ISSN: 2233-7857

International Journal of Future Generation Communication and Networking

Volume No. 16

Issue No. 3

September - December 2023

ENRICHED PUBLICATIONS PVT. LTD

S-9, IInd FLOOR, MLU POCKET,
MANISH ABHINAV PLAZA-II, ABOVE FEDERAL BANK,
PLOT NO-5, SECTOR-5, DWARKA, NEW DELHI, INDIA-110075,
PHONE: - + (91)-(11)-47026006

ISSN: 2233-7857

International Journal of Future Generation Communication and Networking

Aims and Scope

SERSC is an international center for supporting distinguished scholars and students who are researching various areas of Science and Technology. SERSC wishes to provide good chances for academic and industry professionals to discuss recent progress in various areas of Science and Technology.

SERSC organizes many international conferences, symposia and workshops every year, and provides sponsor or technical support to researchers who wish to organize their own conferences and workshops.

SERSC also publishes high quality academic international journals in various areas of Science and Technology

ISSN: 2233-7857

International Journal of Future Generation Communication and Networking

ISSN: 2233-7857

International Journal of Future Generation Communication and Networking

(Volume No. 16, Issue No. 3, September - December 2023)

Contents

A Unified Comprative Phonon Dynamical Study of Europium Oxide (EuO) and Europium Sulphide (EuS)

S. P. Singh[1], Mudit P. Srivastava[2], Awanish K. Singh[3]

[1] Deptt. of Physics, Govt.P.G. College, Lohaghat, Champawat, Uttrakhand, India

[2] Deptt. of Physics, SRMIST, Delhi-NCR Campus, Modinagar, Ghaziabad, (U.P.), India

[3] Deptt. of Physics, Shaheed Smarak Govt. Degree College, Yusufpur Mohamdabad, Ghazipur, (U.P.), India

ABSTRACT

A systematic unified comparative theoretical analysis of Europium Oxide (EuO) and Europium Sulphide (EuS) has been investigated by a lattice dynamical model which include the effect of three-body interaction (TBI) in the framework of second neighbor three body rigid shell model (SNTRSM) and second neighbor rigid ion model (SNTRIM). These two includes long range Coulomb interactions, three body interactions and short-range second neighbor interactions. The significance of these two approaches thus obtained, have been applied to study the phonon dispersion curves (PDC), variation of Debye temperature with absolute temperature, phonon density of states and anhormonic properties of Europium Oxide (EuO) and Europium Sulphide (EuS) by the supplication of TRSM (three-body force shell model) and TRIM (three-body force rigid ion model). It is concluded that our theoretical results predicted by SNTRSM on phonon dynamics and derivable properties will be very much close to their measured data. The present approach has revealed much better description of the crystal dynamics of the solid than those reported by other models.

Keywords: Phonon dispersion curves, Rigid shell model, Rigid ion model, Debye temperature PACS Nos. 63.20.-e; 65.40.Ba; 78.30.-j

INTRODUCTON

The electronic structure of Europium sulfide (EuS) and Europium Oxide (EuO) which is a group of Europium Chalcogenides, solidifies in f.c.c. NaCl structure and are likewise called as uncommon earth europium chalcogenides with incredible intrigue. Dissimilar to other uncommon earth mixes europium chalcogenides by and large, show non-blended valance character. The investigation of cross section dynamical conduct of these chalcogenides is fragmented even today because of deficient exploratory information for phonon scattering bends or curves and a little consideration has been paid to it.

Despite the fact that europium chalcogenides have an enormous application as attractive semiconductors, yet no genuine consideration has paid so for. Just barely any data about the optical frequencies [3-5], versatile elastic properties [2] and magnetic [29, 30] have been introduced. Complete test information on phonon scattering isn't accessible for these mixes aside from EuSe, for which restricted data about phonon recurrence has been accounted for by Silberstein et al. [1]. Zeyher and Kress have applied a phenomenological model (OSM) [14] to talk about the phonon dispersion curves or bends (PDCs) and the combined density of states (CDS). Moreover, Osaka et al. [11] have examined the phonon frequencies just for EuSe utilizing Breathing shell model (BSM). For better outcome Mischenko and Kikoin [19] have changed Zayher and Kress overlap shell model (OSM) to foresee the phonon scatterings bends of EuO and EuS. Every one of these analysts changed the dynamical network by consolidating the charge thickness disfigurement impacts. Be that as it may, based on cover accomplishments, their outcomes are for away from progress since none has thought about the many

body associations (the primary significant term is three body connections) for these mixes. Because of the unfilled 4f shells, the ionic radii of uncommon earth particle changes and in this manner covering of the chalcogenides particles, likewise changes. The Europium chalcogenides show the deviation from the Cauchy discrepancy C12=C44. The BSM utilized by Onsaka et al. [11] and Sakale et al. [25] of PDC just clarifies the acoustic branches well. Thusly it is clear that OSM and BSM neglect to clarify the optical parts of PDC of these crystals. It has been discovered that three body associations clarify well the optical branches and Cauchy error both at the same time and effectively to practically all the ionic and semiconducting crystals [17]. Also, these mixes showed solid optical phonon oddities all through the Brillouin zone and exceptional acoustic phonon spread along [qqq] bearings. These realities recommend that kinds of many-body collaborations are liable for the flexible and phonon irregularities in these compounds. These have inspired the current creators to the fundamental need of two phenomenological grid dynamical models. The point of this paper is to test the relevance and utility of second neighbor three-body unbending shell model (SNTRSM) and second neighbor three-body inflexible particle model (SNTRIM) for the acceptable portrayal of phonon scattering relations and other phonon properties of these compound mixes .

THEORY

The general formulation of present Lattice Dynamical model is given by

(i) Three-body force rigid shell model (SNTRSM)

(ii) Three-body force rigid ion model (SNTRIM)

The interaction system of present model thus consists of long range Coulomb and three body interactions (TBI) energies. The next term is the form of SR overlap repulsive energy extended to the next nearest neighbor ions in Europium Chalcogenides. As per the interaction system, the present model may positively be the successful attempt for the dynamical description of these materials.

The general formulation of SNTRSM can be derived from the crystal potential whose relevant expression per unit cell is given by

$$\Phi = \Phi^{C} + \Phi^{R} + \Phi T^{BI} \qquad (1)\ .$$

Where the first two terms represent, respectively, long range Coulomb and three body interactions (TBI) energies. The next term is the form of SR overlap repulsive energy extended to the next nearest neighbor ions. where first term Φ^{C} is Coulomb interaction potential which is long-range in nature, second term Φ^{R} is short range overlap repulsion potential operative up to the second neighbors and third term Φ^{TBI} is three body interaction potential. The secular determinant D(q), is the (6x6) dynamical matrix which is given by:

$$D(q) = (R' + Z_m C Z_m) - (T + S_m C Y_m)(S + K + Y_m C Y_m)^{-1}(T^{*} + Y_m C Z_m) \qquad (2)$$

The Number of adjustable parameters has largely been reduced by considering the short range interaction to act only through the shells. This assumption leads to R=T=S. The expressions derived for elastic constants corresponding to SNTRSM have been obtained as:-

$$\frac{4r_0^4}{e^2} C_{11} = [-5.112 Z_m^2 + A_{12} + \frac{1}{2}(A_{11} + A_{22}) + \frac{1}{2}(B_{11} + B_{22}) + 9.3204\xi'^2] \qquad (3)$$

$$\frac{4r_0^4}{e^2}C_{12}=[0.226Z_m^2-B_{12}+\frac{1}{4}(A_{11}+A_{22})$$

$$-\frac{5}{4}(B_{11}+B_{22})+9.3204\xi'^2] \quad (4)$$

$$\frac{4r_0^4}{e^2}C_{44}=[2.556Z_m^2+B_{12}+\frac{1}{4}(A_{11}+A_{22})$$

$$+\frac{3}{4}(B_{11}+B_{22})] \quad (5)$$

In View of the equilibrium condition $[(d\Phi/dr)_0]$ We obtain.

$$B_{11}+B_{22}+B_{22}=-1.165Z_m^2 \quad (6)$$

Where

$$Z_m^2=Z^2\left(1+\frac{12}{Z}f_0\right) \quad \text{and} \quad \xi^{12}=Zr_0f_0$$

The term f_0 is a function dependent on the overlap integrals of the election wave-funtions and the subscript zero indicates the equilibrium value. By solving the secular equation along [q00] direction and subjection the short and long-range coupling coefficients to the long-wavelength limit $q \rightarrow 0$, two distinct optical vibration frequencies are obtained as:

$$(\mu\omega_L^2)_{q=0}=R_0'\frac{(Z'e)^2}{Vf_r}\cdot\frac{8\pi}{3}\left(Z_m^2+6\xi'^2\right) \quad (7)$$

$$(\mu\omega_r^2)_{q=0}=R_0'\frac{(Z'e)^2}{Vf_r}\cdot\frac{4\pi}{3}Z_m^2 \quad (8)$$

Since, in these compounds, $\omega_L=\omega_r$ at Γ - point, therefore, Esq. (7) and (8) lead to the expression:

$$\frac{Z_m^2+6\xi'^2}{\xi'^2}=-\frac{f_L}{2f_r} \quad (9)$$

Where the abbreviations stand for

$$f_r=1-\left(\frac{\alpha_1+\alpha_2}{v}\right)\cdot\frac{4\pi}{3}Z_m^2$$

By solving the dynamical matrix along [0.5, 0.5,0.5] directions at L-Point modified expressions for $\omega_{Lo}(L)$, $\omega_{To}(L)$, $\omega_{LA}(L)$, and $\omega_{TA}(L)$, are as follows.

$$m_1\omega_{LA}^2(L)=R_0+\frac{e^2}{V}(2A_{11}+B_{11}-\frac{e^2d_1^2}{a_1}$$

$$+\left(\frac{e^2}{V}\right)C_{1L}(Z_m+d_1)^2\left[1+\left(\frac{\alpha_1}{V}\right)C_{1L}\right]^{-1} \quad (10)$$

$$m_2\omega_{LO}^2(L)=R_0+\frac{e^2}{V}(2A_{22}+B_{22}-\frac{e^2d_1^2}{\alpha_1}$$

$$+\left(\frac{e^2}{V}\right)C_{1L}(Z_m+d_2)^2\left[1+\left(\frac{\alpha_2}{V}\right)C_{1L}\right]^{-1} \quad (11)$$

$$m_2\omega_{TO}^2(L)=R_0+\frac{e^2}{2V}(2A_{22}+B_{22}-\frac{e^2d_2^2}{\alpha_2}$$

$$+\left(\frac{e^2}{V}\right)C_{1T}(Z_m+d_2)^2\left[1+\left(\frac{\alpha_2}{V}\right)C_{1T}\right]^{-1} \quad (12)$$

$$m_1\omega_{TA}^2(L)=R_0+\left(\frac{e^2}{2V}\right)(A_{11}+5B_{11}-\frac{e^2d_1^2}{\alpha_1}$$

$$+\frac{e^2}{V}C_{1T}(Z_m+d_1)^2\left[1+\left(\frac{\alpha_1}{V}\right)C_{1T}\right]^{-1} \quad (13)$$

where

$C_{1L}^{'}=-\left[\left(C_{1xx}+2C_{1xy}\right)+\left(V_{1xx}+2V_{1xy}\right)Z_m^{-2}Zx_0f_0^{'}\right]0.5,0.5,0.5$

$C_{1T}^{'}=-\left[\left(C_{1xx}+C_{1xy}\right)+\left(V_{1xx}+2V_{1xy}\right)Z_m^{-2}Zr_0f_0^{'}\right]0.5,0.5,0.5$ where $\left(C_{1xx}+C_{1xy}\right)$ and $\left(V_{1xx}+V_{1xy}\right)$ are Coulomb and three - body coupling coefficients evaluated at L-point. polarizability is negligibly small and the negative ion polarizability of nitride ion is almost zero. Therefore, it has been considered to utilize the second neighbour three-body force rigid ion model (SNTRIM) for further calculations of phonon frequencies.

In an attempt to solve the expressions for SNTRIM, all the Eqs (1-6) will remain the same , only the difference is in the expressions from Eqs. (7-13), which can be written as follows:

$$\left(\mu\omega_L^2\right)_{q=0}=R_0+\frac{8\pi e^2}{3V}(Z_m^2+6\xi^{'2}) \quad (14)$$

$$\left(\mu\omega_T^2\right)_{q=0}=R_0-\frac{4\pi e^2}{3V}(Z_m^2) \quad (15)$$

Since, in these compounds, $\omega_L=\omega_T$ at $\Gamma-$point, therefore, Eqs (14) and (15) lead to the expression:

$$Z_m^2=-4Zr_0f_0^{'} \quad (16)$$

Again, by solving the dynamical matrix along [0.5, 0.5, 0.5] directions at L-point, the modified expressions for $\omega_{Lo}(L)$, $\omega_{To}(L)$, $\omega_{LA}(L)$, and $\omega_{TA}(L)$ are derived as follows:

$$\omega_{LO}(L)=R_0+\frac{e^2}{v}(2A_{22}+B_{22})+\frac{e^2}{v}C_{1T}^{'}Z_m^2 \quad (17)$$

$$m_2\omega_{TO}^2(L) = R_0 + \frac{e^2}{v}(A_{22} + 5B_{22}) + \frac{e^2}{v}C'_{1T}Z_m^2 \quad (18)$$

$$m_1\omega_{LA}^2(L) = R_0 + \frac{e^2}{v}(2A_{11} + B_{11}) + \frac{e^2}{v}C'_{1L}Z_m^2 \quad (19)$$

$$m_1\omega_{TA}^2(L) = R_0 + \frac{e^2}{v}(A_{11} + 5B_{11}) + \frac{e^2}{v}C'_{1T}Z_m^2 \quad (20)$$

where R_0 and C'_{1T} have already been defined.

COMPUTATIONS AND RESULTS.

The input data along with their relevant references and calculated model parameters from SMTRSM and SNTRIM for EuO and EuS are given in Table-1 and Table-2. A comparative result on phonon dispersions curves from the two models have been shown in Figure-1and Figure-2. These results have also been compared with the observed data of Kress et al [1].for visual comparison.

Table 1 Input data and model parameters for EuO

[$C_{ij}(in10^{12}\,dyne\ cm^{-2})$, v(in THz), $r_0(in10^{-8}\,cm)$ **and** $\alpha_i(in10^{-24}\,cm^3)$]

Input Data		**Model Parameters**		
Properties	**Values**	**Parameters**	**TRSM**	**TRIM**
C_{11}	19.2*	Z^2_m	0.7392	0.7238
C_{12}	4.25	$r_0f'0$	-0.0119	-0.0119
C_{44}	5.42	A	7.6432	7.564
$V_{LO}(\Gamma)$	13.05	B	-0.861	-0.8432
$V_{TO}(\Gamma)$	5.460	d_1	0.4145	-
r_0	2.572	d_2	1.1721	-
α_1	2.07	Y_1	-2.0541	-
α_2	2.40	Y_2	-0.8448	-

Table 2-Input data and model parameters for EuS

[$C_{ij}(in10^{12}\,dyne\ cm^{-2})$, v(in THz), $r_0(in10^{-8}\,cm)$ **and** $\alpha_i(in10^{-24}\,cm^3)$]

Input Data		**Model Parameters**		
Properties	**Values**	**Parameters**	**TRSM**	**TRIM**
C_{11}	13.1	Z^2_m	0.6745	0.6522
C_{12}	1.10	$r_0f'_0$	-0.3005	-0.3005
C_{44}	2.73	A	8.5110	8.396
$V_{LO}(\Gamma)$	8.01	B	-0.7858	-0.7598
$V_{TO}(\Gamma)$	5.35	d_1	0.01634	-
r_0	2.984	d_2	1.4081	-
α_1	1.5	Y_1	-0.7943	-
α_2	5.5	Y_2	-2.1497	-

*** Value extrapolated from measured PDC**

**** Reasonable value taken from ionic radii**

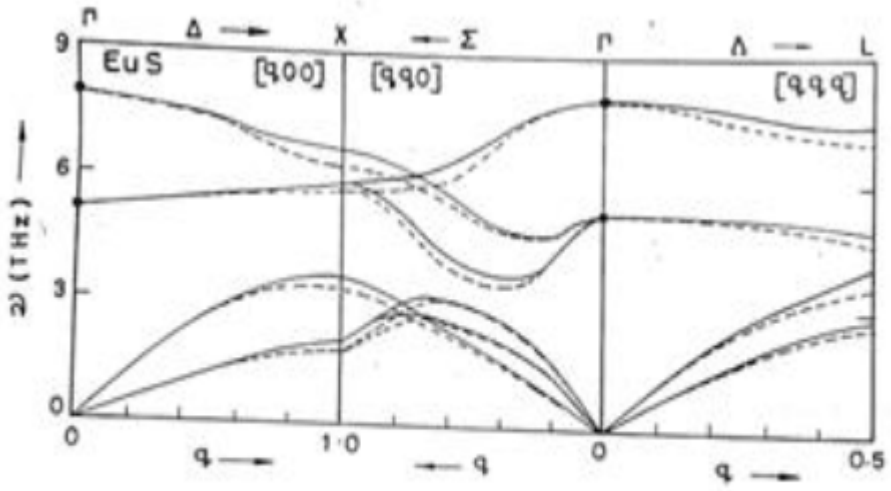

Fig. 1. Phonon dispersion curves for EuS

• Experimental points —— TRSM ----- TRIM

DISCUSSION AND CONCLUSION

From figure 1 and 2, it is clear that the results reported from SNTRSM for EuO and EuS. EuS are comparatively more close to ensured data on PDCs. There are certain features in PDC of EuS which deserve special mention. The three body interactions have influenced both LO and TO branches much more than acoustic braches (LA and TA). Another striking feature of the present study is noteworthy from the excellent reproduction of optical and acoustic branches.

The model parameters of TRSM and TRIM have been used to calculate the phonon spectra for allowed 48 non-equivalent wave vectors in first Brillouin zone. The frequency along with symmetry directions have been plotted against the wave vectors to obtain the phonon dispersion curves (PDCs) from both the models. These curves are compared with each other and with inelastic neutron scattering technique.

Since neutron scattering provide us only a very little data for symmetry direction, we have studied the specific heat for complete description of frequencies. For this purpose the specific heat has been computed at different temperature using Blackmann's technique [35] and corresponding Debye temperature have been plotted against absolute temperature (T). .

It may be concluded that SNTRSM provides agreement which is certainly better than those fitted by experimental researchers and SNTRIM, are very much close to the experimental values. Although, qualitatively the agreement achieved from our present model SNTRSM is comparatively better than some of the model values. In addition, some other researchers [18-24] of the field have also tried their best to explain PDCs and other properties of europium chalcogenides but only with moderate success.

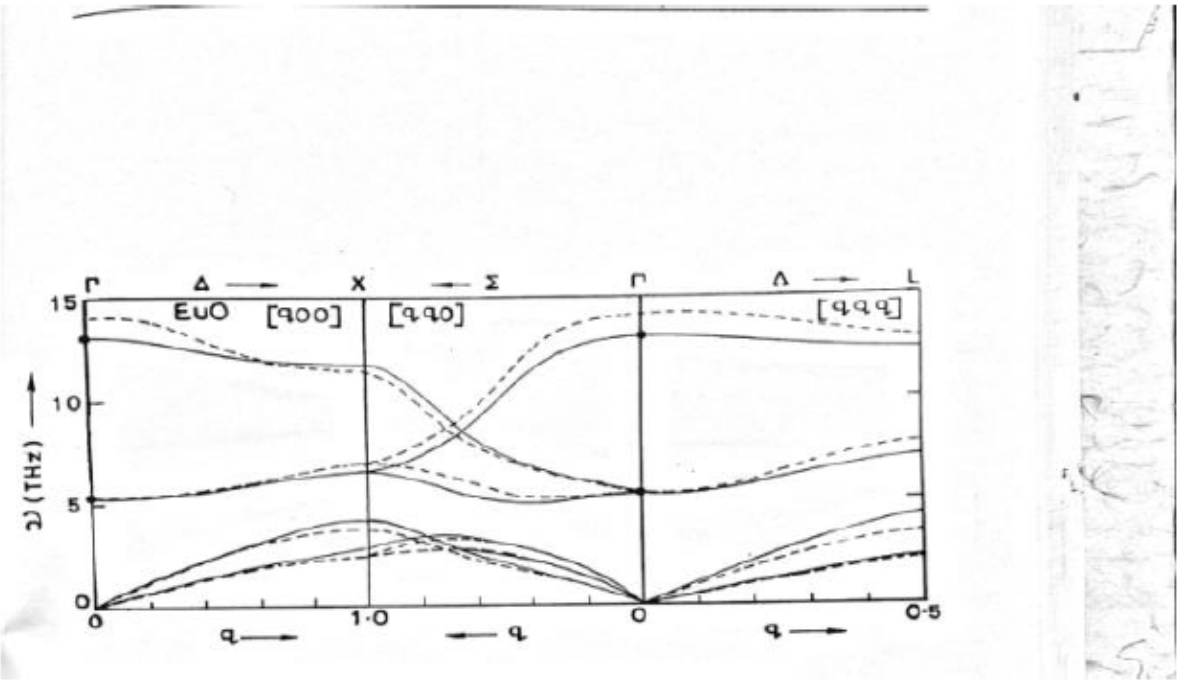

Figure-2 Phonon dispersion curves of EuO.
Experimental points -------TRSM
---------TRIM

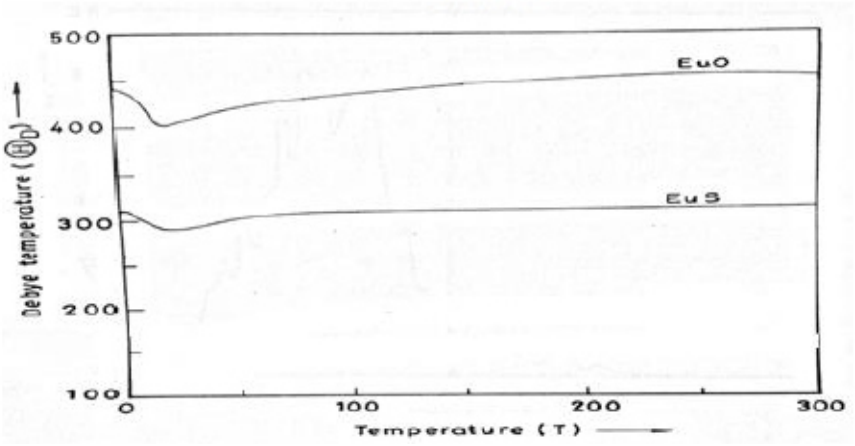

Figure-3 Debye temperature variations of EuO and EuS

Furthermore, in order to increase the merit of this work, we have tested the adequacy of our model by calculating [33] two phonon Raman/IR spectra and variation of Debye temperatures shown in figure-3. In order to interpret them the critical point analysis has been used following the method prescribed by Burstein et al [36].

It may be concluded that the inclusion of the effect of short range overlap repulsive interaction upto second neighbours in the framework of TRIM and TRSM is important in EuO and EuS. These are probably the first reports of its kind and this will help the other workers to analyze their data in future.

Furthermore, It is expected that slight discrepancies still occurring between theory and experiment may be further improved by including the effect of free carrier screening (FCS), Van der Waals interactions

(if data are available in future) and by including anharmonicity of vibrations in the present model (SNTRSM).

REFERENCES

1. *Silberstein R.P, Tekippe V.T. and Dresseelhaus M.S., Phy. Rev (1977) 2728.*
2. *R.W.G. Wyckoff in Crystal Structure, (Wiley, New York) 1963.*
3. *Guntherod G., Phy, Cond. Matter 18 (1974) 37.*
4. *Holah G.D., Webb J.S Deneriss, R.B and C.R. Pidgron, Solid State Commun. 13 (1973)209.*
5. *Axe J.D, J. Phys. Chem. Solids 30 (1966) 1403.*
6. *Schroder U., Solid state Commun 4(1966)347.*
7. *Shapiro Y. and Reed T.B, in 17th Conference on Magnetism and Magnetic Materials, Chicago, 1971, AIP Conf. Pro . No. 5 (AIP, New York, 1972) p.857.*
8. *Chatterjee A., Singh A.K. and Jayaraman A., Phys. Rev. B6, (1972), 2285.*
9. *Holah G.D, Webb J.S., Dennis R.B. and Pidgeon C.R., Solid State , ommun. 13, 209(1973)*
10. *Bilz H., Gliss B. and Hanke W., in Dynamical Properties of solids, edited by G.K. Horton and A.A. Maradudin (North Holland, Amsterdam, 1974.*
11. *Onsaka Y., Sakurai O. and Tachiki M., Solid State Commun. 23 (1977) 589.*
12. *Kress W., Reichardt W., Wagner V., Kugel G. and Hennion B., in Lattice Dynamics, edited by M Balkanski [Flammarion Paris] 1977,*
13. *Guntherodt G. et at., Phys. Rev, B20 (1979) 2834.*
14. *Zeyher R. and Kress W., Phys. Rev B20 (1979) 2850.*
15. *Guntherodt G., Jayarman A., Kress W.and Bilz H., Phy. Lett. 20 (1981) 824, Guntherodt G., Jayaraman A., Bilz H., Kress W., Falicov L.M., Hanke W. and M.B. Maple [Eds.] Valence Fluctuations in Solids North Holland Amsterdam (1981)*
16. *L.M Falicov, W. Hanke and M.B. Maple (Eds.), Valence Fluctuations in Solids North Holland Amsterdam (1981)*
17. *Singh R.K., Phys. Reports 85 (1982) 259*
18. *Sanyal S.P and Singh R.K., Physica B+C 132 (1985) 201.*
19. *Mischenko A.S. and. Kikoin K.A, J. Phys. Codens. Matter 3 (1991) 5937.*
20. *Jha P.K. and Sanyal S.P., Indian J.Pure and Appl. Phy. 31 (1993)469.*
21. *Jha K. and Sanyal S.P., Indian Journal of Pure and Applied Physics Vol. 32, October 1994, pp.824-829.*
22. *Jha P.K. and Sanyal S.P., Pramana J.Phys. 43(1994) 193.*
23. *Jha P.K. and. Sanyal S.P, Pramana Indian J. Pure and Appl. Physics 32 (1994) 824.*
24. *Jha P.K. and Sanyal S.P., Pramana, Solid State Commun. 105 (1998) 455.*
25. *Sakake U.K., Jha P.K. and Sanyal S.P., Bull. Mat. Science 23 (2000)333.*
26. *Brill R., Solid Stat. Phys. Academic Press, New York 20,1 (1967)*
27. *Witte H. and Wolfed E., Z. Phys. Chem. 4, 36 (1965) and Rev. Mod. Phys. 30, 51 (1958)*
28. *Vogl E. and Waidelied W., Angrew Z. Phys.25, 98 (1968).*
29. *P. Wachter in Handbook on Physics and Chemistry of Rare-Earths (North Holland, New York), 1979.*
30. *Mauger A. and Godart C., Physics Reports 141 (1986) 51.*
31. *Woods A.B.D., Cochran W. and Brockhouse B.N., Phys. Rev. 119.980 (1960)*
32. *Lundqvist S.O., Ark. Fys. 6, 25 (1952).*
33. *Singh S P, Ph D Thesis, "Three body Interaction of lattice dynamics of Europium chalcogenides" (VBS Purvanchal University, Jaunpur), 2005.*
34. *Dr. Mudit P. Srivastava, Ph.D. Thesis, "A Comprehensive Study of Lattice Dynamics of Cesium Halides" (V.B.S. Purvanchal University, Jaunpur,U.P.) 2007.*
35. *Blackmann M., Z, Phys, 82, 421 (1933) and Trans. Roy. Soc. A 236, 102 (1955).*
36. *Burstein E., Jhonson F.A. and Landon R., Phy. Rev. 139 A, 1239 (1965).*
37. *Upadhyaya K S, Ajay Kr. Singh, Pandey Atul, Pathak S N & Singh A K, Pramana, 64(2005) 299.*
38. *S. P. Singh, Mudit P. Srivastava and Awanish K. Singh, Int. J. Advd. Sc. & Research, Vol.3, Issue-6, pp 29-32,(2018).*

Analysis oOf Delaminated Hybrid Carbon Fiber Composites

[1]Hassan A. Alessa, [2]Steven L. Donaldson
[1, 2]University of Dayton, 300 College Park,
Dayton, OH 45469 USA

ABSTRACT

Fiber reinforced composite materials have been used increasingly in primary and secondary structures in such applications as aircraft, satellites, automobiles, biomedical industries, marine, and sporting goods. This growth is due primarily to the characteristics of composite materials, which include high specific stiffness, high specific strength, and low density. Both carbon and glass fibers are often used as reinforcing fibers, embedded in polymer matrix material. The glass fibers are inexpensive, have high strength to weight ratio, but low stiffness. Carbon fiber is more expensive, but has a high strength to weight ratio and high stiffness.

The delamination between composite layers is one of primary weaknesses in composite material structure. The mode I peeling, mode II shearing, and mixed-mode I/II are the most common delamination fracture crack driving modes between interfaces. Delamination can then lead to a reduction in the structural stiffness. If the structure has compression loading, buckling failure may ensue. The best design approach may find a compromise between less weight and less cost by using a hybrid material approach of both glass and carbon fibers. This research focused on a hybrid materials consisting of both glass and carbon fiber embedded in a polymer matrix, undergoing mode I, mode II, and mix mode I/II static interlaminar fracture. Glass fiber panels, carbon fiber panels, and hybrid panels were fabricated using the wet layup / vacuum bag technique. The non-hybrid all-glass, all-carbon, and hybrid glass/carbon were experimentally characterized by quasi- static testing in load frames. The specimen and material geometries (especially at material interfaces) were analyzed using the finite element method. The program Abaqus was utilized, including the cohesive zone method (CZM). Finally, the resulting fracture surfaces were investigated using a scanning electron microscope. The result showed the fracture toughness values of hybrid material (FG/CF) were between that of fiber glass and carbon fiber. Also, fracture toughness increased due to fiber bridging under static mode I, mode II, and mixed mode I/II.

INTRODUCTION

The application of composite material has been expanding in many structural engineering fields in recent years. This increased use of composite materials is due to their low density, strength, high stiffness, long fatigue life, corrosion resistance and ability to tailor their structural properties. [1].Large structures such as ships, aircrafts, wind turbine blades, cars bodies, and satellites, are fabricated from many materials and parts. Sometimes the structures have failure related to poor design or structural aging. The most common mechanical failure in composite material is delamination, which is separation of the ply layers. Delamination occurs between interfaces because it is the weakest zone in composite materials. The delamination failure modes include mode I, mode II and mix-mode I/II Figure1.1.

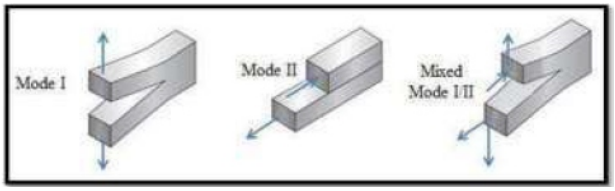

Figure1.1 Mode I, Mode II and Mixed mode I/II. [15]

Composite structures require durability, damage tolerance, long fatigue life cycle, long life, and affordable cost for their light weight. Both carbon and glass fibers are often used as reinforcing fibers, embedded in polymer matrix material. The glass fibers are inexpensive, have high strength to weight ratio, but low stiffness. Carbon fiber is more expensive, but has a high strength to weight ratio and high stiffness. A hybrid fiber approach is a combination more than two fiber types, in an effort to take advantage of each material, to optimize the balance between properties and cost. For example, the incorporation of carbon longitudinal spars in fiberglass wind turbine blades, wind of air craft and sailboats [2, 3, 4, 5].

The primary method to gain information regarding mode I, mode II and mix mode I/II delamination resistance is by experimental mechanical testing. The test responses can then be simulation by using finite element analysis software. This simulation program helps to understand the failure behavior, especially due to mixed model loading. The last step is to examine the resulting fracture surfaces carefully, to help identify energy-absorbing mechanisms that correlate to the mechanical test results.

LITERATURE REVIEW:

The most common delamination fracture failure type studies have been under mode I loading. Many of people had been done mode I fracture on composite material experimental and simulation. The studies considered to serve as an important back ground to the current work are discussed below. In 1982, Whitney, Browning and Hoogsteden conducted mode I experiments with four different materials (AS-1/3502, AS-4/3502, T300/V3778A, AS-1/ Polysulfone, and Bidirectional Cloth) carbon fiber reinforced polymer. They calculated the critical energy release rate by using four methods (Area method, Beam analysis, Empirical Analysis, and Center Notch) with different initial crack. [6]. In 1989, N. Sela,O. Ishai and L.Banks, investigated how adhesive thickness effect on fracture toughness of carbon fiber reinforced plastic between 0.04mm -1.01mm. They found if increase the thickness of adhesive will increase fracture toughness and the adhesive thickness range between 0.1-0.7mm [22].

In 1996, John A. Nairn studied the effect of residual stresses of mode I for double cantilever beam on adhesive and laminate [7]. In 2007, A.J. Brunner, B.R.K. Blackman, P. Davies used alternating 0°/90° layers and increased fiber bridging between two beam by that increased delamination resistance [12]. P.N.B. Reis1a, J.A.M. Ferreira,

F.V. Antunes, J.D.M. Costa, C. Capela studied crack initial length on carbon/ epoxy. After they obtained the results of experimental, the specimens were analyze by finite element to creates carve P vs. With different energy release rate and crack length [13]. In 2002, Mehdi Barikani, Hossein Saidpour, and Mutlu Sezen used modified beam theory to study the temperature effect on fracture toughness with different epoxy. They found increasing the temperature decreased fracture toughness [8,9].

In 2008, Solaimurugan, and Velmurugan did mode I fracture with kinds of fiber glass woven and UD with stitched and without stitched. The specimen‟s fiber interface had many orientation designs for UD fiber had 0/0, 30/-30, 45/-45, 60/-60, 90/-90 and 0/90 interfaces and woven had 30/-30, 45/-45 and 90/90 interfaces. Kevlar fiber roving of Tex 175 g/km was the material stitching between two beams. The stitching increase the toughness of specimen three times compare with specimen without stitching [10, 11, 12].

In 1997, Julio F. Davalos did experimental and simulation on hybrid material mode I between wood and fiber- reinforced plastic (FRP) and was using contoured specimen for mode I. The fracture toughness of each wood- wood and FRP-FRP higher than FRP-wood hybrid and he used two method the first one Rayleigh-Ritz and Jacobian derivative method (JDM) [13]. In 1999, Shun-Fa Hwang, Bon-Cherng Shen fabricated mode I specimen hybrid material (carbon fiber and fiber glass). The both beams of mode I specimen had two materials fiber glass and carbon fiber with different fiber orientation and specimen hybrid material (carbon fiber and fiber glass) obtained higher interlaminar fracture toughness compare with non-hybrid specimen [14]. In 2012 Mohammadreza Khoshravan, Farhad Asgari Mehrabadi fabricated mode I specimen hybrid material of carbon fiber/aluminum and did fracture toughness tested. They used modified beam theory (MBT) and compliance calibration method (CCM) to calculate mode I fracture toughness. They studied how crack length effect on crack failure and they used FEA to analyses stress distribution on long of specimen and width of specimen [15].

In 1998, M. N. Charalambides, A. J. Kinloch and F. L. Matthews investigated on repair carbon fiber reinforce plastic (CFRP) by using scarf joint and applied mode II test experimental and FEA.) [16]. In 2000, P. Compston, P.-Y.B. Jar, P.J. Burchill, K. Takahashi investigated fiber glass reinforced using three different resins and with different fiber volume fracture to compare interlaminated delamination fracture toughness of mode II[31]. In 2003, Stevanovic, Kalyanasundaram, Lowe, and Jar studied how poly (acrylonitrile-butadiene-styrene) (ABS) affected on fracture toughness when mixed with various vinyl-esters (VE) in interface by different mixed ration. ABS was increase the fracture toughness when added with VE less 7% and reduce the fracture toughness when added with VE higher than 7% [64]. In 2006, B.R.K. Blackman, A.J. Brunner, J.G. Williams used specific carbon fiber epoxy (HTA-1200 carbon fiber 113 epoxy resin) for mode II test. In 2007, Masahiro Arai, Yukihiro Noro, Koh-ichi Sugimoto, Morinobu Endo used nano-fiber carbon fiber in specimen inter face with different density for calculate mode II fracture toughness. From the experiments result, increasing density of nano-carbon fiber is increase the fracture toughness [17].

Single leg Bending is one of mixed mode I/II test method Figure1.2.6. In 2003, Gregory D. Tracy, Paolo Feraboli, Keith T. Kedward investigated mix mode single leg four point binding on (RFI) carbon fiber /epoxy laminate of material (IM7-AS4/350-6 hybrid composite system) [18]. In 2007, Cole S. Hamey investigated in Mix mode and fabricated the specimen out of two different kind of wood structures and bind together by epoxy. He used Single Leg Bending (SLB) specimen for experimental test [19]. In 2011, L.F.M. da Silva, V.H.C. Esteves1, F.J.P. Chaves, the specimen fabricated for mix mode of steel/ adhesive / steel. The steel was DIN 40CRMnMo7 and epoxy adhesive was 2015 from Huntsman [20].

MATERIALS AND PROPERTIES

Materials

This research was conducted using composite materials fabricated from S1-HM Unidirectional (UD) fiber glass, EPON Resin 828, EPI-CURE Curing Agent 3223 (Hardener), TORAYCA T300 unidirectional carbon fiber and fluorinated ethylene propylene (FEP) Optically Clear Film made with Teflon.

The fiber glass was donated from AGY-South Carolina. The resin and the hardener were donated from Momentive Specialty Chemicals in Stafford-Texas.

EPON Resin and Curing Agent

The epoxy system used had two main components; first component is the epoxy resin 828 and the second part is curing agent 3223. These two components were equally important since both reacted and contributed to the final structure and properties. The curing agent 3223 was added 10% by weight to the epoxy resin 828 to cure. [1]

Resin

EPON 828, Figure 2.1, is liquid bisphenol A Epichlorohydrin based epoxy resin which contains Phenol, 4,4O - (1- methylethylidene) bis-polymer with (chloromethyl) oxirane [1]

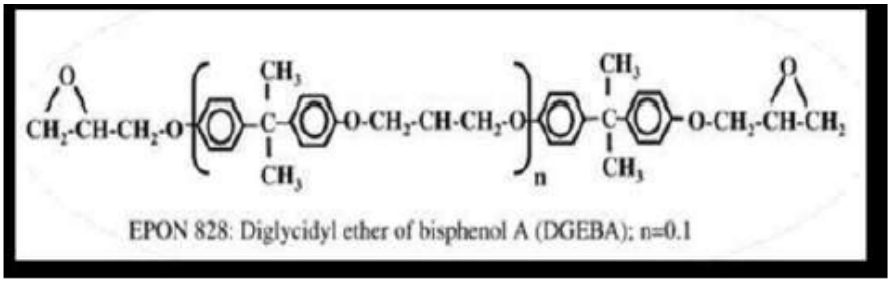

Figure 2.1 EPON 828

And it is one of bifunctional phenolic glycidyl ethers under Diglycidylether of Bisphenol-A (DGEBA), Figure 2.2 DGEBA has two common reactions to ring- opining polymerization and crosslinking, either catalyzed homopolymerization or bridging reactions incorporating a coreactive crosslinking agent into the network (1). These reactions will be discussed in more details in mechanisms section.

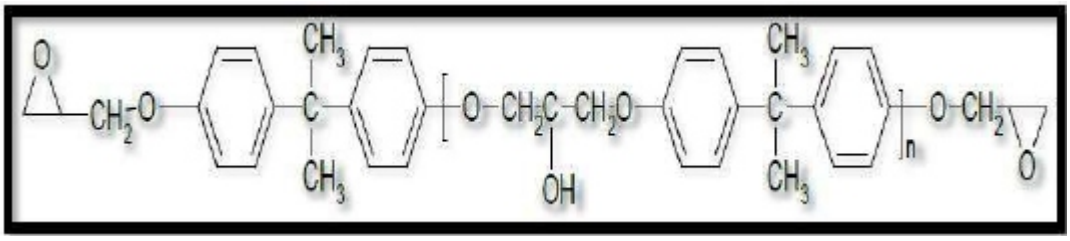

Figure 2.2 Diglycidylether of Bisphenol-A (DGEBA), n = 0, for the derivatives, n > 0.

Curing Agent: EPI-CURE 3223

DIETHYLENETRIAMINE (DETA), N-(2-aminoethyl-1, 2-ethanediamine) is a linear ethyleneamine with two primary and one secondary amine as shown in figure 2. It is a single-component with clear, colorless, and an ammonia-like odor product [4].

DETA is a liquid agent widely used with epoxy resins for fast cures or where room temperature cures are required (Appendix A). Due to exothermic heat of the reaction and the pot life of the catalyzed resin is quite short; this agent is restricted to small casting applications. Although DETA has good properties at room temperature when it is used in curing process (6).

3 PANEL FABRICATIONS AND TENSILE TEST

Panel Fabrication and Sample Cutting:

The simulation using Abaq requires material properties data as input to the9 models. The material properties were collected using tensile test ASTM standard D3039 [4] [5] with strain gage MM (CEA-06-250UW-120). The results were used to calculate , and for the glass and carbon composites used.

They were several steps used to fabricate the specimens for the tensile tests. The fabrication lay-up is shown in Figure 3.1. First, the dry fiber plies were cut into pieces with dimension 19" x 18" (482.6 mm x 457.2mm) for fiber glass. The dimensions for dry carbon fiber pieces were 12" x 12" (304.8mm x 304.8mm). The table surface was cleaned by wiping with acetone. Third, the sealing tape was placed (High Temp Sealant Tape-Yellow) with dimensions of 19.25" x 18.25" (488.95mm x 463.55mm) for fiber glass and for carbon fiber sealing tape dimension 12.25" x 12.25" (311.25 mm x 311.25 mm) was used. Fourth, the non-porous Teflon (234 TFNP non- adhesive non-porous) was placed over the sealing tape to build a dam structure, which kept the resin contained.

The dimension used for the dry fiber glass was 22" x 21" (558.8 mm x 533.4 mm) and for carbon fiber 15" x 15" (381 mm x 381 mm). Fifth, the resin/harder were well mixed 10:1 by weight, then the epoxy was poured on the Teflon (dam structure). The epoxy was then distributed equally by a squeegee. The first piece of fiber was laid up on Teflon (dam structure), then epoxy was poured on the fiber and was distributed equally by a squeegee. These steps were repeated for the next layers of fibers. The [0]T fiber glass piece was laid up with one layer for fiber orientation The [90]s specimens were laid up with two layers having fiber orientation The [45/-45]T were laid up using two layers with fiber orientation...The [05]T carbon fiber pieces were laid up using five layers for fiber orientation . The carbon [904]s were laid up with eight layers having fiber orientation . Finally, the carbon [45/- 45]5s were laid up ten layers for fiber orientation . After the fiber was laid up and resin applied, a layer of non- porous Teflon with thickness 0.003" (0.0762 mm) was placed on top, then an aluminum caul plate with thickness 0.118" (3 mm), after that Teflon with thickness 0.003" (0.0762 mm). Following that, the breather layer was then covered by vacuum bagging with vacuum port and seals the vacuum bagging on the edge by sealing tape and leaks were checked. Finally the vacuum pump was connected to vacuum port and turns on the vacuum pump and keeps it running for 24 hours.

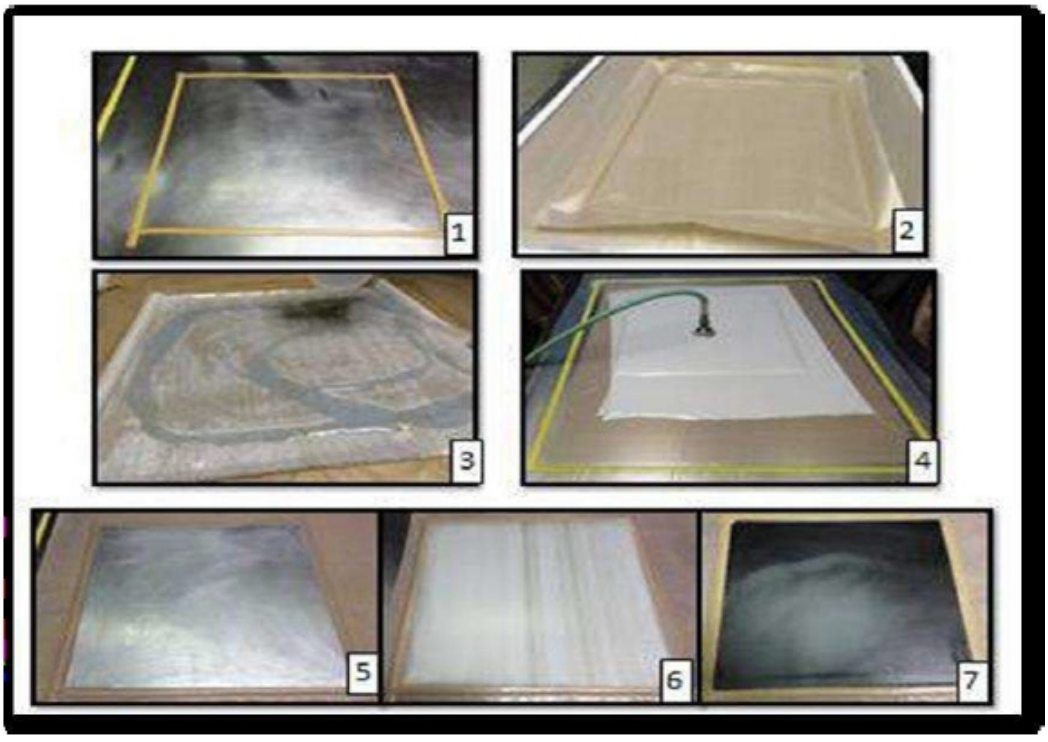

Figure 3.1 Panel Fabrication for Tensile Test and mad tensile specimen

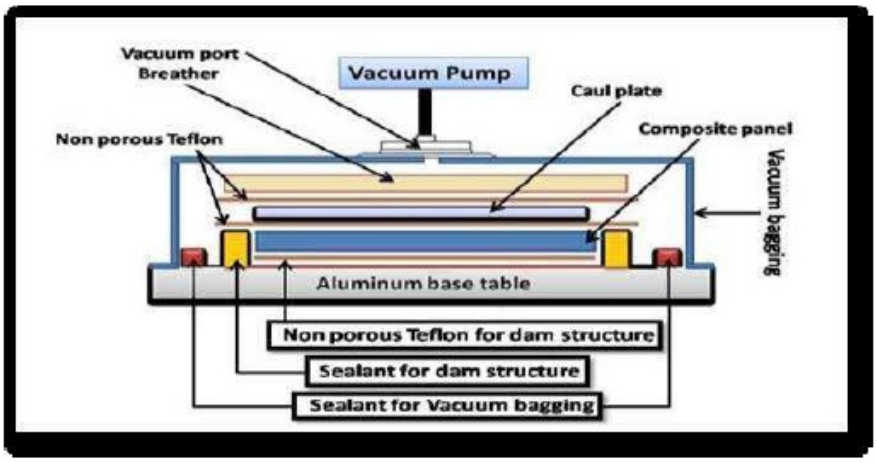

Figure 3.2. (1-7). Panel fabrication steps:

1. Dam structure by sealing tape, 2. Non-porous Teflon, 3. Fiber layup and poured resin, 4. Panel under vacuum for 24 hours, 5. Panel after cure, and vacuum bag and breather removed showing aluminum caul plate, 6. Panel of fiber glass, 7. Carbon fiber panel.

The composite panels were then stored for ten days in room temperature to make certain they were fully cured. Then, the composites panels were then cut with dimension 10" (250 mm) over length for unidirectional and symmetric, but were cutting with dimension 7" (175 mm) over length for unidirectional. The tabs were fixed by super glue with 2.25" (56 mm) length and 0.062" (1.5 mm) thickness for unidirectional panel, 1" (25 mm) length and tab thickness for unidirectional panel. The composite panels were cut into tensile specimens with dimension 0.5" (15mm) x 10" (250mm) x 0.04" (1mm) for fiber orientation unidirectional, tensile specimen with dimension 1" (25mm) x 7" (175mm) x 0.08" (2mm) for fiber orientation 9 unidirectional, and tensile specimen with dimension 1" (25mm) x 10" (250mm) x 1" (25mm) for fiber orientation symmetric. They were cut using a wet diamond saw to avoid micro cracks in the specimen.

Install strain gage on tensile specimen;

The following material and tools were used to install the specimen strain gages: M-Bond 200 adhesive, Teflon tape, sand paper 320-grit, Q-tips, strain gage, tweezers. Figure 3.2 shows the strain gage installation steps: first, clean the gauging area with solvent, such as GC-6 isopropyl alcohol. The solvents have to use one way.[6] The second step is to remove any surface scale and make the surface smooth on the gauging area by sand paper 320- grit. Wiping the gagging area by wetted with M-Prep Conditioner A in one way Figure 3.2.(2-3). After that Wiping the gagging area and scrub with a cotton-tipped wetted with M-Prep Neutralizer Figure 3.2. (3-4). Take the strain gage from package by using tweezers and place on a clean glass plate. Install Teflon tape completed on the terminal and gage. Lift the Teflon tape at angle to glass plate Figure 3.2. (5-7). The specimen angle fiber orientation, install two Teflon tape with strain gage on center of specimen first will be side by side to fiber direction for fiber orientation and Second one horizontal to fiber direction.

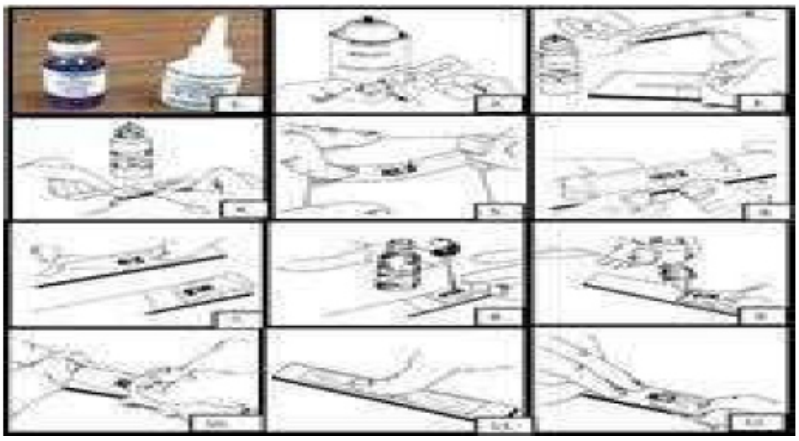

Figure 3.2. (1-12) M-Bond 200 adhesive, (2-12).install strain gage steps [6]

The specimen angle fiber orientation was installed Teflon tape with strain gage on center of specimen and vertical with fiber orientation.The specimen angle fiber orientation was installed Teflon tape with strain gage on center of specimen and with angle to fiber orientation Take of one side the Teflon tape from spacemen until reach end of strain gage and strain gage coated by M-Bond 200 catalyst and wait until dry. Put one drab of M-Bond 200 adhesive Figure 3.2. (8-9).The first contact area between spacemen and strain gage. Pull the tape by angle degree and start install Teflon tape with strain gage on spacemen and wipe- out of adhesive Figure 3.2.(4-10). Hold strain gage by thumb to produce the pressure and heat from the thumb on strain gage at least one minute Figure 3.2. (5-11). Remove the Teflon tape my peeling the tape out of spacemen. Figure 3.2. (6-12).

Soldering the wire with strain gage connector:

Warm up the solder iron and clean up the head of solder iron and make sure the solder tip clean too by pass the solder iron tip on a wet sponge until get it shines.

Tin the head of solder iron, strain gage connector, and the head of wire by lead (tinning is coating a head of soldering tip by thin layer of lead). Tinning helping the heat flow from the tip of soldering to between the components you are soldering.

Heat the wire by head of the tip until reach the same the temperature and try to connect the wire on strain gage connector and feed them by lead. Remove the lead first after that the solder tip. Install small piece of masking tape on wire and end spacemen toake sure the connecting area between wire strains gages do not move to avoid strain gage damaging. Repeat this processing with all spacemen.

Tensile testing

Static tensile tests were conducted following the ASTM standard D3039 and D 3039M-08 [7] using the specimens with fiber orientation, fiber orientation, and fiber orientations, as shown in Figure 3.4.Five samples from each, and fiber orientation and different material (fiber glass and carbon fiber) of the six panels were tested to calculate young's modulus, and for fiber glass and carbon fiber.

Table 3.4 .1 The average of tensile test specimens dimensions:

	Width (b)	Length (L)	Thickness (h)	Area (A)
Carbon fiber unidirectional	0.54" (13.57mm)	10" (250mm)	0.04" (1.03mm)	0.0177" (13.91mm)
Carbon fiber unidirectional	1.08" (27.34mm)	7" (175mm)	0.09" (2.27mm)	0.095" (0.095mm)
Carbon fiber symmetric	1.03" (20.91mm)	10" (250mm)	0.079" (1.61mm)	0.0813" (33.57mm)
Fiber glass unidirectional	0.53" (13.5mm)	10" (250mm)	0.04" (0.98mm)	0.020" (13.17mm)
Fiber glass unidirectional	1.028" (26.121mm)	7" (175mm)	0.073" (1.84mm)	0.075" (48.169mm)
Fiber glass symmetric	1.015" (25.77mm)	10" (250mm)	0.076" (1.93mm)	0.077" (49.62mm)

Static tensile tests were conducted using a screw-driven mechanical test frame, Instron 5500R, as shown in Figure 3.4(1). The first step was that the specimens were installed in the grips and the strain gage wires connected to the strain gage input card of the scanner panel (Vishay, Model 5100B Scanner, System 5000) Figure 3.4.(2-4). Load and displacement were reset, and the test was started at a displacement rate of 2mm/min [0.05in/min]. After that, the test was stopped and repeated with the other specimens, as shown in Figure 3.4. (5-8).

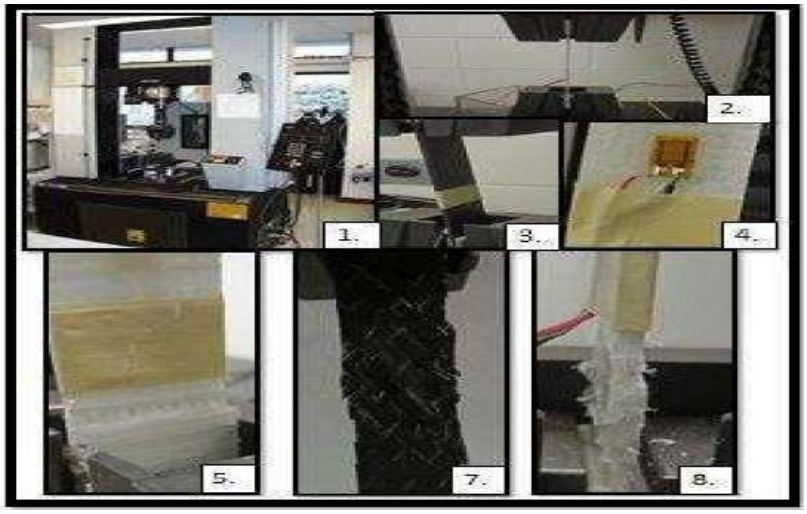

Figure 3.4.(1-8)
(1) Instron 5500R frame, (2-4) specimen was installed in upper and lower grips of Insttron machine , (5-8) specimens after tinsel tests

Calculations

Table 3.5.1 Property of fiber glass-S1-HM UD / Epon 828 epoxy composite

FG-S1-HM UD TENSILE MODULUS		
	5.431 Msi	37448.305 Mpa
Tensile strength	2207.5 lb.	9822.804 N
	1.712 Msi	11806.780 Mpa
Tensile strength	402.76 lb.	1792.178 N
	0.308 Msi	2654.051 Mpa
Tensile strength	662.86 lb.	2949.553 N
	0.175	

Property of carbon fiber T300/ Epon 828 epoxy composite

CF-T300		
	25.821 Msi	178031.971 MPa
Tensile strength	4829.967 lb.	21492.101N
	0.956 Msi	6596.138 MPa
Tensile strength	349.92 lb.	1557.053 N
	0.384 Msi	2124.237 MPa
Tensile strength	3779.12 lb.	16816.106N
	0.373	

4. PANEL FABRICATION AND TESTS OF MODE I, MODE II AND MIXED MODE I/II

Panel Fabrication:

The overall goal of this paper is to discuss the developments of hybrid DCB for mode I, hybrid ENF for mode I, and mix mode I/II. It will also address the key tasks involved in the development of all three types of composites material such as: (1) Carbon-fiber/Epoxy composite (2) Glass-fiber/Epoxy and (3) Hybrid (Carbon and Glass fibers) composites. The development of a reliable, and , analysis of hybrid DCB, hybrid ENF, and single leg bending (ASLB). The first step in this research was to match bending stiffness of fiber glass and carbon fiber for hybrid DCB, ENF, and ASLB.

Table 4.1 Matched bending stiffness of carbon fiber and fiber glass:

	Thickness m	S1-HM UD TENSILE MODULUS EI	TORAYCA T300 EI	Thickness m	
	1.00E-03	50.8	8.466	0.0001	
	2.10E-03	106.68	1.69E+01	0.0002	
	2.20E-03	111.76	25.4	0.0003	
	2.30E-03	1.17E+02	33.866	0.0004	
2 layers	2.40E-03	121.92	42.333	0.0005	
	2.50E-03	1.27E+02	50.8	0.0006	
	2.60E-03	132.08	59.266	0.0007	
	2.70E-03	137.16	67.7333	0.0008	
	2.80E-03	142.24	76.2	0.0009	
	2.90E-03	147.32	84.666	0.001	
	3.00E-03	152.4	93.133	0.0011	
	3.10E-03	157.48	101.6	0.0012	
	3.20E-03	162.56	110.066	0.0013	
	3.30E-03	167.64	118.533	0.0014	
	3.40E-03	172.72	127	0.0015	8 layers
	3.50E-03	177.8	135.466	0.0016	

They were several steps necessary to fabricate the tensile test specimens. First, the dry glass fiber plies were cut into pieces with dimensions 19" x 18" (482.6 mm x 457.2mm). The dimension for cutting the dry carbon fiber was 12" x 12" (304.8mm x 304.8mm). Second, the surface of tje table was cleaned from remaining resin or dirt and wiped using acetone. Third, sealing tape with dimensions 19.25" x 18.25" (488.95mm x 463.55mm) for fiber glass, and tape dimension 12.25" x 12.25" (311.25 mm x 311.25 mm) were used for carbon fiber were placed on the tool. Fourth, the non-porous Teflon sheet with dimensions

22" x 21" (558.8 mm x 533.4 mm) for glass fiber and 15" x 15" (381 mm x 381 mm) for carbon fiber was laid up over the sealing tape to build a dam structure to keep the resin contained. Fifth, the resin / hardener were well mixed with 10:1 (by weight) and the epoxy was poured onto the Teflon (dam structure). The epoxy was then distributed equally using a squeegee. The first piece of dry fiber was laid up on the Teflon (dam structure), then epoxy was poured on fiber and was distributed equally by a squeegee. These steps were repeated for the next layers of fibers Fiber Glass Panel The dry glass fiber panels had two distinct sides, as shown in Figures 4.1 and 4.2. The side shown in Figure 4.1 had a small amount of 90° cross weave placed to increase the handing capacity of the primarily unidirectional tows. This face was designated as the 90-face. The opposite face is shown in Figure 4.2.2. It shows the back face of the layer, with the V cross- weaves. This face was designated as the V-face. Therefore, there were three possible combinations of planes for crack growth between glass fiber layers, so the panel fabrication needed to account for this. The first type of fiber glass orientation was denoted as 90/V. Two pieces of fiber glass were laid up with 90 directions facing down Figure 4.2.1. Then, the Teflon insert (0.005") was laid up on top second layer. After that, two more layers were laid up with 90 directions facing down.

Figure 4.1 Fiber glass 90

Figure 4.2 Fiber glass V

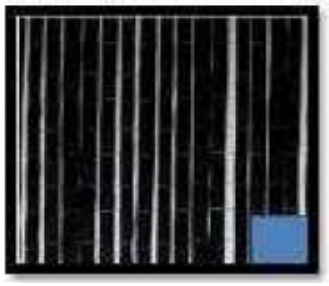

Figure 4.3 Carbon fiber T300

The second model of fiber glass orientations called for 90/90 at the center interface. Two wet pieces of fiber glass were laid up with 90 directions facing up and V directions facing down. Then, the Teflon insert 0.0005" (0.0127mm) was laid up on top second layer. After that, two more wet layers were laid up with 90 directions facing up and V direction facing down. The third model of fiber glass orientations called for V/V at the center interface. Two wet pieces of fiber glass were laid up with V directions facing up and 90 directions facing down. Then, the Teflon insert 0.0005" (0.0127mm) was laid up on top second layer. After that, two more wet layers were laid up with V directions facing up and 90 directions facing down.

Carbon Fiber Panel

The carbon fiber plies did not have any preferred „face" or side, as shown in Figure 4.3. They were laid up with ten layers, with distributed epoxy equally on each piece between layers. Then the Teflon insert was laid up on top of the ten layers of carbon fiber. After that, another ten layers of carbon fiber laid up on top Teflon insert.

Hybrid of Carbon Fiber and Fiber Glass Panel:

They are two types of fiber orientation with the hybrid specimens. The first type of hybrid is referred to as carbon fiber/90 glass fiber. First, two layers of fiber glass with the V direction facing down and 90 facing up were laid down and saturated with resin. The Teflon insert was then laid up on fiber glass 90 faces. After that, ten layers of carbon fiber were laid up.

The second model of hybrid specimens is referred to as carbon fiber/V glass fiber. Two wet layers of fiber glass the 90 directions facing down were laid up, with the V surface facing up. The Teflon insert was then laid up on fiber glass V face. After that, ten wet layers of carbon fiber were laid up.

After the wet fiber plies were laid up, they were covered by a non-porous Teflon 3 mil sheet 3, followed by the aluminum plate, Teflon sheet, breather layer, and vacuum bag. The vacuum bag was connected to a central vacuum port and the vacuum port connected to the vacuum pump. The vacuum pump was run for 24 hours. Following that, each panel was stored for ten days to get full curing. A total of twelve panels were fabricated: three of fiber glass panels, three carbon fiber, and six hybrid panels.

Sample Cutting

After ten days (for full cure) the panels were cut into specimens. The fiber glass panel Figure 4.4.4.(1) was cut into two pieces for Mode I and Mode II specimens. The Mode I piece has size 8.5" (469.9mm) x 6.25" (158.75mm), and the Mode II piece had a size of 8.5" (469.9mm) x 6.25" 8.25" (209.55mm). The panels edges were parallelized by using a roller sander, as shown in Figure 4.4.4.(5). The carbon fiber Figure 4.4.4.(2) and hybrid Figure 4.4.4.(3) panels were also cut into two pieces, as shown in Figure 4.4.4.(4). The Mode I pieces for both the carbon and hybrid were 12" (304.8mm) x 5.25" (133.35 mm)], and the Mode II pieces for both carbon and hybrid were 12" (304.8mm) x 6.72" (184.15mm)]. The specimen edges were also parallelized.

The dimensions of the Mode I fiber glass specimens were 7" (177.8mm) x 1"(25.4mm). The Mode II glass fiber specimens were 8" (203.2mm) x 1" (25.4) as shown in Figure 4.4.1. The carbon fiber and hybrid Mode I specimens dimensions were 5" (127mm) x 1"(25.4mm), and 7" (177.8mm) x 1" (25.4) for the Mode II specimens, as shown in Figure 4.4.2. The hybrid mixed-mode specimen dimensions were 8" (203.2mm) x 1"(25.4mm) as shown in Figure 4.4.3. The mode I specimen had 2.5" Teflon insert implanted in the panels, whereas the Mode II and mix-mode had a 2" Teflon insert.

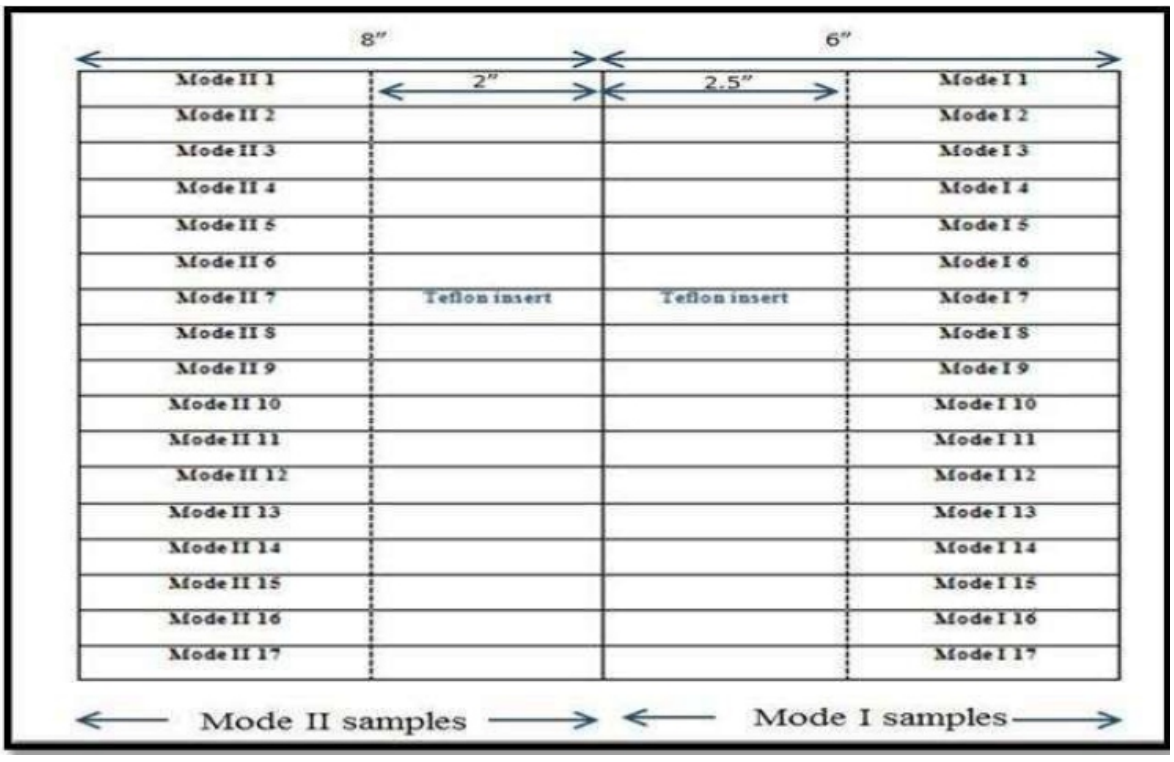

Figure 4.4.1 Fiber glass panels dimension

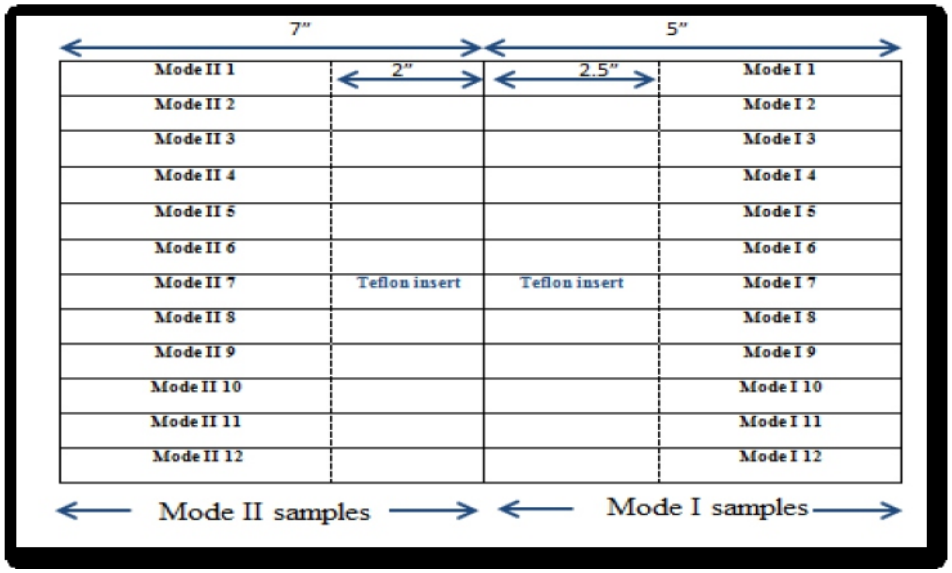

Figure 4.4.2 Carbon and hybrid fiber panels dimension.

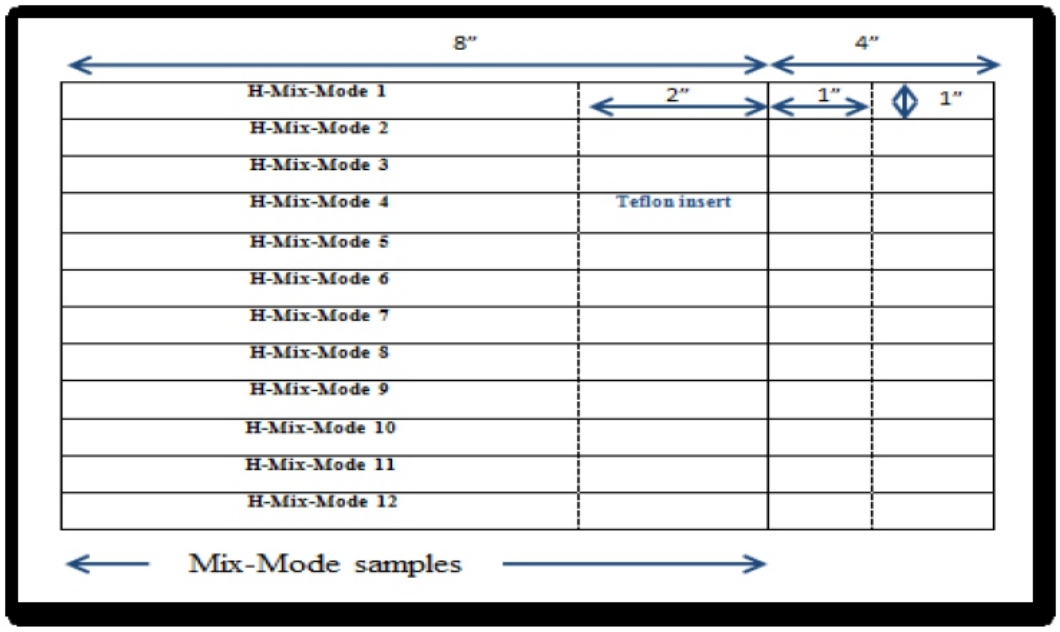

Figure 4.4.3 Hybrid mix-mode panels dimension.

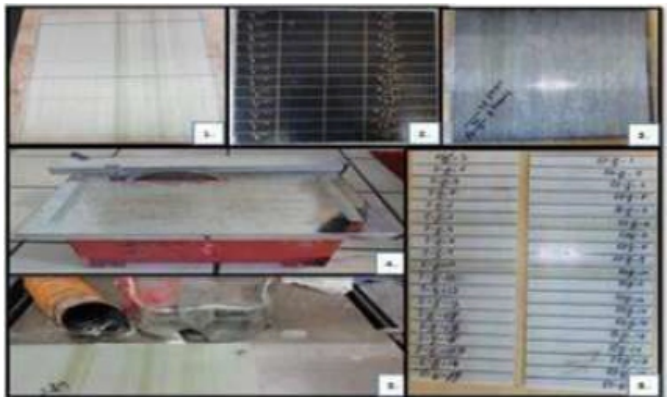

Figure 4.4.4. (1-6) 1. Fiber glass panel, 2. Carbon fiber panel, 3. Hybrid (CF/FG) panel, 4. Wet diamond saw, 5. Parallelizing the panels, 6. The panels were parallelized and ready for cutting to make specimens.

Mechanical Testing

This research was conducted under static test conditions for mode I (Double Cantilever Beam, DCB), mode II (End Notched Flexure, ENF) and mixed-mode I-II (Single Leg Bending, SLB). The goal of the project was to study the interlaminar fracture toughness of hybrid composite materials.

Sample's Preparation for Mechanical Testing

Specimens for mode I, mode II and mix-mode were prepared for mechanical testing. Mode I specimen preparation followed ASTM D5528 standard [8], each sample edge was filed with 600 grit sand paper to produce smooth edges. Next, the specimen dimensions of spacemen length, width and thickness were recorded. The bonding regions of aluminum T- tabs were filed by sand paper until shiny. T-tabs were bonded (using cyanoacrylate "super glue") on each side of the specimen at the ends containing the Teflon insert. The spray gun shown in Figure 4.5.1.1(1) was used to coat mode I specimens just ahead of insert side by using water based Polly Scale white paint, as shown in Figure 4.5.1.1(2) to visualize the crack delamination growth. Ten vertical lines were marked on each specimen at five millimeter length intervals, as shown in Figure 4.5.1.2.

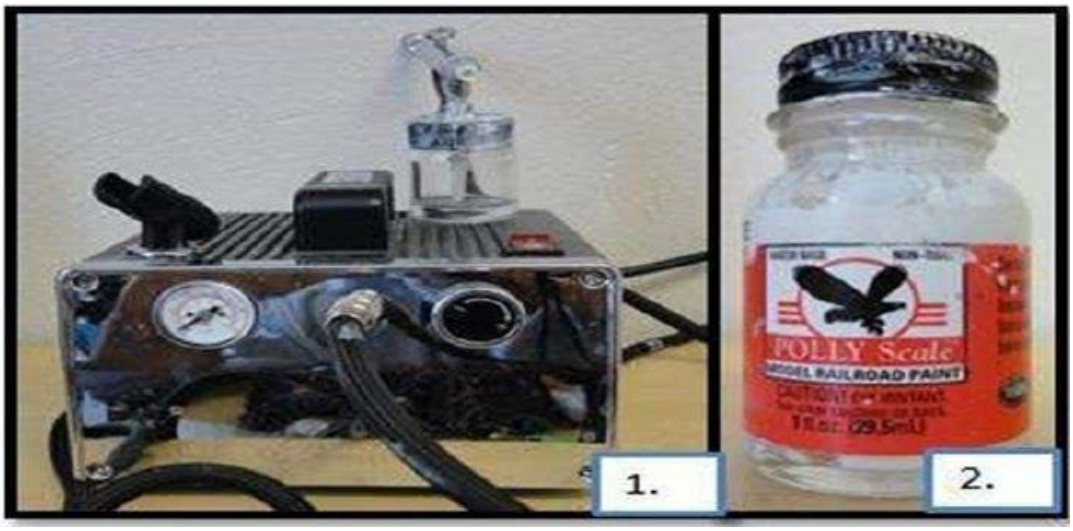

Figure 4.5.1.1 Spray paint gun and air pump, (2) Polly Scale white paint water base

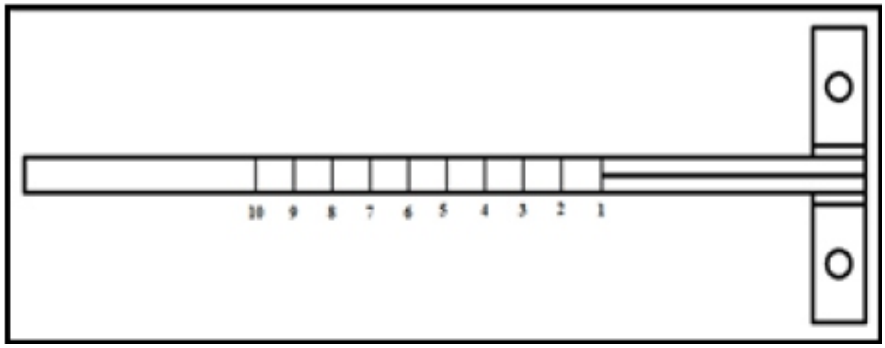

Figure 4.5.1.2 The DCB specimen marked with vertical marks every 0.2" (5mm) starting at insert.

Mode II preparation, each sample edges was filed by 600 grit sand paper to have smooth edge. Second steps get the dimension of spacemen length, width and thickness. The spray gun was used to coat mode I specimen just ahead of insert side by using (water based Polly Scale white paint).

The mode II specimens were marked with vertical two marks the first end insert the second one after the insert 1.2" (30.48mm).

Mix-mode preparation, each sample edges was filed by 600 grit sand paper to have smooth edge. Second steps get the dimension of spacemen length, width and thickness. The spray gun was used to coat mode I specimen just ahead of insert side by using (water based Polly Scale white paint).

The mix-mode specimens were marked with vertical two marks the first end insert the second one after the insert 1.2" (30.48mm) and cut one of ENF a leg 1.5" (38.1mm) length to make SLB.

DCB Mode I Fracture Static Test:

The Mode I Double Cantilever Beam (DCB) test was developed to measure the interlaminar fracture toughness under peeling stress. The mode I testing conducted in this study was using the unidirectional fiber (UD) laminates, except with the minor cross-stitch as discussed previously. The fibers directions were along the long axis of the specimens Figure 4.5.2.1.The mode I static testing was conducted following ASTM standard D5528 [8]. Five samples of each of six design were tested to calculate GIC, the mode I interlaminar fracture toughness.

Table 4.6.2 The dimensions (average) of DCB specimen:

Mode I	Width b	Length L	Thickness h	Initial delamination length ao
FG-90-V	1.034" (26.26mm)	7" (177.8mm)	0.174" (4.428mm)	2.5" (63.5mm)
F.G-90/90	1.03" (26.14mm)	7" (177.8mm)	0.181" (4.59mm)	2.5" (63.5mm)
F.G-V/V	1.02" (25.9mm)	7" (177.8mm)	0.183" (4.66mm)	2.5" (63.5mm)
CF	1.04" (26.4mm)	7" (177.8mm)	0.234" (5.9436mm)	2.5" (63.5mm)
H-CF-FG-90	1.03" (26.11mm)	5" (127mm)	0.184" (4.66mm)	2.5" (63.5mm)
H-CF-FG-V	1.03" (26.13mm)	5.5" (139.7mm)	0.19" (4.76mm)	2.5" (63.5mm)

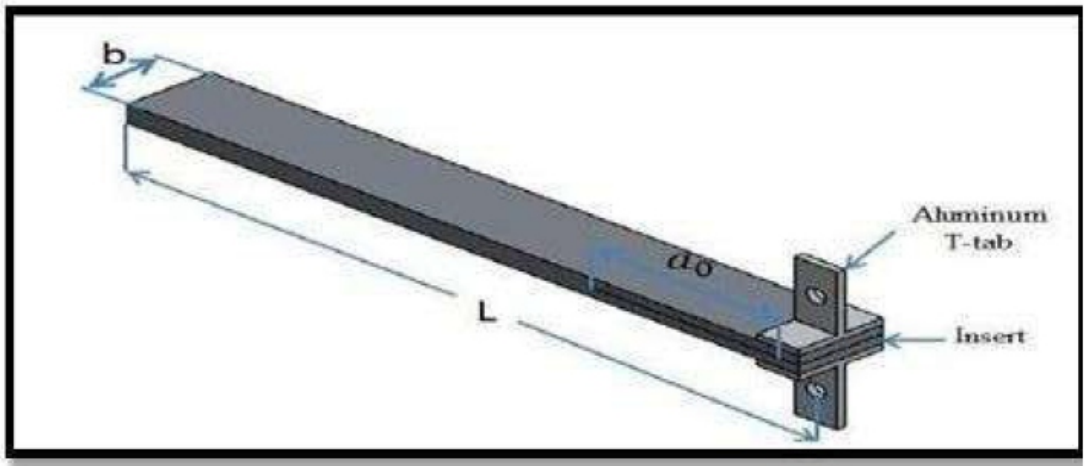

Figure 4.5.2.1. Mode I specimen with T-tab attachment

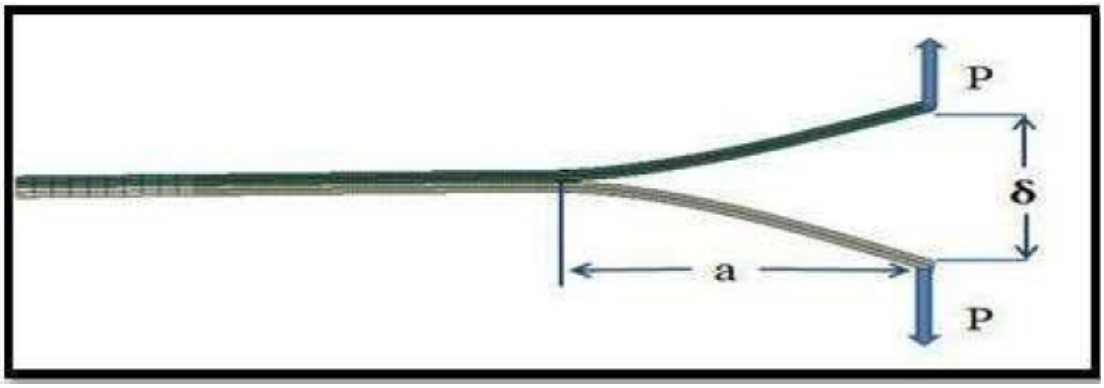

Figure 4.5.2.2 The DCB specimen is in open mode of the static test.

An Instron 5500R Model 1123 was used to provide the mechanical force for the mode I tests. It was a screw- driven mechanical test frame. It was measuring the load P, and opening distance, Figure 4.5.2.2. The max load of load cell used was 200 lb. The speed displacement rate was 0.1"/min. during the test. A magnifier and bright light source were employed to follow the crack propagation. When the crack propagated and arrived to a mark point, a custom tapping device was used to digitally mark on curve (P vs. δ) to calculate GIC.

In order to conduct the tests, first, each the mode I specimen was attached to the Instron machine by using two pins Figure 4.5.2.3.(1-2). Second, the load and displacement were reset. Note this test did not require mechanically precracking the specimen before the test, because the thin Teflon inserts 0.5 mil was used according ASTM Standard D5528 [8]. Testing was then conducted at a displacement rate 0.1"/minute while the crack propagation was monitored using magnifier and bright light source. The tapping device was taped 10 times, each time when the crack reaches a vertical line during the crack propagation.

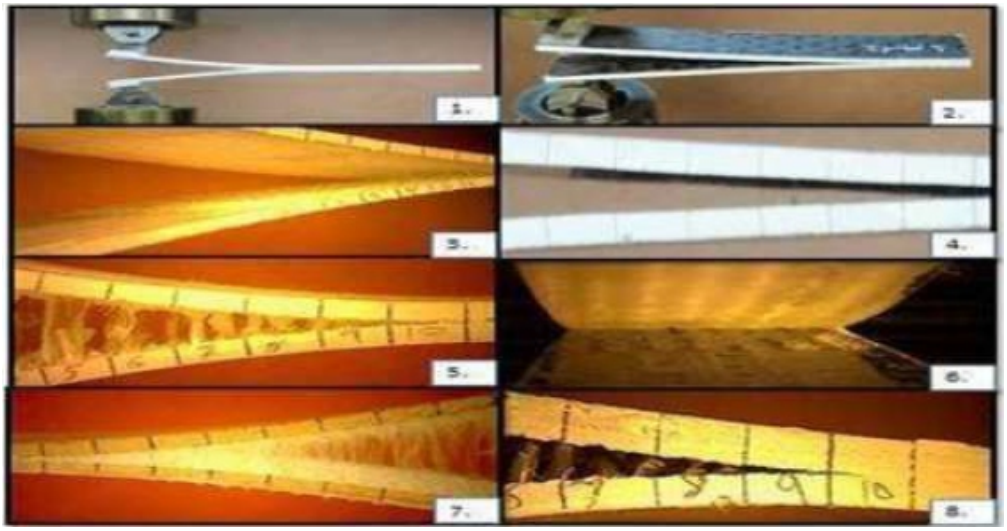

Figure 4.5.2.3
(1-2)Specimen installed in Instron machine by T taps, (2,4)The carbon fiber, (3) fiber glass V-V, (5) fiber glass 90-90, (6) H-CF/FG-V, (7) fiber glass 90-V, (8) H-CF/FG-90

The FG and CF specimens were attached to the Instron machine by pins in the T-tab as shown in Figure 4.5.2.3 (1-2). The carbon fiber fracture and fiber glass V-V did not show fiber bridging. Figure 4.5.2.3 (3-4). The fiber glass 90-V and fiber glass 90-90 did show fiber bridging. Figures Figure 4.5.2.3 (5) (7). The fracture area of the hybrid H- carbon fiber/ fiber glass V-V did not have fiber bridging, but the carbon fiber side of the specimen appeared to be covered with the fiber of the fiber glass. Figure 4.5.2.3 (6). The hybrid H-carbon fiber/ fiber glass 90 showed fiber bridging Figure 4.5.2.3 (8).

Mode II-ENF Static Test:

The Mode II End Notch Flexure (ENF) test was designed to measure the interlaminar shear fracture energy under the shearing mode. The mode II test used in this study was conducted using the unidirectional fibers (UD fibers), except for the slight cross-stitch used to hold the UD fiber tows together, as discussed previously. The fibers were aligned with the length of the specimen. The mode II static test was conducted following the ASTM draft standard by Davidson [9]. Five samples mode II of each six of designs were tested to calculate GIIC mode II interlaminar shear fracture toughness. The specimen is shown in Figure 4.6.3.1.

Table 4.6.3 The dimensions (average) of ENF specimens

Mode II	Width b	Length L	Thickness h	Initial delamination length ao
FG-90-V	1.03" (26.26mm)	8" (203.2 mm)	0.174" (4.43mm)	2" (50.8mm)
F.G-90/90	1.03" (26.14mm)	8" (203.2 mm)	0.18" (4.43mm)	2" (50.8mm)
F.G-V/V	0.97" (24.67mm)	8" (203.2 mm)	0.18" (4.60mm)	2" (50.8mm)
CF	1.04" (26.4mm)	8" (203.2 mm)	0.234" (5.94mm)	2" (50.8mm)
H-CF-FG-90	1.02" (25.87mm)	7" (177.8mm)	0.181" (4.60mm)	2" (50.8mm)
H-CF-FG-V	1.03" (26.19mm)	7" (177.8 mm)	0.189" (4.79mm)	2" (50.8mm)

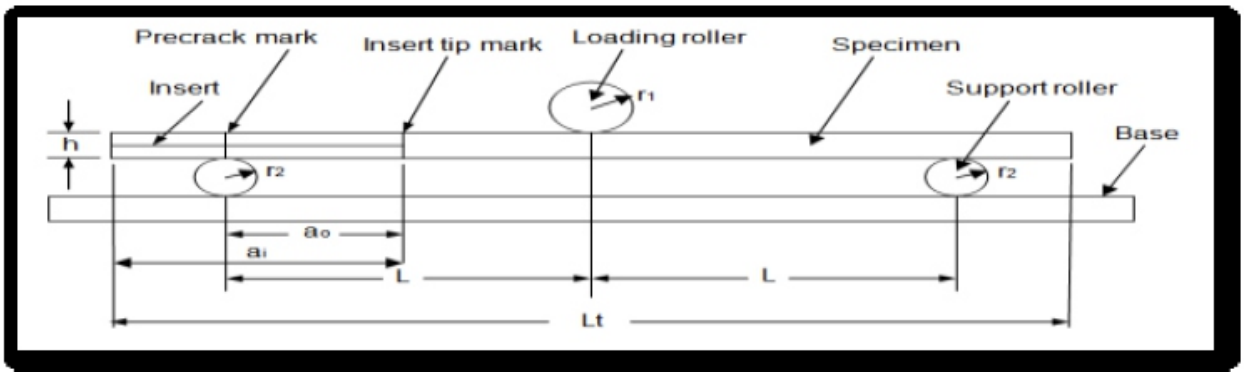

Figure 4.6.3.1 Mode II –ENF static test setup [9]

A screw-driven Instron mechanical test frame was used for the three point bending flexural test required to calculate mode II fracture energy. It measured the load and opening displacement. The maximum load

of the load cell was used was 500 lb. The displacement rate was 0.025 in/min. During the test, a magnifier and bright light source were used to follow the crack propagation.

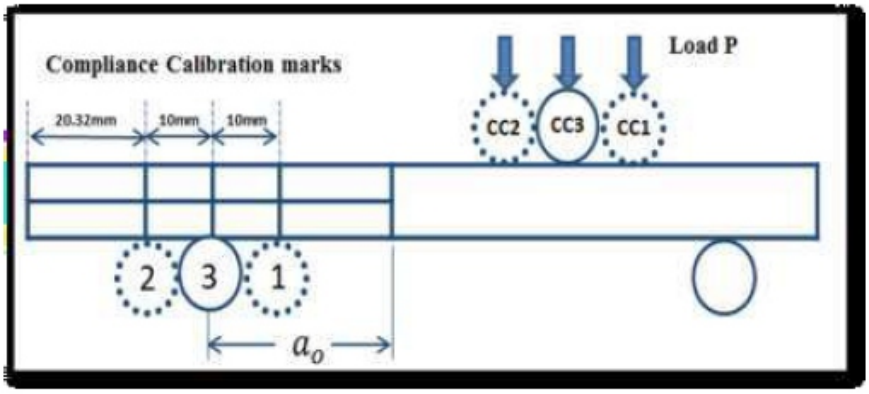

Figure 4.6.3.2 The three positions of CC and the fracture test marks.

The ENF static test was conducted using two main steps. Precracking was not necessary for the specimen since it had a 0.5 mil thickness Teflon insert. Three compliance calibration (CC) runs were made before each actual test. Each specimen was marked with four marks by a thin vertical line, as shown in Figure 4.6.3.2. The locations of the vertical lines were as follows, as shown in Figure 4.6.3.2: line labeled 1 was 1.7" (40.32 mm) from the left edge of the specimen, line labeled 2 was 0.8" (20.32 mm) from the left edge, the line labeled 3 was 1.2" (30.32 mm) from the left edge of the specimen. The fourth line (at the right edge of the dimension a0 in Figure 4.6.3.2) was at the end of the Teflon insert, which was 2" (50.8 mm) from the end of the specimen.

Compliance Calibration Processing

Each specimen was tested in three point flexure. The dimension in Figure 4.6.3.1 were L = 2 inches (50.8mm), Lt = 8inches (203.2) ai =2 inches (50.8mm) a0 =0.8 inches (20.32mm) . During the compliance calibration, each specimen was loaded to 50% of maximum load (without crack propagation), followed by complete unloading. The specimen was then shifted to the second position for CC2 and the process repeated. The specimen was then shifted to the third position for CC3, where the specimen was loaded to maximum failure load causing crack propagation. The load P and the displacement δ during CC1, CC2 and CC3 were recorded.

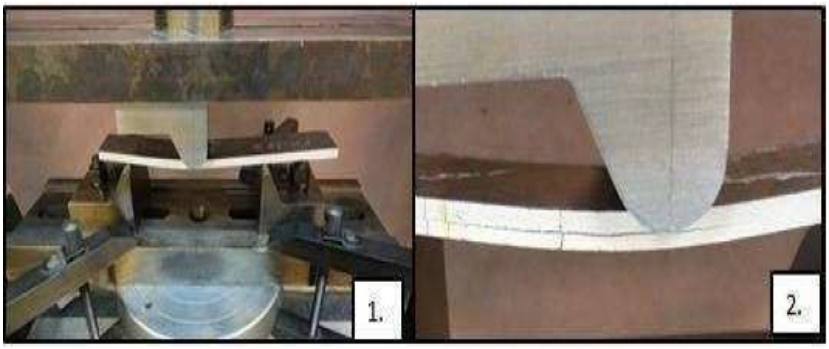

Figure 4.5.6.3.3Carbon fiber specimen for mode II set on flexure during mode II test, (2) The crack propagate until end of the load area from upper roller 0.8" (20.32mm)

The Mode II specimens testing resulted in specimens that were still fully joined, since the crack did not propagate fully along the length of the specimens, as designed. Therefore, the amount of fiber bridging could not be ascertained by looking at the specimen edges. Figure 4.5.6.3.3.

Mixed-Mode I / II

The Single Leg Bending (SLB) test was designed to test the interlaminar mix-mode I-II critical fracture energy. The mix-mode SLB tests conducted in this study were tested using the unidirectional fibers (UD fibers) specimens. The fiber directions were along the length of the specimen. The mixed-mode static test was done following the Single Leg Bending (SLB) specimen by Szekrenyes an Uj [10].

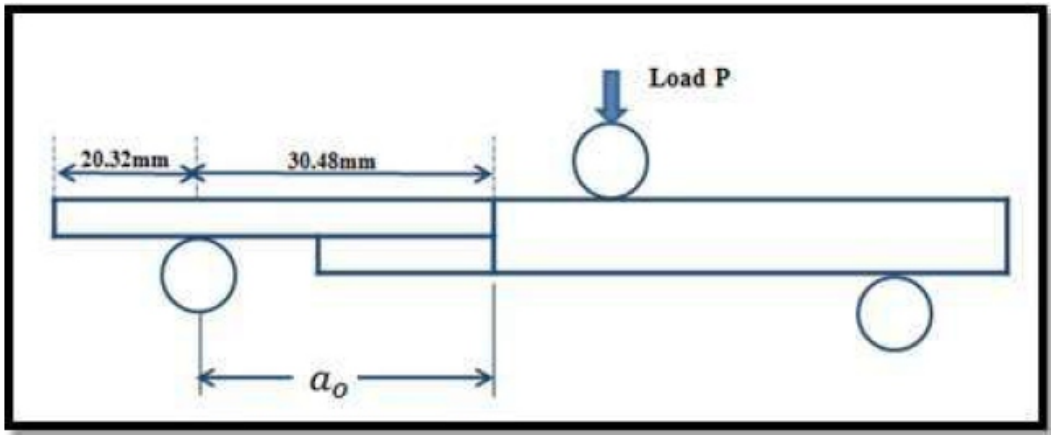

Figure 4.6.5 Single-Leg Bending (SLB) specimen on three points bending flexural for mix mode fracture test marks.

Five mixed-mode samples of each of six designs were tested to calculate GMix-C mix- mode interlaminar mix- mode (shear and open mode) fracture toughness. Figure 4.6.5. The design is similar to an ENF specimen, but with cut one leg and made shorter than the other by 1.5" (38.1mm). The Instron machine was used to conduct the three point flexural loading. It measured the load and traveling distance. The max load of load cell used was 500 lb. The displacement rate was 0.025 in/min. During the test a magnifier and bright light source were used to follow the crack propagation.

Table 4.6.5 Mix-mode specimen average dimensions

Mode II	Width b	Length L	Thickness h	Initial delamination length ao
FG-90-V	1.03" (26.22mm)	8" (203.2 mm)	0.177" (4.48mm)	2" (50.8mm)
F.G-90/90	1.032" (26.213mm)	8" (203.2 mm)	0.17" (4.424mm)	2" (50.8mm)
F.G-V/V	1.032" (26.213mm)	8" (203.2 mm)	0.176" (4.486mm)	2" (50.8mm)
CF	1.016" (25.8mm)	8" (203.2 mm)	0.218" (5.54mm)	2" (50.8mm)
H-CF-FG-90 Single-Beam-C.F	1.014" (25.745mm)	8" (177.8mm)	0.181" (4.60mm)	2" (50.8mm)
H-CF-FG-V Single-Beam-C.F	1.02" (25.898mm)	8"(177.8 mm)	0.066" (1.68mm)	2" (50.8mm)
H-CF-FG-90 Single-Beam-FG	1.0636" (27.015mm)	8"(177.8mm)	0.0876" (2.225mm)	2" (50.8mm)
H-CF-FG-V Single-Beam-FG	1.004" (25.5mm)	8"(177.8 mm)	0.088" (2.22mm)	2" (50.8mm)

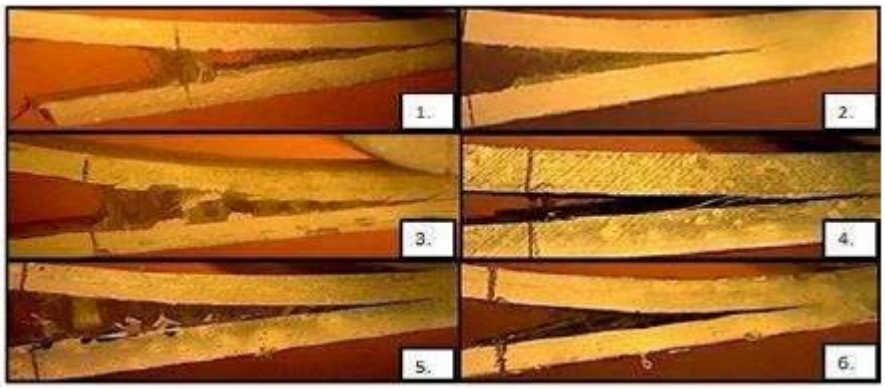

Figure 4.6.6 Mix-mode FG 90/V specimen is on three point flexural. (2)Mix-mode FG V/V specimen is on three points flexural. (3) Mix-mode FG 90/90 specimen is on three points flexural. (4) Mix-mode CF specimen is on three points flexural. (5)H- Mix- mode CF/FG90 specimen is on three points flexural. (6) H- Mix-mode CF/FGV specimen is on three points flexural.

Figure 4.6.6 (1, 3, 5) shows the edges of the specimens under load. The fiber glass 90- V, fiber glass 90-90, and H-CF/FG-90 had fiber bridging. Figure 4.6.6 (4) shows that the carbon fiber fracture moved from layer to another layer. Figure 4.6.6 (2) shows that the fiber glass V-V fracture had little fiber bridging. Figure 4.6.6 (6) hybrid H-CF/ FG V-V had fiber bridging cause by the carbon fiber layers.

5. RESULTS:

1. Mode I Fracture

The summary of the Mode I initiation results are shown in Figure 8.24. The pure carbon fiber composite showed the lowest GIc. This was followed by 90/90 glass fiber, but at approximately double the value. The next higher results in the all-glass specimens were the V/V specimens; with the highest glass (as well as the highest of all the specimens) were the V/90 specimens. The hybrid specimens, both C-90 and C-V results were similar, and in the range of the all-glass specimens. This is consistent with a visual observation of the fracture surfaces, which showed both faces containing glass. The cracks appeared to propagate in the glass layers of the hybrid specimens. The summary of the Mode I average results are shown in Figure 8.25. Again, the all- carbon specimen had the lowest value of GIc. This was followed by all-glass V-V specimen. The all-glass V/90 and 90/90 showed much higher values, which is consistent with the extensive fiber bridging observed. The 90/90 showed the most fiber bridging, which is consistent with the fact that it had the highest GIc value. The two hybrid designs had results in between the all-glass and all-carbon specimens. Additionally, the C/90 showed more fiber bridging than the C/V, and also a higher average toughness. It should be noted that all of the specimen designs containing 90 had the highest toughness values, which was consistent with the extensive fiber bridging observed in specimens with 90 interfaces.

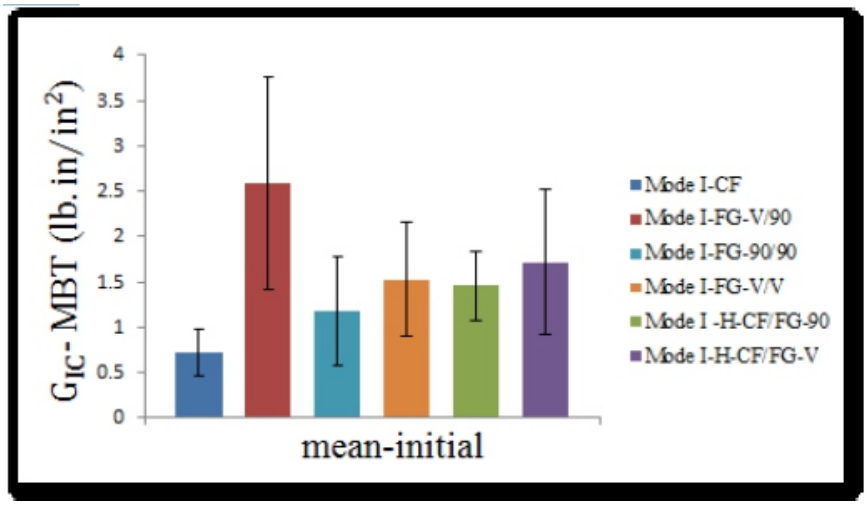

Figure 5.1 Mean initial of mode I strain energy release rate of all mode I specimens by using Modified Beam theory (MBT).

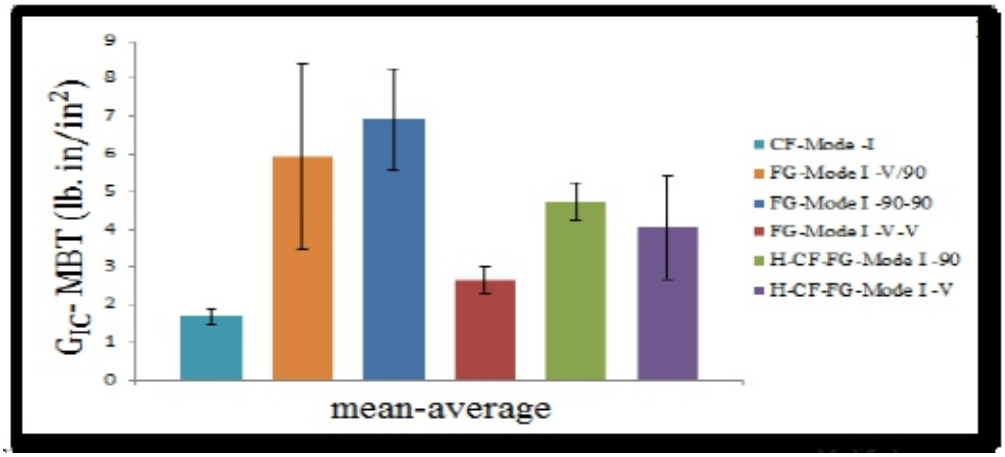

Figure 5.2 Mean average of mode I strain energy release rate of all mode I specimens by using Modified Beam theory (MBT).

2. Summary of Mode II Fracture

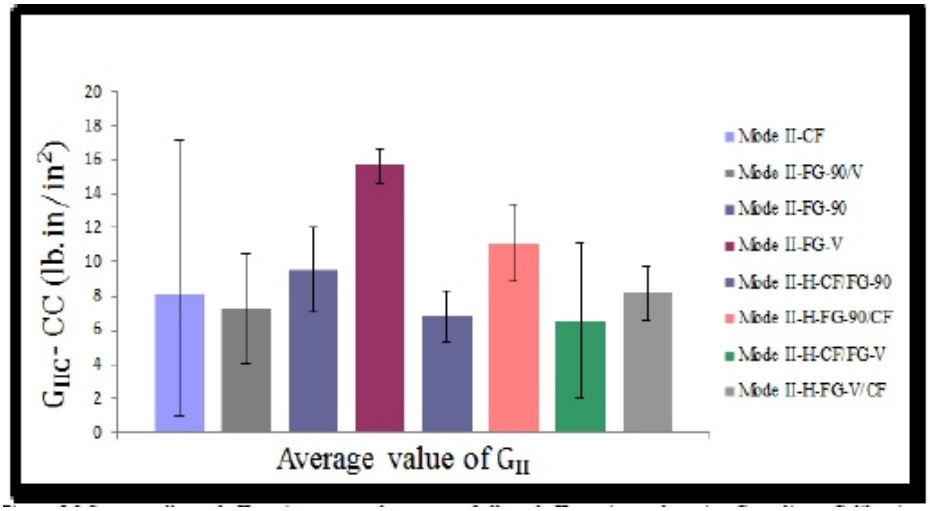

Figure 5.3 Summary‟s mode II strain energy release rate of all mode II specimens by using Compliance Calibration Method.

The summary of the Mode II results can be seen in Figure 8.3.7. The lowest values are for the hybrid specimens tested with carbon fiber as the upper layer. This is followed by the all glass 90/V fracture, then the all-carbon. These values were all similar in value, especially considering the error bands. The next all-glass is the 90/90.

The flipped hybrid specimens follow. Finally the all-glass V/V is the highest. The fiber bridging could not be observed during the test, but could be observed in the scanning electron microscope images, which will be discussed in a later section.

6. CONCLUSIONS:

The applications of hybrid composites (such as carbon and glass fiber) materials have been expanding in many fields such as aircraft, wind turbine generators, bridges and infrastructure, sporting goods such as helmets, and marine applications. A composite material may be preferred in applications because of their high strength and stiffness to weight ratio, long fatigue life, and corrosion resistance. In many applications they can be easy to fabricate and offer low cost. [48]. The use of hybrid materials offers the ability for designers to balance the high stiffness and strength of carbon fiber, with the high strength and low cost of glass fiber composites. The present study represents of delamination interface of carbon fiber, fiber glass and hybrid-(fiber glass/carbon fiber) under mode I, mode II and mix-mode I/II static.

The key mechanical test results are summarized in Figures 9.1-9.6.

1. CF and FG-V/V had lowest value of mode I, while FG-90/V and FG-90/90 had the highest values of The H-CF/FG-90 and H-CF/FG-V had values between CF and FG. The H-CF/FG-90 was slightly higher than H-CF/FG-V.
2. FG-V/V had the highest value of The lowest values were from the hybrid H-CF/V specimens.
3. The H-CF/FG-90 was better than H-CF/FG-V in mode II and mixed mode I/II.

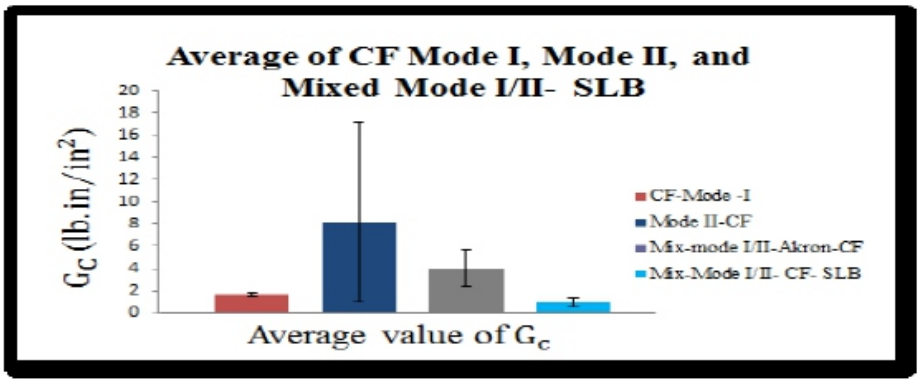

Figure 6.1 the average of CF mode I, mode II, and mixed mode I/II- SLB

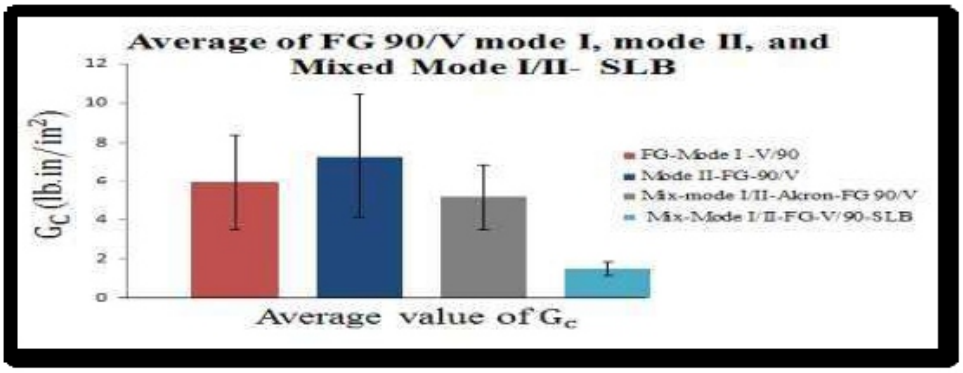

Figure 6.2 the average of FG 90/V mode I, mode II, and mixed mode I/II- SLB

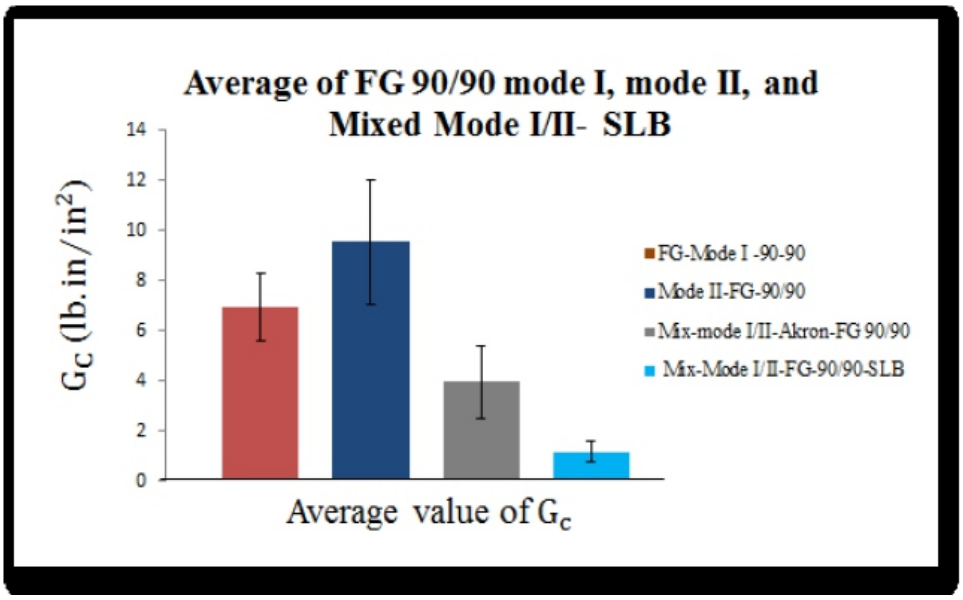

Figure 6.3 the average of FG 90/90 mode I, mode II, and mixed mode I/II- SLB

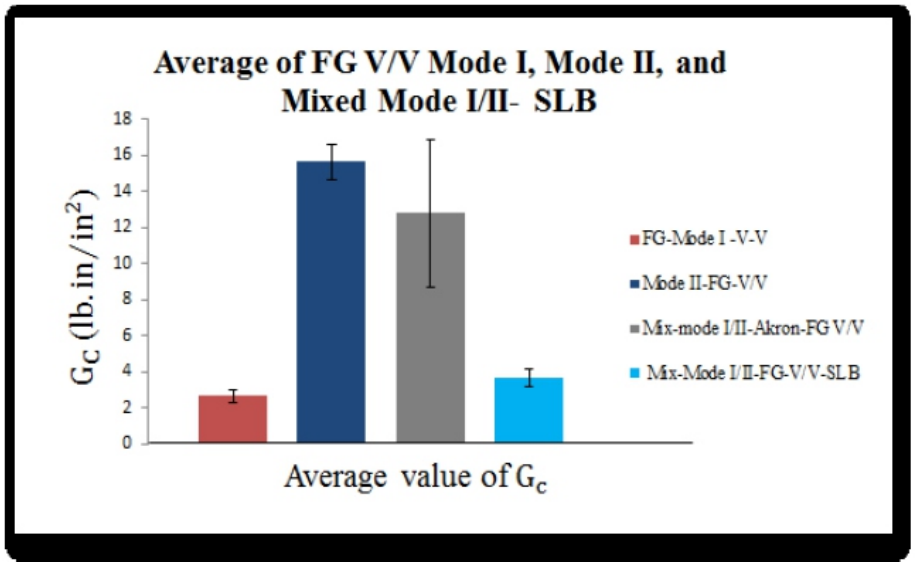

Figure 6.4 the average of FG V/V mode I, mode II, and mixed mode I/II- SLB

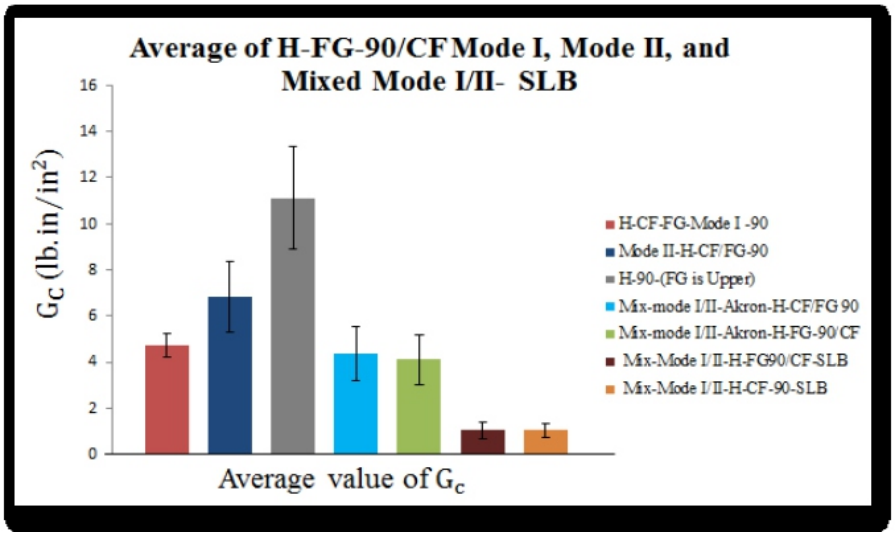

Figure 6.5 the average of H- FG-90/CF mode I, mode II, and mixed mode I/II- SLB

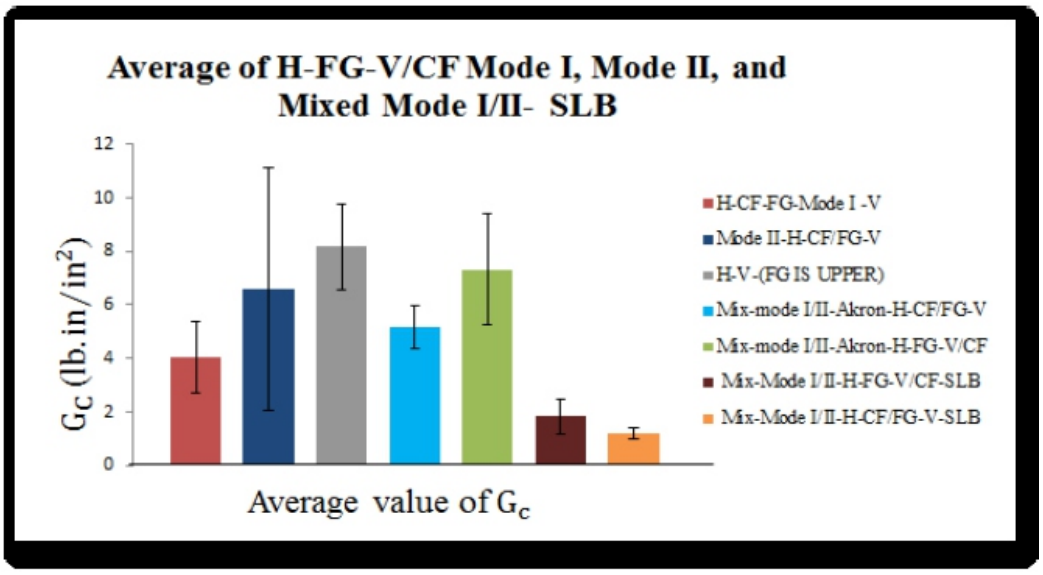

Figure 6.6 the average of H- FG-V/CF mode I, mode II, and mixed mode I/II- SLB

REFERENCES:

1. *J.M. Whitney, C.E. Browing and W. Hoogsteden "A Double Cantilever Beam Test for Characterizing Mode I Delamination of Composite Materials" Air Force Wright Aeronautical Laboratories Wright-Patterson, Air Force Base, Ohio 45433, 1982.*
2. *N. Sela,O. Ishai and L.Banks-Sills ,"The effect of adhesive thickness on interlaminar fracture toughness of interleaved CFRP specimens",1989.*
3. *A.J. Brunner, B.R.K. Blackman, P. Davies "A status report on delamination resistance testing of polymer–matrix composites" Science Direct, Engineering Fracture Mechanics, 2007.*
4. *P.N.B. Reis1a, J.A.M. Ferreira, F.V. Antunes, J.D.M. Costa, C. Capela "Analysis of the initial delamination size on the mode I interlaminar fracture of carbon/epoxy composites".*
5. *Mehdi Barikani, Hossein Saidpour, and Mutlu Sezen. "Mode-I Interlaminar Fracture Toughness in Unidirectional Carbon-fibre/Epoxy Composites".2002.*
6. *Mohammadreza, Khoshravan, Farhad Asgari Mehrabadi. "Fracture analysis in adhesive composite material/aluminum joints under mode-I loading; experimental and numerical approaches", International Journal of Adhesion & Adhesives, SciVerse Science Direct,2012*
7. *Moslem Shahverdi, Anastasios P. Vassilopoulos, Thomas Keller "A phenomenological analysis of Mode I fracture of adhesively-bonded pultruded GFRP joints",2011*
8. *Shun-Fa Hwang, Bon-Cherng Shen. "Opening-mode interlaminar fracture toughness of interply hybrid composite materials".1999.*
9. *Masahiro Arai, Yukihiro Noro, Koh-ichi Sugimoto, Morinobu Endo "Mode I and mode II interlaminar fracture toughness of CFRP laminates toughened by carbon nanofiber interlayer".Science Direct.Composites Science and Technology.2007.*
10. *L.F.M. da Silva, V.H.C. Esteves, F.J.P. Chaves "Fracture toughness of a structural adhesive under mixed mode loadings" Mat.-wiss. u.Werkstofftech. 2011, 42,*
11. *"Fracture Toughness Testing: Part One" http://www.keytometals.com/page.aspx?ID=CheckArticle&site=kts&NM=291*
12. *Andras Szekre, Jozsef Uj" Comparison of some improved solutions for mixed- mode composite delamination coupons,2005*
13. *Book of Mechanics of Materials fifth edition by Ferdinand P.Beer, E.Russell Johnston , Jon T. DeWolf, David F. Mazurek*
14. *Book of engineering mechanics of composite materials second edition by Isaac M. Daniel Ori Ishai*
15. *ASTM 2734 Method (Epoxy Burn Off)*
16. *"Wind Energy Composite Materials Handbook from Gurit", accessed 1/18/2013, 2013, http://www.gurit.com/wind-energy-hand-book.aspx.*
17. *"Design News - Features - Sandia Sizes up Wind Turbine Blade Design ", accessed 1/18/2013,*

18. *http://www.designnews.com/document.asp?doc_id=230008&dfpPParams=ind_1 82,aid_230008&dfpLayout=article.*
19. *Mansour H. Mohamed, Kyle K. Wetzel, "3D Woven Carbon/Glass Hybrid Spar Cap for Wind Turbine Rotor Blade", Journal of Solar Energy Engineering NOVEMBER 2006, Vol. 128*
20. *W.C. de Goeij, M.J.L. van Tooren, A. Beukers "Implementation of bending- torsion coupling in the design of a wind-turbine rotor-blade", Applied Energy 63 (1999) 191-207*
21. *Dayton A. Griffin, Global Energy Concepts, LLC , 5729 Lakeview Drive NE, #100 ,Kirkland, Washington 98109 "Blade System Design Studies Volume I: Composite Technologies for Large Wind Turbine Blades"*
22. *John F. Mandell,Douglas S. Cairns,Daniel D. Samborsky, Robert B. Morehead and Darrin H. Haugen "Prediction of Delamination in Wind Turbine Blade Structural Details", ASME 2003 Wind Energy Symposium*
23. *Paul S. Veers,Thomas D. Ashwill, Herbert J. Sutherland, Daniel L. Laird and Donald W. Lobitz, John F. Mandell, Walter D. Musial, Kevin Jackson, Michael Zuteck, Antonio Miravete, Stephen W. Tsai, James L. Richmond, "Trends in the Design, Manufacture and Evaluation of Wind Turbine Blades", Wind Energ. 2003; 6:245–259 (DOI: 10.1002/we.90)*
24. *Cheng Ong,Design, manufacture and testing of a bend-twist D-spar", 1999 http://arc.aiaa.org/doi/abs/10.2514/6.1999-25*

Statistical Analysis of Malware in Anroid with the Techniques of Machine Learning

Hemant Kumar, Akshay Chamoli, Subodh Kuma
Jamia Hamdard , hemant.sscbs@gmail.com
Jamia Hamdard , akachamoli@gmail.com
Jamia Millia Islamia , subodhkumar588@gmail.com

ABSTRACT

The use of smartphones continues to sour, with Android leading the way. Google claims to have around 1.4 billion active mobile devices across the globe. According to The Telecom Regulatory Authority of India, India has become the second country globally with a user threshold of 1.03 billion users. The massive user base has caught the eyes of cybercriminals trying to attack Android using malware. Malware is malicious software created to destroy computer or electronic systems without the knowledge of the user using the system. This work aim has created an efficient malware detection system with machine learning-enabled features for Android Environment so that they can sense malware applications with the help of static features. The system extracts various permissions and API Tags from the Android applications. It uses these features along with five unique machine learning techniques for classifying whether the application is malicious or benign. The experimental results are promising as we have achieved high accuracy in detecting Android malware with all the classifiers. We have also analyzed the effect of a number of Android applications used in the database on the accuracy of classifiers .

1. INTRODUCTION

Android applications are generally used in cell phones as a mobile software application and are created by Google to run on Android platforms like smartphones, tablets, Google TV, and other devices compatible with running Android featured operating system. Android applications utilize advanced hardware and software to bring benefits and values to their users. According to statista.com, the number of accessible applications in the Google Play Store outperformed 1 million applications in July 2013 and was most recently positioned at 2 million applications in February 2016 [1]. Google says there are 1.4 billion active mobile devices [2] worldwide. According to The Telecom Regulatory Authority of India, India has become the second country globally with a user threshold of 1.03 billion users [3]. The Android platform's openness makes it attractive to users, but the freedom or openness users appreciate is also a pitfall of the forum. Cybercriminals nowadays are finding more complex ways to get into android systems and breach the security of the system. Cybercriminals exploit it by posting malware spreading apps in deceitful attempts to steal personal information. In this case user's mobile security is compromised. So the users who download malicious apps unknowingly face a mobile privacy threats. The research carried out by Pulse secure, found that 97% of malware focusses the Android operating system [4].

Malware is malicious software and is developed for damaging the computer system irrespective of the knowledge of the user [5]. Trojan horse, worm, virus, spyware are all classified as malware. It is necessary to analyze malicious apps to understand the risk associated and their intentions. There are various types of analysis, including Static Analysis and Dynamic analysis as the broad domain. Examining malicious software without performing the process is called static analysis whereas, exploration of the infected file during its completion is known as dynamic analysis [5, 6]. It is also called behavioral analysis. In this project, we have used static analysis of malicious apps. The disassembly

method is one of the old procedures of static analysis. Machine learning classifiers are used for classifying malicious applications having permissions, API Tags, and a combination of both [7, 8, 9, 10, 11].

Our contribution in the paper are as follows:

1. Extraction of Android App static features by using Androguard.
2. Classification of Android applications as malicious or benign by using five machine learning classifiers: Naïve Bayes, KNN, Logistic Regression, C4.5, and SVM.
3. Analyze the effect of three sets of static features (permissions only, API Tags only, and permissions and API tags) on the performance of the classifiers.
4. Analyze the effect of the number of Android applications on the performance of classifiers.
5. Based on our database we have also compared the top ten Android app permissions and API tags of both benign and malicious apps and then concluded the dangerous permissions and API Tags.

2. Related Work

In the domain of static analysis for malware detection in Android applications, several studies have already been processed. Sanz et al. [12] introduced PUMA (Permission Usage to detect Malware in Android), a process for sensing malevolent applications using the consent usage of each application. They used machine learning models to perceive whether an application is malicious or not. A dataset of 357 benign and 249 malicious applications was used in the technique, and Android Asset Packaging Tool (AAPT) was used to get permissions from the APK file. Justin Sahs et al. [13] used a machine learning process to detect Android malware. The technique used Androguard (an open-source project) to get features from APKs and then used these features to train a One-Class SVM. The system was limited to just permissions (built-in and non-standard) and CFGs of the input applications. One more approach towards Permission-Based Malware Detection which is proposed by Aung et al. [14] have used K-means clustering, Random Forest DT (decision tree) and CART (Classification and Regression Tree) algorithm. The accuracy rate improved to 91.75% with Random Forest DT and the most efficient orignal positive rate of 97.8% with CART.

Aafer et al. [15] presented DroidAPIMiner: generic data mining technique to develop a classifier for applications having inbuilt android feature. Their procedure had compared performance of four classifiers: ID5, C4.5, KNN and SVM in terms of both the process of various feature extraction i.e. approval based and API calls based feature set with package level and parameter information. The data set taken for this paper consists of 3987 malware samples from Android Malware Genome Project and 500 benign applications from each category in Google Play [16]. They reported KNN with an efficient performance model and has given the accuracy of 99.9%. The false positive rate is very low as 2.2% when around 189 features are taken from a feature set. Akanksha Sharma et al. [17] gave a proactive technique for static malware detection. The features which were removed based on API calls as well as permissions. Correlation based as well as information gain feature selection process and used to select most efficient features. The dataset created from the selected feature set was validated using Naive Bayesian and K-Nearest Neighbor classifiers. They used APKAnalyser for reverse engineering.

3. Proposed Methodology and Implementation

The suggested procedure consists of these four steps. They are:

STEP 1: Creation of an efficient database having a variety of Android malware belonging to different malware families and benign apps from various categories of applications such as communication, education, health etc. We have created 4 sets of databases having a different number of Android apps.

STEP 2: Extracting features such as Android permissions and API tags and creating three sets of features- permissions only, API tags only, and permissions and API tags.

STEP 3: Preprocessing the three sets of features by using the filter to remove unnecessary features.

STEP 4: Building the models of a Machine learning classifier using the 3 sets of features and also by using 4 different databases of apps and subsequently analyzing the performance of various classifiers based on the feature set and database set.

I. Creation of Database

Here we label the procedure we monitored to get data from the android application file. The basic steps we have followed for each application are:

1. First, we downloaded the android apps of different malware families from AndroMalShare [18] and goodwares from Google Play Store [16] as shown below.

Malware Families	Count	Goodware Families	Count
DroidkungFu	10	Arcade	5
FakeInst	10	Tools	22
Opfake	10	Business	8
Geinimi	10	Communication	10
FakeLogo	10	Education	11
Kmin	10	Entertainment	9
Adrd	10	Lifestyle	10
YZHCSMS	10	Music & Audio	8
PJApps	10	Photography	7
Legacy	10	Puzzle	7
		Shopping	9

2. We decompressed the android apps using Androguard [19] and extracted the selected features like Permissions requested and API Tags for each android app by using our python scripts.
3. We build a dataset in a CSV file format with the extracted data.

In step 2, we processed the AndroidManifest.xml file to extract the data.

Using our python scripts we extracted the permissions and created the feature vectors in the following way.

For each Android app, we retrieved the selected features "permissions requested" and "API Tags".

The selected features with their values are kept as a binary number (0 or 1) and is signified as a sequence of comma separated values which is also called as CSV format.

0,0,0,0,0,0,0,0,0,0,0,0,0,0,0,0,0,0,0,0,0,0,0,0,0,0,0,0,0,0,0,0,0,0,0,0,0,0,0,0,0,0,0,0,0,0,0,0,0,0,0,0,0,0
,0,0,0,0,0,0,0,0,0,0,0,0,0,1,0,0,0,0,0,0,0,0,0,0,0,0,0,0,0,0,0,0,0,0,0,0,1,1,0,0,0,0,0,1,0,0,0,0,0,0,0,0,0,1,0,0,
0,0,0,0,0,0,0,0,0,0,0,0,0,0,0,0,0,1,0,0,0,0,1,0,0,0,0,0, MALICIOUS

Figure 1: Feature Vector created using extracted android permissions

0,0,0,0,1,0,0,0,0,0,0,0,0,0,0,0,0,0,0,0,0,0,0,0,0,0,0,0,0,0,0,0,0,0,0,0,0,0,0,0,0,0,0,0,0,0,0,0,0,0,0,0,0,0
,0,0,0,0,0,0,0,0,0,0,0,0,0,1,0,0,0,0,0,0,0,0,0,0,0,0,0,0,0,0,0,0,0,0,0,0,0,0,0,0,0,0,0,0,0,0,0,0,0,0,0,0,0,
0,0,0,0,0,0,0,0,0,0,0,0,0,0,0,0,0,0,0,0,0,0,1,0,0,0,0,0,BENIGN

Figure 2: Feature Vector created using extracted API Tags

Features

Features used in the dataset are the Permissions requested, API Tags (Tags defined in Androguard[19] corresponding to APIs used in the app), and Permissions requested and API Tags used by the Android Applications[20].

Few samples of permission features are:

• **android.permission.READ_PHONE_STATE:** Permits access in read only mode. This is crucial agreement in order harm an android application

• **android.permission.INTERNET:** Permits the applications for opening network sockets for the usage of internet. If any application doesn't require the internet and still it request the INTERNET access then it can be used for malicious purpose

• **android.permission.CALL_PHONE:**
Permits the application to initiate a phone call without accessing the Dialler user interface for the user to approve the call. Malevolent use of this permission can incur charges to the user.

• **android.permission.ACCESS_COARSE_LOCATION:**
Permits an app to access approximate location. Attackers can use this permission maliciously to track the location of the user.

• **android.permission.ACCESS_WIFI_STATE:** Permits applications to access information about Wi-Fi networks. By making use of android permissions. INTERNET along with this permission access, attackers gain access to sensitive information.

Few Samples of API Tags are:

• **Android:** It consists of resource classes and is used by the applications which are included in the platform and is used to define application approvals for system features.

• **Bluetooth:** Offers classes that manages Bluetooth functionality, which includes various features such as device scanning, connection establishment among devices for communication and management of data transfer among devices.

• **Location:** Consists of the framework API classes that defines services enabling location based features.

• **Reflection:** brings reflective access to description info.

• **Widget:** Consists of the components essential to create "app widgets", which users use to integrate with other applications (such as the home screen) to speedily access application data and services without starting of a new activity.

II. Preprocessing the Database

In Machine Learning applications, an enormous number of extricated highlights, some of which excess or immaterial, present a few issues, for example, deceiving the learning calculation, over-fitting, lessening over-simplification, and expanding model intricacy and run-time [21,22]. These antagonistic impacts are significantly more critical when applying Machine Learning strategies on cell phones since they are regularly limited by preparing and capacity abilities, just as battery power. Therefore Applying the Remove Useless in weka [13], filtered out the dataset in a preparatory stage and enabled the malware detector to work more proficiently, with a quicker detection period. Yet, decreasing features should only be performed when a high level of accuracy can be preserved.

We have preprocessed the database using "Remove Useless". It is an unsupervised attribute filter used to remove attributes that do not vary at all or that vary too much

III. Building the model using classifiers and detecting the malware

Our job is to develop a model that can classify an app as either malicious or benign. To do that, we have used five different machine learning algorithms for classification Naïve Bayes Classifier, KNN, Logistic Regression, C4.5, and Support Vector Machine. These five different classifiers belong to other classifiers' families, KNN belongs to the lazy classifier, Naïve Bayes. Logistic Regression belongs to the family of Probabilistic classifier, C4.5 belongs to the Decision tree, and The ML technique capable of dividing the training data set by optimal separation is done with the Support Vector Machine technique [24, 25].

We examined two experiments.

First Experiment: In the first experiment, we have extracted around 135 permissions, 41 API tags from 200 apps. We created four databases having 50 instances, 100 instances, 150 instances and 200 instances of permissions, API Tags, and permissions plus API Tags mixed respectively. So basically this experiment consists of three parts that are:

1. Permission Based Analysis
2. API Tags Based Analysis
3. Permissions plus API Tags based Analysis

•All these three parts consist of these two steps.

STEP-1- Preprocess each database using "Remove Useless" filter in Weka [13].

STEP-2-Classifiy each database using five different machine learning algorithms in Weka [13].

1. Naïve Bayes 2. KNN 3. Logistic Regression 4. C4.5 5. SVM
To test our created grouping models, we have utilized cross approval technique with 10 folds, i.e., our dataset is part multiple times into 10 unique sets for learning (90% of the absolute dataset) and testing (10% of the complete information). Note the Accuracy, True Positive Rate, and False Positive Rate of every classifier.

Compare the ACCURACY and TIME EFFICIENCY of each classifier.

Second Experiment: In this experiment, we have extracted top ten permissions and API Tags from the dataset of both benign and malicious apps. We have then compared the top ten permissions and API Tags from both benign and malicious apps and have concluded dangerous permissions and API Tags.

4. RESULT AND ANALYSIS

Results of both the experiments are given below:

1st Experiment Results:
We generate the classification model using five different classifiers described earlier for permissions, API Tags, and permissions plus API Tags as features and run them for four different datasets, a dataset of 50 instances,100 instances, 150 instances and 200 instances respectively. We have used Weka [13] for classification.

Table 1: The result of each classifier on permissions based dataset

Classifier	Dataset of 50 instances		Dataset of 100 instances		Dataset of 150 instances		Dataset of 200 instances	
	Acc.	TPR	Acc.	TPR	Acc.	TPR	Acc.	TPR
Naïve Bayes	90%	0.840	95%	0.900	90.66 %	0.933	92%	0.960
KNN(k=5)	86%	0.760	90%	0.820	89.33 %	0.827	95%	0.950
Logistic Regression	90%	0.880	93%	0.960	95.33 %	0.960	96.5 %	0.960
C4.5	90%	0.880	95%	0.980	93.33 %	0.933	96%	0.970
SVM	90%	0.880	97%	0.960	98%	0.973	98%	0.980

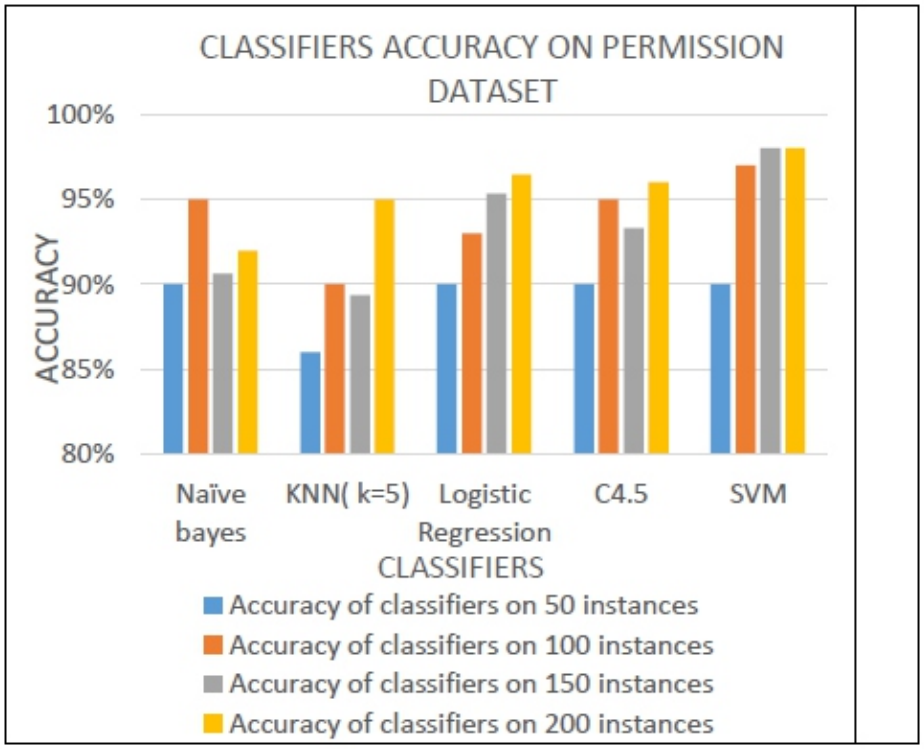

Figure 3: Bar Graph showing classifier wise accuracy for permission based analysis

In permission based analysis we found that the accuracy of SVM is the highest i.e., 98% in the dataset of 200 and 150 instances while KNN holds the lowest accuracy i.e. 86 % in case of 50 instances. Also, we found that in most of the cases, as we increase the number of instances the accuracy of classifier increases with the slight exception in case of Naïve Bayes

Table 2: The result of each classifier on API Tags based dataset

Classifier	Dataset of 50 instances		Dataset of 100 instances		Dataset of 150 instances		Dataset of 200 instances	
	Acc.	TPR	Acc.	TPR	Acc.	TPR	Acc.	TPR
Naïve Bayes	86%	0.960	93%	0.960	89.33 %	0.933	91%	0.940
KNN(k=5)	86%	1.000	90%	1.000	91.33 %	1.000	93.5 %	1.000
Logistic Regression	82%	0.800	87%	0.880	89.33 %	0.907	92.5 %	0.930
C4.5	84%	0.920	91%	0.980	93.33 %	1.000	93%	0.970
SVM	86%	0.880	92%	0.980	94%	0.973	95.5 %	0.980

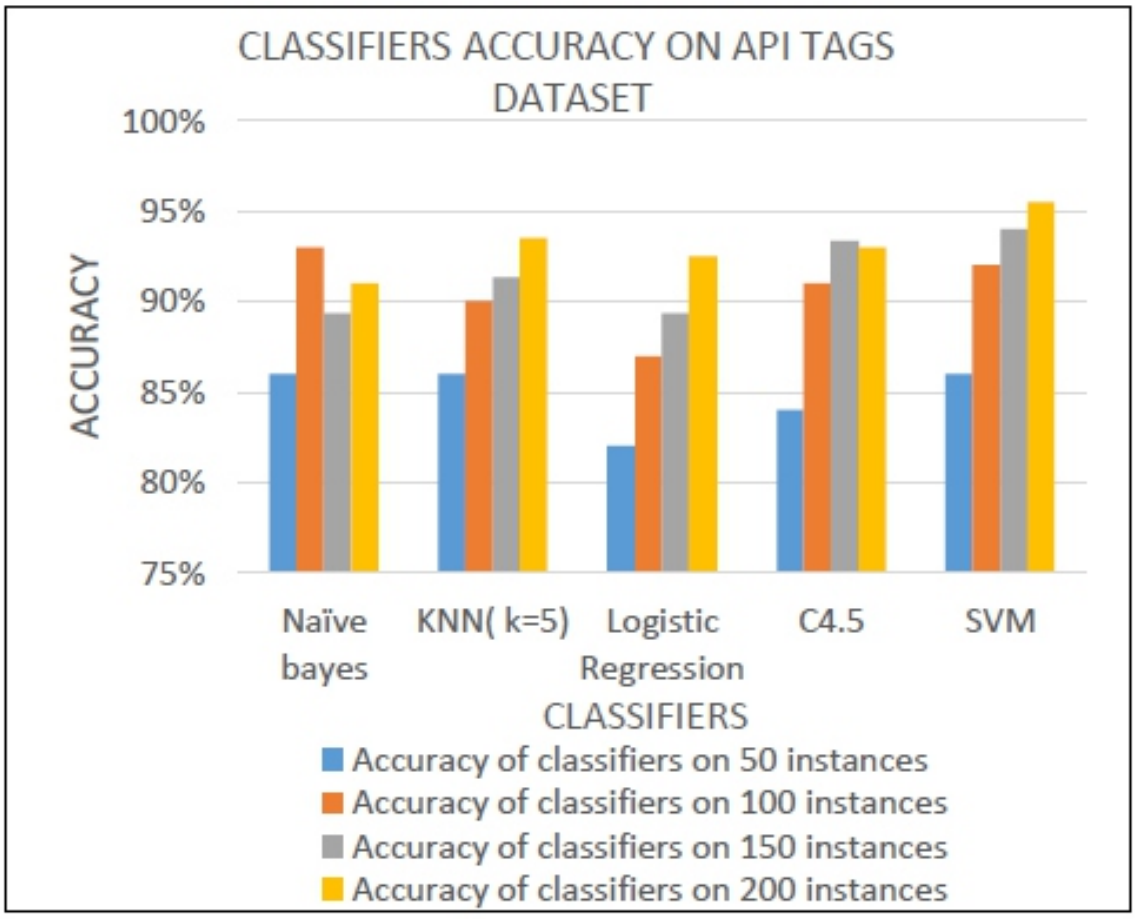

Figure 4: Bar Graph showing classifier wise accuracy for API Tags based analysis

In API Tags based analysis we found that the accuracy of SVM is highest i.e., 95.5% after that Logistic regression and C4.5 give better result in terms of accuracy while KNN holds the lowest accuracy i.e. 86 % in case of 50 instances. Also, we found that in most of the cases ,as we increase the number of instances the accuracy of classifier increases with the slight exception in case of naïve Bayes where the accuracy attain a peak at dataset of 100 instances

Table 3: The result of each classifier on Permission plus API Tags based dataset

Classifier	Dataset of 50 instances		Dataset of 100 instances		Dataset of 150 instances		Dataset of 200 instances	
	Acc.	TPR	Acc.	TPR	Acc.	TPR	Acc.	TPR
Naïve Bayes	96%	0.960	96%	1.000	94.66 %	0.987	96%	0.990
KNN(k=5)	94%	0.960	96%	0.960	96%	0.960	97.5 %	0.980
Logistic Regression	96%	0.960	98%	1.000	96.66 %	0.960	98%	0.980
C4.5	88%	0.920	96%	0.980	95.33 %	0.947	98%	0.990
SVM	96%	1.000	96%	0.940	97.33 %	0.960	98.5 %	0.980

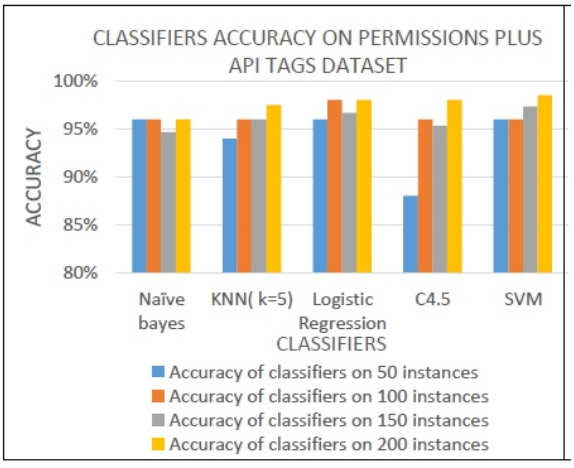

Figure 5: Bar Graph showing classifier wise accuracy for permission plus API Tags based analysis

In permissions plus API Tags based analysis we found that SVM turns out to be the best classifier as the accuracy of SVM is highest i.e. 98.5. Also, we found that in most of the cases as we increase the number of instances the accuracy of the classifier also increases.

2nd Experiment result:

We found the top ten permissions from each of the database of 100 malicious apps and 100 benign apps collected separately.

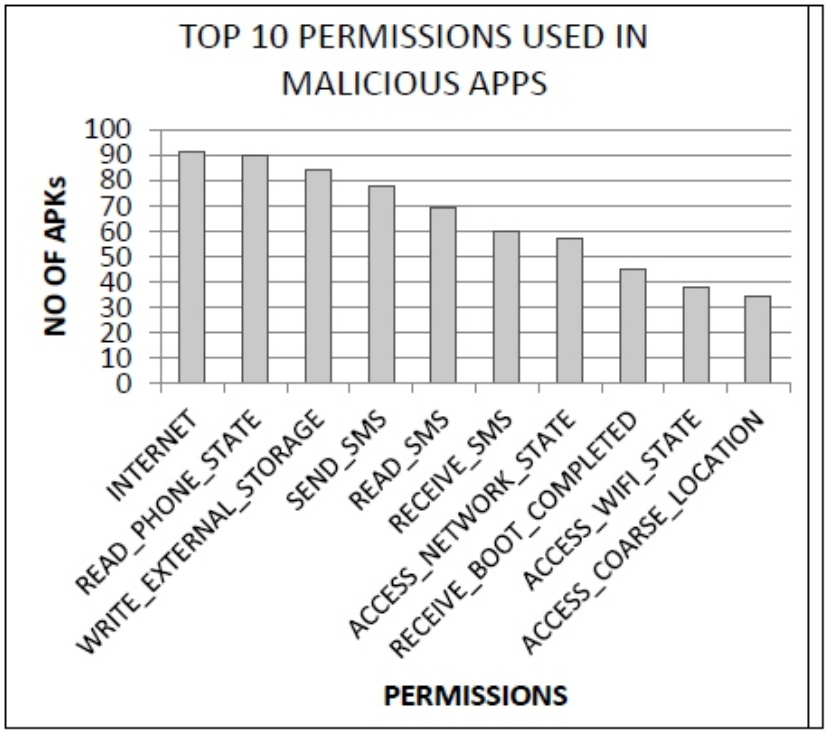

Figure 6: Bar graph showing top 10 permissions used in malicious apps

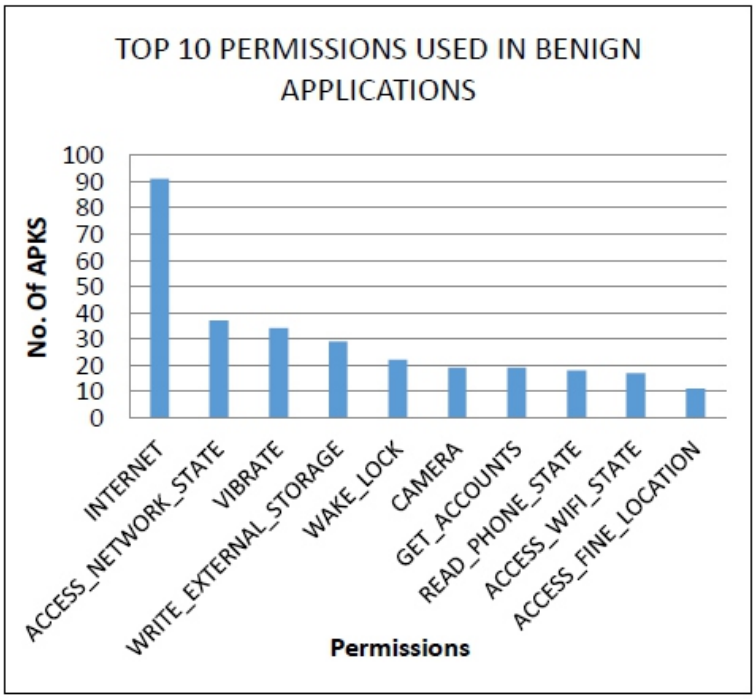

Figure 7: Bar graph showing top 10 permissions used in benign apps

We also found the top ten API Tags from each of the database of 100 malicious apps and 100 benign apps collected separately.

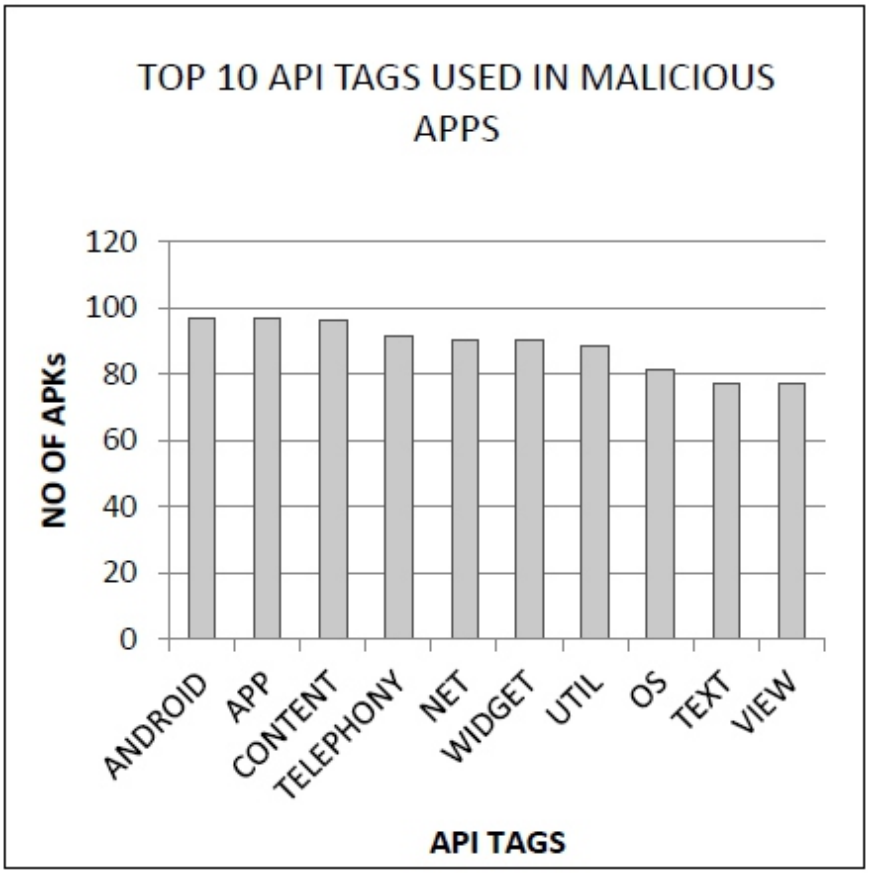

Figure 8: Bar graph showing top 10 API Tags used in malicious apps

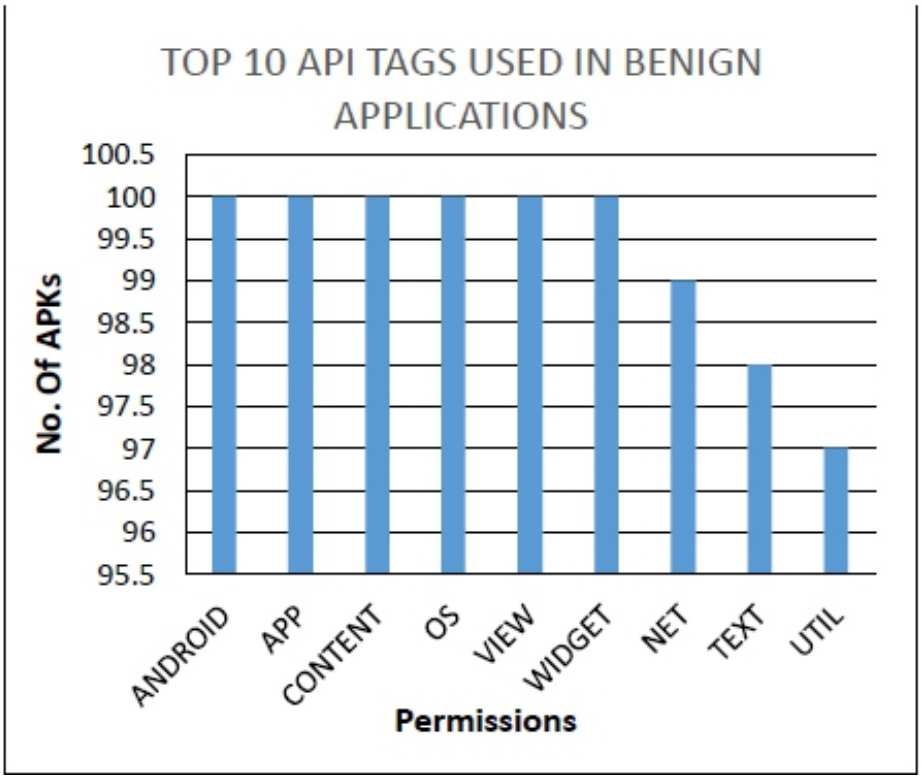

Figure 9: Bar graph showing top 10 API Tags used in benign apps

After comparing figure 6 and figure 7 we conclude that SEND_SMS, READ_SMS, RECEIVE_SMS, RECEIVE_BOOT_COMPLETED and ACCESS_COARSE_LOCATION are the permissions mostly used only in malicious applications. Similarly, from figure 8 and figure 9 we can see that TELEPHONY is the API Tag mostly used only in malicious applications.

5. CONCLUSION

In this paper, we have examined about Android applications comprised of both malicious and non-malicious. In Malicious apps, we have used ten malware families which have already been discussed in earlier chapters.

We have used five classification algorithms to detect the malware and subsequently evaluated the classifiers on the basis of accuracy.

Taking into the consideration all databases, SVM classifier turned out to be the best classifier in detecting the malware.

Out of all the three datasets i.e. Permissions, API Tags, Permissions plus API Tags as features, Permission plus API Tags based features comes out be the best for the detection of malware on the basis of features.

Analyzing all the datasets thoroughly, the top ten Android Permissions used in malicious applications are INTERNET, READ_PHONE_STATE, WRITE_EXTERNAL_STORAGE, SEND_SMS, READ_SMS, RECEIVE_SMS, ACCESS_NETWORK_STATE, RECEIVE_BOOT_COMPLETED, ACCESS_WIFI_STATE,ACCESS_COARSE_LOCATION.

Top ten API Tags used in malicious applications are ANDROID, APP, CONTENT, TELEPHONY, NET, WIDGET, UTIL, OS, TEXT, VIEW After comparing the top most permissions and API Tags in both malicious and benign apps we conclude that SEND_SMS, READ_SMS, RECEIVE_SMS, RECEIVE_BOOT_COMPLETED and ACCESS_COARSE_LOCATION are the dangerous permissions and TELEPHONY is the dangerous API Tag.

REFERENCES

[1] http://www.statista.com/statistics/266210/number-of-available-applications-in-the-google-play-store/

[2] http://www.androidcentral.com/google-says-there-are-now-14-billion-active-android-devices-worldwide

[3] http://www.techi.com/2015/12/india-now-has-more-than-a-billion-smartphone-users/

[4]http://www.scmagazineuk.com/updated-97-of-malicious-mobile-malware-targets-android/article/422783/

[5] Odusami, Modupe, Olusola Abayomi-Alli, Sanjay Misra, Olamilekan Shobayo, Robertas Damasevicius, and Rytis Maskeliunas. "Android malware detection: A survey." In International Conference on Applied Informatics, pp. 255-266. Springer, Cham, 2018.

[6] Xiao, Xi, Shaofeng Zhang, Francesco Mercaldo, Guangwu Hu, and Arun Kumar Sangaiah. "Android malware detection based on system call sequences and LSTM." Multimedia Tools and Applications 78, no. 4 (2019): 3979-3999.

[7] Milosevic, Nikola, Ali Dehghantanha, and Kim-Kwang Raymond Choo. "Machine learning aided Android malware classification." Computers & Electrical Engineering 61 (2017): 266-274.

[8] Li, Jin, Lichao Sun, Qiben Yan, Zhiqiang Li, Witawas Srisa-An, and Heng Ye. "Significant permission identification for machine-learning-based android malware detection." IEEE Transactions on Industrial Informatics 14, no. 7 (2018): 3216-3225.

[9] Demontis, Ambra, Marco Melis, Battista Biggio, Davide Maiorca, Daniel Arp, Konrad Rieck, Igino Corona, Giorgio Giacinto, and Fabio Roli. "Yes, machine learning can be more secure! a case study on android malware detection." IEEE Transactions on Dependable and Secure Computing 16, no. 4 (2017): 711-724.

[10] Martín, Ignacio, José Alberto Hernández, and Sergio de los Santos. "Machine-Learning based analysis and classification of Android malware signatures." Future Generation Computer Systems 97 (2019): 295-305.
[11] Chen, Xiao, Chaoran Li, Derui Wang, Sheng Wen, Jun Zhang, Surya Nepal, Yang Xiang, and Kui Ren. "Android HIV: A study of repackaging malware for evading machine-learning detection." IEEE Transactions on Information Forensics and Security 15 (2019): 987-1001.
[12] Sanz, B., Santos, I., Laorden, C., Ugarte-Pedrero, X., Bringas, P.G., Alvarez, G.,: PUMA: Permission Usage to detect Malware in Android, Springer, Berlin Heidelberg, 2013
[13] Justin Sahs , Latifur Khan, A Machine Learning Approach to Android Malware Detection, Proceedings of the 2012 European Intelligence and Security Informatics Conference, p.141-147, August 22-24, 2012
[14] Zarni Aung, Win Zaw. "Permission-Based Android Malware Detection" in International Journal of Scientific & Technology Research Volume 2, Issue 3, March 2013
[15] Aafer, Y., Du, W., Yin, H.: DroidAPIMiner: Mining API-level features for robust malware detection in android. In: Zia, T., Zomaya, A., Varadharajan, V., Mao, M. (eds.) SecureComm 2013. LNICST, vol. 127, pp. 86–103. Springer, Heidelberg (2013)
[16] https://play.google.com/store?hl=en
[17] Akanksha Sharma and Subrat Kumar Dash,: Mining API Calls and Permissions for Android Malware Detection, proceedings of 13th International Conference, CANS 2014, Heraklion, Crete, Greece, October 22-24, 2014.
[18] http://sanddroid.xjtu.edu.cn:8080/
[19] https://github.com/androguard/androguard
[20] Jung, Jaemin, Hyunjin Kim, Dongjin Shin, Myeonggeon Lee, Hyunjae Lee, Seong-je Cho, and Kyoungwon Suh. "Android malware detection based on useful API calls and machine learning." In 2018 IEEE First International Conference on Artificial Intelligence and Knowledge Engineering (AIKE), pp. 175-178. IEEE, 2018.
[21]Gong, Zhiqiang, Ping Zhong, and Weidong Hu. "Diversity in machine learning." IEEE Access 7 (2019): 64323-64350.
[22]Cai, Jie, Jiawei Luo, Shulin Wang, and Sheng Yang. "Feature selection in machine learning: A new perspective." Neurocomputing 300 (2018): 70-79.
[23] www.cs.waikato.ac.nz/ml/weka/
[24] A. Dey, "Machine learning algorithms: A review," Int. J. Comput. Sci. Inf. Technol., vol. 7, no. 3, pp. 1174–1179, 2016.
[25]M. Mohri, A. Rostamizaden, and A. Talwalkar, Foundations of Machine Learning, 2nd ed. Cambridge, MA, USA: MIT Press, 2018.

People Perception Towards Covid-19 Preventive and Management Measures by State Government of Andhra Pradesh, India: A Study On North Coastal Andhra Pradesh Region

DR. Peteti Premanandam,
Associate Professor, Head of the Department, Political Science & Public Administration, Andhra University, Visakhapatnam, Andhra Pradesh (State), India

ABSTRACT

The main aim of this study is to understand the people perception towards Covid-19 preventive and management measure which has been taken by the Andhra Pradesh State government. Covid-19 Pandemic is a new type of challenge or Non-Programmed activity which was never faced by the Andhra Pradesh State government, India in the past. In this article the researcher studies how the state government has taken preventive and management measure to control the spreading of Covid-19 Pandemic under the leadership of Y.S.R. Jagan Mohan Reddy, Honourable Chief Minister of Andhra Pradesh. 1650 Questionnaire/schedules are distributed among three districts (Visakhapatnam, Vizianagaram and Srikakulam) of North Coastal Andhra Pradesh Region but 1026 questionnaire/schedules are received form the sample respondents. The researcher collected the required data through well structured & tested questionnaires and schedules. The researcher used the Stratified sampling technique which comes under the Probability sampling method and also followed the Covid-19 pandemic guidelines for data collection.

Keywords: Covid-19, Pandemic, Perception, people, Prevention and Management

INTRODUCTION:

In December 2019, the epicentre for the COVID-19 disease is Wuhan city in Hubei Province of China and has become a pandemic as per the World Health Organisation (WHO). The World Health Organization (WHO) has given name to this virus as 2019-nCoV (Novel Coronavirus 2019, 2020) which was later renamed as Severe Acute Respiratory Syndrome Coronavirus 2 (SARS-CoV-2) by the International Committee on Taxonomy of Viruses. The diseases caused by this virus is called as coronavirus disease 2019 and abbreviated as COVID-19 (CO: corona, VI: virus, D: disease and 19: 2019 year). The Carona virus has exact resemblance (87%) with coronavirus of Bat (bird) and so, it is suspected to develop from the bats. This virus is out broken in pneumonia type of disease with respiratory problems and it is leading to death due to respiratory system failure. The patients show flu-like symptoms with breathing problems and high fever. Still, there is no treatment of this disease. However, control, prevention and management measures are the best options.

The disease has spread in 215 countries and territories with about 4,07,14,604 patients and more than 11,23,887 deaths globally. India is the second most affected country with about 75,97,063 patients and more than 1,15,236 deaths after the United States of America (cases: 84,59,041 and deaths: 2, 25,241). On 30th January, 2020 , the first case in India was confirmed in Kerala's Thrissur district, who was a student and had returned home from Wuhan University of China for a vacation.

Prevention and the management

The prevention and management are very crucial issues to control the COVID-19 Pandemic. Besides, there is a great need for the collective efforts of the people and the government. The regular and the proper care of the homes and hospitals are very important to control this calamity. Therefore, it is urgently advised and requested that all the persons should follow the preventive & management measures, and quarantine strictly otherwise the situation may be the worst.

The constitution of India establishes a federal structure, viz., there are separate governments at union and states levels, and there is a division of powers between the Central and State governments. The "Public health and sanitation; hospitals and dispensaries" subject comes under State list or list II of Indian Constitution. From the above inference, the Public health sector comes under the immediate supervision and control of the state government. Hence, for the Preventive and management measures towards Covid-19 Pandemic in India, the concerned State Governments have been playing an operative role and the Union government of India doing the Coordinating and regulative activities.

This paper studies the perception of people towards the Covid-19 Preventive and Management measures has taken by Andhra Pradesh state government under the leadership of Y.S.R, Jagan Mohan Reddy, Honourable Chief Minister of Andhra Pradesh. The Andhra Pradesh State is one of the 28 states of India and its consists of about 5.4 crores population according to Unique Identification Aadhar organisation of India. The report of Andhra Pradesh State Health Department on 12th March, 2020, the first Covid-19 positive case noted in Nellore district to 24 years old man, who returned from Italy and tested Covid-19 positive. Present the virus has spread to all the total 13 districts of the state and East Godavari district has the highest number of cases. On 20th October, 2020 the total Covid-19 cases in Andhra Pradesh is 7,83,155 and deaths 6453.

The selected area of study is "North Coastal Andhra Pradesh region" (also called as Uttarandhra Region in Telugu language) and it comprises of three districts viz. Visakhapatnam, Vizianagaram and Srikakulam.

REVIEW OF RELATED LITERATURE:

The availability of literature on 'prevention and management of Covid-19 Pandemic' is hardly available due to new subject and recent origin (Non-Programme activity). The 'review of related literature' is presented below.

Sara Marelli et al., (July, 2020) found that the impact of lockdown was greater in students than in workers, and also in females than in males. With regard to psycho-emotional aspects, about one-by-third of our sample showed anxious depressive symptoms. The results of this study may provide support for the implementation of some interventions for well-being in pandemic condition.

Lei Qin et al. (2000) found that by using Social Media Search Indexes (SMSI) to predict the outbreak of COVID-19 Pandemic among populations in affected areas could be effective, and demonstrated a high correlation with new suspected and, confirmed COVID-19 pandemic infection cases. SMSI is an effective early predictor, that would enable the health government departments to point potential and high-risk outbreak areas. So, the health government departments should prepare in advance for epidemic prevention and plan new public health policies earlier.

Tia Sheree Gaynor & Meghan E. (September 2020) concluded in their research-findings that existing disparities exacerbate COVID-19 pandemic outcomes for Black people. Targeted universalism (means setting universal goals and using targeted process to achieve those goals) is proposed as an administrative framework to reach the needs of all people affected by COVID-19 Pandemic disease.

Judd E. Hollander et al., (April: 2020)[11] concluded that Disasters and pandemics pose peculiar challenges to health care delivery sector. Though Tele-Health not solve them all, it's well suited for scenarios in which infrastructure remains intact and clinicians are available to see patients. Payment and regulatory structures, state licensing, credentialing across hospitals, and programme implementation all take time to work through, but health systems that have already invested in telemedicine are well positioned to ensure that patients with Covid-19 pandemic receive the care they required. In this occasion, it may be an effectively perfect solution.

CDC COVID-19 Response Team (March:2020) found that the risk of deadly COVID-19 pandemic in USA increases with age. The Team recommend Social distancing for all ages to slow the spread of the virus, protect the health care system, and help protect vulnerable older adults. Further, avoid cruise travel and nonessential air travel, and stay home as much as possible to further reduce the risk of being exposed. The people and communities should cooperate to help slow the spread of COVID-19 and protect older adults.

Hasan Muhammad Baniamin et al. (2020) [13] summarised different factors that account for both the control and the spread of COVID-19. The study identified countries according to their relative success in preventing the virus and mitigating its spread. Such initial success may not last due to fresh waves of the disease. The factors identified in this study generate inputs for policymakers and practitioners of different countries to consider when making and evaluating policy. Countries that are not affected yet or still in the initial state of the spread of the disease may learn from the factors identified in this study.

Imran Ali et al. (2020) realised that Covid-19 pandemic is spreading rapidly among the persons who are taking it non-seriously and not following the advice of WHO, and commands of the local governments. So, the study requested that all the persons should follow the preventive measures, managements and quarantine strictly otherwise the situation may be worsened. In outline, the collective efforts should require globally to fight against Covid-19 like diseases in future.

Huijuan Jin et al., (April:2020) revealed that people who infected with Covid-19 may show neurological symptoms first. Neurologists and Healthcare providers could pay close attention to these symptoms and have a high index of suspicion when evaluating patients in an endemic area. The Early recognition of this disease may help in providing of treatment. And also, the isolation of patient at early stage to prevent clinical worsening and spreading of deadly virus.

Amerigo Giudice et al., (2020) concluded that COVID-19 has spread worldwide in a pandemic way and infection control measures are mandatory to limit contagion, especially for healthcare professionals who meet potentially infected patients. In any case, the decrease of infectious risk remains a major challenge for dentists, among the most exposed health professionals.

Objectives of the Study

1 To study the perception, opinion and satisfaction levels of North Coastal Andhra Pradesh Region people towards Covid-19 preventive and management measures has taken by state government of Andhra Pradesh.

2 To study, how the State Administrative mechanism is responsive, proactive and effective in Prevention and Management of Covid-19 pandemic.

3 To study which Strategies, methods and techniques followed by Andhra Pradesh State government to Control and prevention of spread of Covid-19 Pandemic disease.

limitations of the study

1. The study was delimited to Geographic area of North Coastal Andhra Pradesh region of Andhra Pradesh only.
2. The study does not cover the total population of North Coastal Andhra Pradesh Region people, due to restraint of time & resources.
3. The majority of the Respondents are those who are affected Covid-19 affected persona and their family members.
4. Due to Covid-19 lockdown limitations rules, the person to person interaction is hardly possible and majority of information gathered through Telephone, WhatsApp calls, etc.

RESEARCH METHODOLOGY

The researcher has done a descriptive research on the topic "People perception towards Covid-19 Preventive and Management Measures by State Government of Andhra Pradesh, India: A Study on North Coastal Andhra Pradesh Region". The Stratified sampling technique (population divided into groups based on some characteristics and then within each group, a simple random sample is used) has been used for distribution of Questionnaire and Schedule for primary data collection. To collect information through questionnaire and schedule, the researcher mostly used Telephone and Internet networks like Gmail, skype, WhatsApp's, Facebook, SMS, etc, due to Covid-19 rules. Secondary data were collected from the available, books, journals, records, and websites. The data has been analysed with the statistical tools like averages and percentage analysis. The study is quantitative and to some extent qualitative in nature. The research period started from 21st June, 2020 and ended on 20th October, 2020.

ANALYSIS AND DISCUSSION:

The Researcher has been received response from 1026 (One thousand and twenty-six) sample respondents out of total distributed 1650 Questionnaires & schedules in North Coastal Andhra Pradesh Region. The majority of the Respondents are those affected by Covid-19 Pandemic and their family members. According to 2011 census of India, the total population of this region is 9,338,177. The selected area of study is "North Coastal Andhra Pradesh region consists of 3 districts viz. Visakhapatnam, Vizianagaram and Srikakulam. The distribution is given below table.

Table 1: Number of Covid-19 cases and Sample Respondents from three Districts of North Coastal Andhra Pradesh Region

Sl. No.	Name of the Districts	Population (Census-2011)	Total Covid-19 Positive Cases	Total Covid-19 deaths	Sample Respon-dents	Percen-tages (%) of Samples
1	Visakhapatnam	2,703,114	51490	455	412	40%
2	Vizianagaram	2,344,474	36415	222	294	29%
3	Srikakulam	4,290,589	40808	327	320	31%
Total: -		**9,338,177**	**91985**	**1,004**	**1026**	**100%**

Source: Primary data

Figure: -1

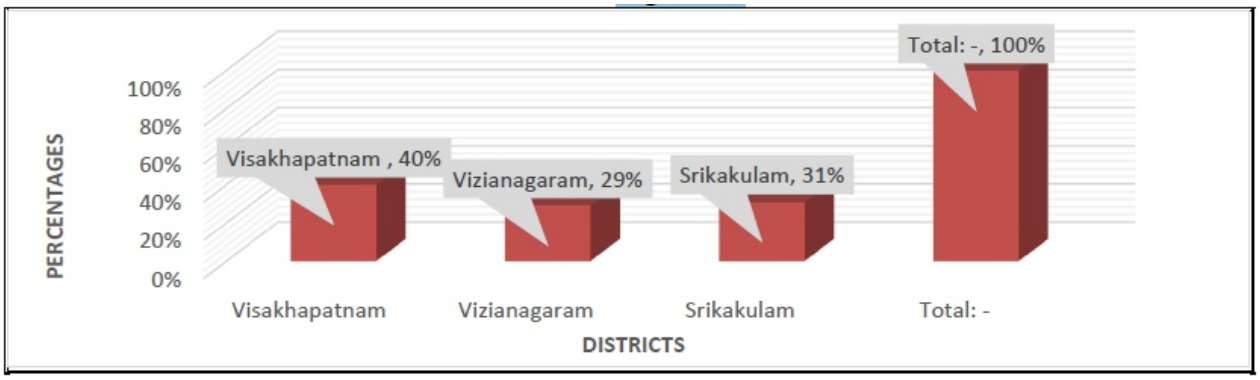

Table 2: The Sample Respondents' Socio-Economic Profile

Sl. No.	Variables	Particulars	No. of Respondents	Percentages (%)
1	**Age group**	Below 25years	174	17%
		25-55years	493	48%
		55 Above	359	35%
		Total	**1008**	**100%**
2	**Gender Group**	Males	564	55%
		Females	462	45%
		Total	**1026**	**100%**
3	**Geographical Regions**	Rural	595	58%
		Urban	431	42%
		Total	**1026**	**100%**
4	**Community-wise**	OC	211	21%
		BC	512	50%
		SC	199	19%
		ST	81	8%
		Minorities	23	2%
		Total	**1026**	**100%**

Source: Primary data

Inference

From the above table, the highest respondents age group is 'between 25-55 years' age group (48%) then followed by '55 years above' age group (35%), and 'below 25 Years' age group (17%). In Gender Group variable, the male (55%) is the highest then followed by female (45%). In Geographical region group,

the 'rural region' (58%) group is the highest then followed by 'Urban region' (42%). Among 'community groups', the highest is 'BC community' (50%) then followed by 'Open Community (OC)' (21%), 'SC Community' (19%), 'ST Community' (8%) and 'Minority Community' (2%).

In the Socio-economic Profile clearly evident that the respondents belong to the age group 'between 25 to 55 years' (48%), male (55%), rural region (58%) and BC Community group (50%) are the highest.

Table 3: The Respondents perception towards Andhra Pradesh Government's methods and techniques using for prevention of Covid-19 Pandemic.

Particulars	Number of Respondents	Percentage
Effective	866	84%
Neutral	91	9%
Ineffective	69	7%
Total	**1026**	**100%**

Source: Primary data

Figure: -2

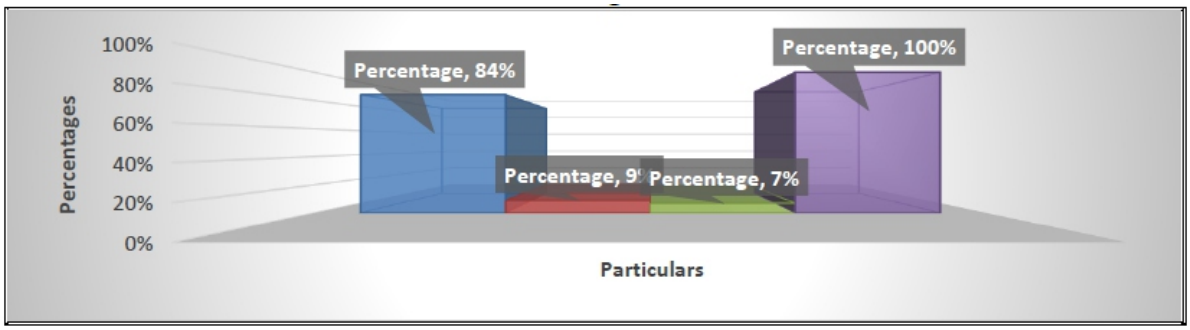

Inference

In this table, the 'Effective' option (84%) is the highest then followed by 'Neutral' option (9%) and 'Ineffective' option (7%). Hear, 84% of North Coastal Andhra Pradesh sample respondents perception towards the State government using methods and techniques for prevention of Covid-19 Pandemic are effective. Hence, the North Coastal Andhra Pradesh Region people believed that the State Government used methods and techniques like trace-test-treat method, Containment zones, Social distancing, work from home, etc., to control (mass community spread) Covid-19 Pandemic are "Effective".

Table: - 4: Respondents perception towards AP state government's awareness campaign about Covid-19 Pandemic.

Particulars	No. of Respondents	Percentage
Good	834	81%
Cannot say	91	9%
Bad	101	10%
Total	**1026**	**100%**

Source: Primary data

Figure: -3

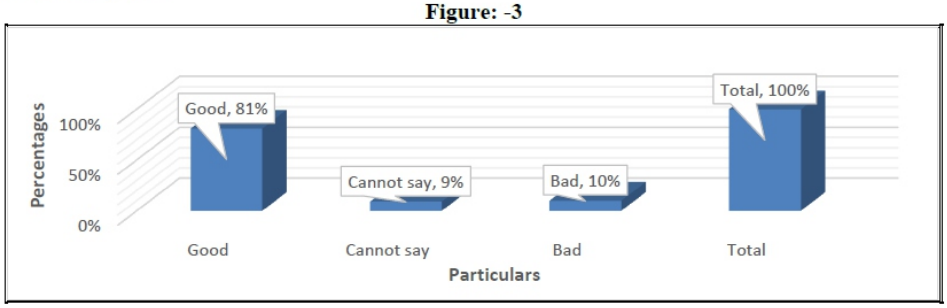

Inference

In this table, the 'Good' option (81%) is the highest then followed by 'Bad' option (10%) and 'Cannot say' option (9%). The table, clearly shows that 81% of sample respondents perception towards AP state government's awareness campaign about the Covid-19 Pandemic is good. Hence, the North Coastal AP people accepted the State government is good in creating awareness about Covid-19 Pandemic dangers and its preventive measures through their Communication networks like media, Government officers, etc.

Table: -5: Respondents perception towards the State government's supply of nutritional food and regulation of food prices

Particulars	No. of Respondents	Percentages
Satisfied	834	81%
Neutral	91	9%
Dissatisfied	101	10%
Total	**1026**	**100%**

Source: Primary data

Figure-4

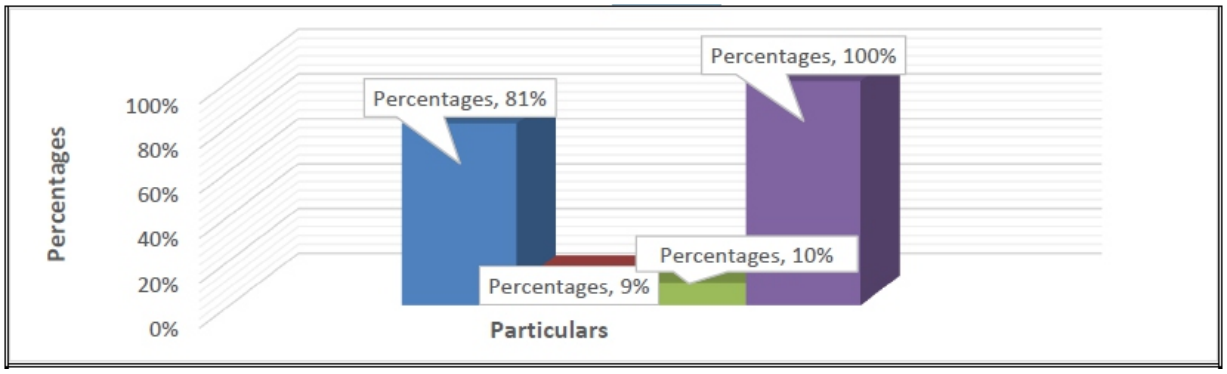

Inference

In this table, the 'satisfied' option (81%) is the highest then followed by 'Dis-satisfied' option (10%) and 'Neutral' option (9%). The table, clearly shows that 81% of respondents satisfied towards the State government's supply of nutritional food and regulation of food prices. So, North Coastal Andhra Pradesh people are satisfied with the AP State Government in time supply of nutritional and essential food items (to boost the immunity system) to people through PDS (Public Distribution System) & AWC (AnganWadi Centres) at free of cost, Rythyu Bazars at cheap prices and other markets at regulating prices to control the Covid-19 Pandemic.

Table: -6: Respondents perception towards government's strictly implementation of Containment zones, Red zones and Buffer zones rules.

Particulars	No. of Respondents	Percentage
Satisfactory	789	77%
Cannot Say	111	11%
Not Satisfactory	126	12%
Total	**1026**	**100%**

Source: Primary data

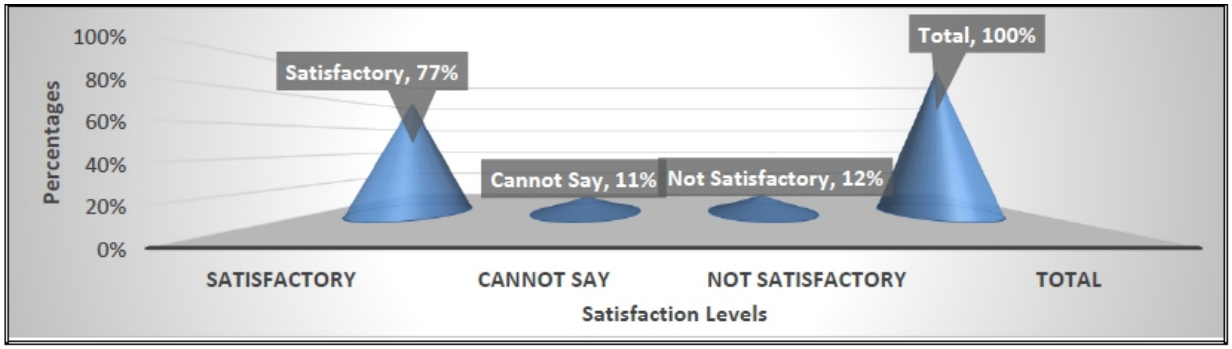

Inference

In this table, the 'Satisfactory' option (77%) is the highest then followed by 'Not Satisfactory' option (12%) and 'Cannot say' option (11%). Hear, it clearly indicates that 77% of respondents satisfactory towards State government strictly implementation of Containment zones, Red zones and Buffer zones rules. So, the people of North Coastal Andhra Pradesh are satisfactory towards the state government strict implementation of lockdown rules in Containment zones, Red zones and Buffer zones of rural and Urban areas to restrict the spread of Covid-19.

Table: -7: Respondents perception towards role of Andhra Pradesh State Police Department in implementation of Lockdown rules to prevention of Covid-19.

Particulars	No. of Respondents	Percentages
Good	767	75%
Neutral	118	12%
Bad	141	13%
Total	**1026**	**100%**

Source: Primary data

Figures: - 6

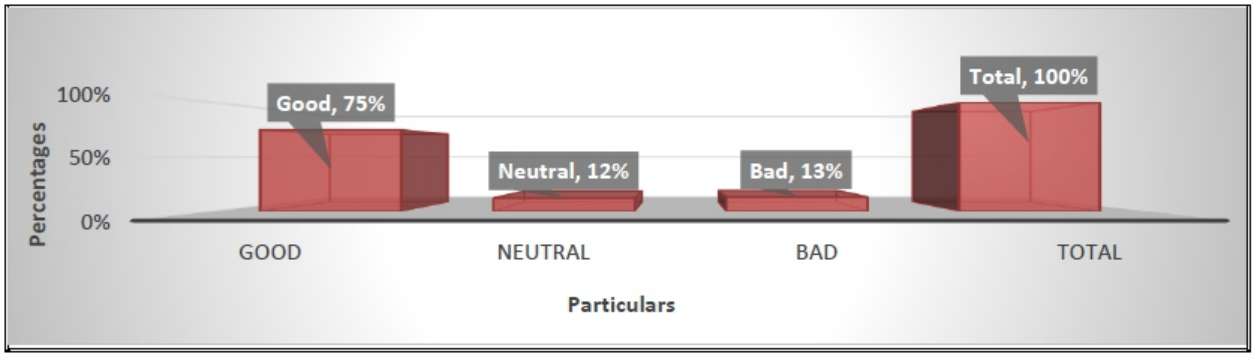

Inference

In this table, the 'Good' option (75%) is the highest then followed by 'Bad' option (13%) and 'Neutral' option (12%). Hear, it clearly indicates that majority (75%) of respondents accepted the role of Andhra Pradesh State Police Department in the implementation of Lockdown rules are good. So, the North Coastal Andhra Pradesh people opinioned that the Andhra Pradesh state police department has played a good role in the implementation of Lockdown rules like controlling people mobility in public places, social gatherings, functions, etc., to control the Covid-19.

Table: -8: Respondents perception on State government implementation of Central Government Lockdown rules strictly

Particulars	No. of Respondents	Percentage
Successfully	886	86%
Neutral	129	12%
Un-successfully	11	2%
Total	**1026**	**100%**

Source: Primary data

Figure: -7

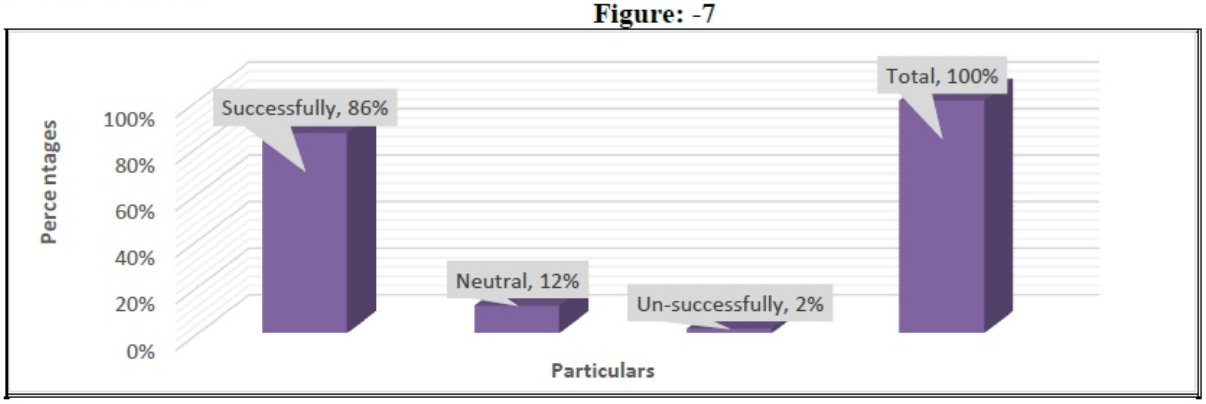

Inference

In this table, the 'Successfully' option (86%) is the highest then followed by 'Neutral' option' (12%) and 'Un-successfully' option (2%). It shows clearly that majority of respondents (86%) agreed that State Government of Andhra Pradesh successfully implemented the Central government Lockdown rules strictly. Hence, The People of North Coastal Andhra Pradesh believed that the State government of Andhra Pradesh successfully implemented the Central government lockdown rules i.e. restriction on public transport (aircraft, train, metro, bus, taxi, etc.), Educational institutions, Gymnasiums, Pilgrimage places, companies, Entertainment places, etc to control the spread of Covid-19 Pandemic disease.

Table: -9: Respondents opinion towards State government Covid-19 Testing percentage.

Particulars	No. of Respondents	Percentages
Yes	819	80%
Don't know	66	6%
No	141	14%
Total	**1026**	**100%**

Source: Primary data

Figure: -8

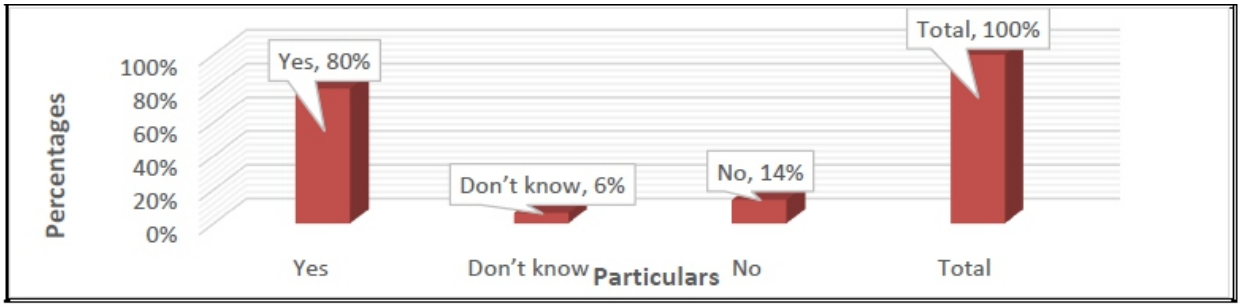

Inference

In this table, the 'Yes' option (80%) is the highest then followed by 'No' option (14%) and 'Don't know' option (6%). It clearly indicates that majority of respondents (80%) accepted "Yes" that the testing capacity of Andhra Pradesh is high and sufficient. Hence, North Coastal AP region people accepted that the Covid-19 Testing (RT-PCR, Trunat and Rapid Kit Testing) capacity of Andhra Pradesh is high and sufficient. Andhra Pradesh State is the highest Testing Capacity in India. And this Testing is conducted according to WHO and ICMR Covid-19 testing guidelines to control the spread of Covid-19 Pandemic.

Table: -10: Respondents perception towards state government conduct of door-to- door survey and trace-test-treat method.

Particulars	No. of Respondents	Percentages
Good	829	81%
Don't know	72	7%
Bad	125	12%
Total	**1026**	**100%**

Source: Primary data

Figure: -9

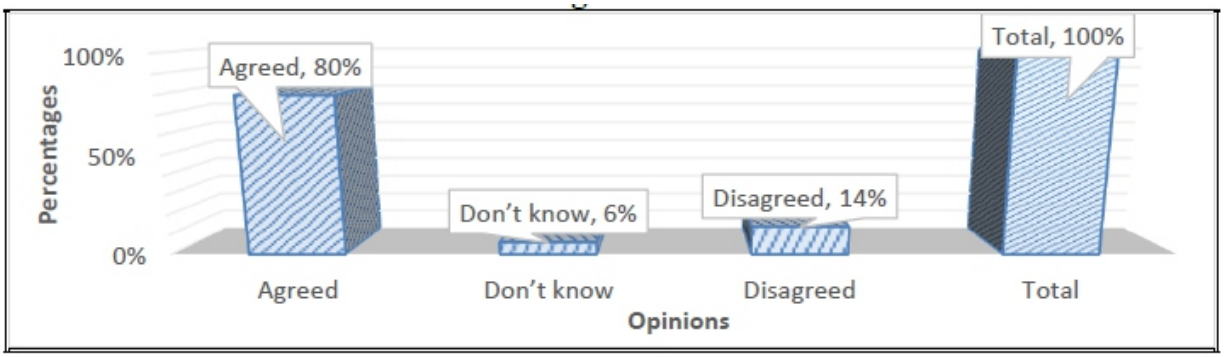

Inference

In this table, the 'Good' option (81%) is the highest then followed by 'Bad' option (12%) and 'Don't know' option (7%). The above data, clearly reveals that the majority of the respondents (81%) expressed "Good" towards the state government conduct of door-to-door survey and trace-test-trace method. Hence, the North Coastal Andhra Pradesh Region people said that the Andhra Pradesh State government conducted of the door-to-door survey, Rapid Health Check-ups and trace-test method delivery are good to prevention and control of Coviid-19 Pandemic. And this work has done with local network of ASHA workers, Auxiliary nurse midwife (ANM), village, and ward volunteer.

Table: -11: Respondent perception towards the provision of Surgical Masks, Covid-19 home isolation kits and other medical items by state Government.

Particulars	No. of Respondents	Percentage
Provided	854	83%
Don't know	81	8%
Not Provided	91	9%
Total	**1026**	**100%**

Source: *Primary data*

Figure-10

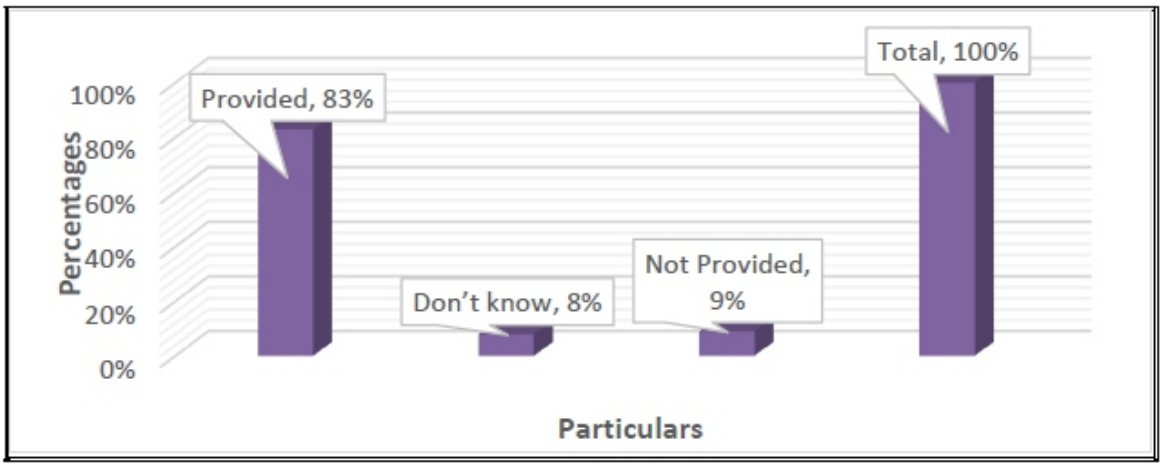

Inference

In this table, the 'Provided' option (83%) is the highest then followed by 'Not provided' option (9%) and 'Don't know' option (8%). It shows clearly shows that majority of respondent (83%) accepted the State government has provided Surgical Masks and Home isolation Kits at free of Cost. So, The North Coastal Andhra Pradesh people accepted the State government has provided the Surgical masks and Covid-19 home isolation medical and other required medical items at free of cost in rural and urban areas and it is also useful to control and prevention of Covid-19 Pandemic disease.

Table -12: Respondents perception towards treatment, facilities and monitoring in District and State COVID Hospitals

Particulars	No. of Respondents	Percentages
Good	833	81%
Don't know	93	9%
Bad	100	10%
Total	**1026**	**100%**

Source: Primary data

Figure-11

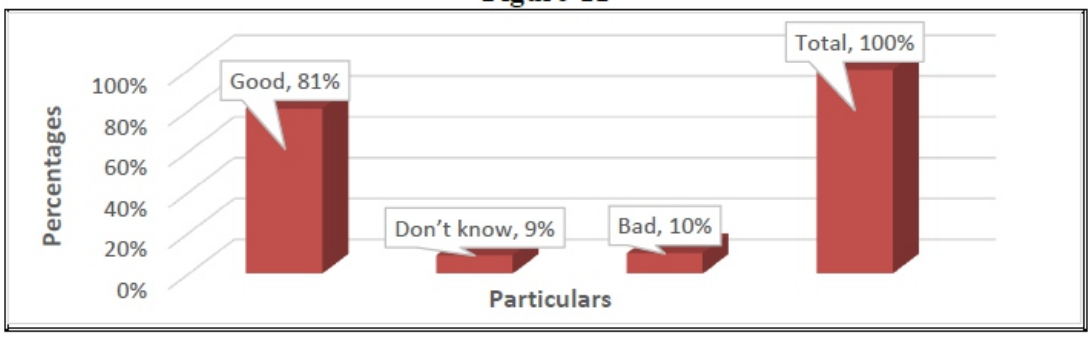

Inference

In this table, the 'Good' option (81%) is the highest then followed by 'Bad' option (10%) and 'Don't know' option (9%). It shows clearly shows that the majority of respondents (81%) agreed the treatment, facilities and monitoring in District and State COVID Hospitals are good. So, the North Coastal Andhra Pradesh region people accepted that the facilities, treatment and monitoring in District and State COVID Hospitals of Andhra Pradesh state government are good to control Covid-19 Pandemic.

Table: - 13: Respondents view towards amenities and facilities in Quarantine Centres.

Particulars	No. of Respondents	Percentages
Good	801	78%
Neutral	100	10%
Bad	125	12%
Total	**1026**	**100%**

Source: Primary data

Figure-12

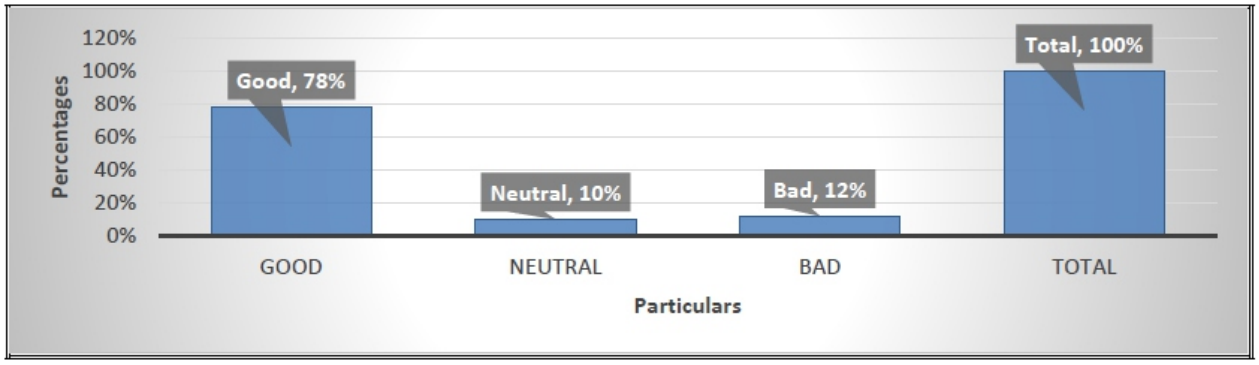

Inference

In this table, the 'Good' option (78%) is the highest then followed by 'Bad' option (12%) and 'Neutral' option (10%). It clearly shows that majority of the respondents (78%) said the amenities and facilities in State Quarantine Centres are good. Hence, the North Coastal Andhra Pradesh region people accepted the Andhra Pradesh State government's Quarantine Centres are good in basic amenities and facilities like Healthy food, drinking water, sanitation material, Hygienic environment, etc. And this State Quarantine are very help in the control of Covid-19 spread by isolation from main stream public.

Table: - 14: Respondents perception towards improvement of Health infrastructure and Recruitment of Medical Staff.

Particulars	No. of Respondents	Percentages
Sufficient	758	74%
Don't know	93	10%
Insufficient	175	16%
Total	**1026**	**100%**

Source: Primary data

Figure: -13

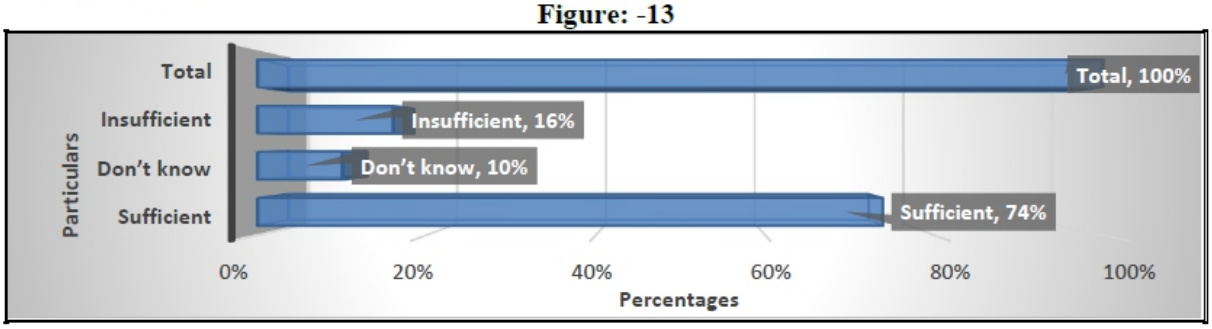

Inference

In this table, the 'Sufficient' option (74%) is the highest then followed by 'Insufficient' option (16%) and 'Don't know' option (10%). It clearly indicates that majority of the respondents (74%) said the Health

infrastructure and medical staff are sufficient. Hence, North Coastal Andhra Pradesh region people said that the Health infrastructure (Building, Ventilators and other hospital equipment) and medical staff (Doctors, Nurses, Pharmacists and others) are sufficient to Prevention and Management of Covid-19 Pandemic.

Table: - 15: Respondent perception towards Frontline workers role in Covid-19 prevention and Management

Particulars	No. of Respondents	Percentages
Agreed	819	80%
Don't know	66	6%
Disagreed	141	14%
Total	**1026**	**100%**

Source: Primary data

Figure: -14

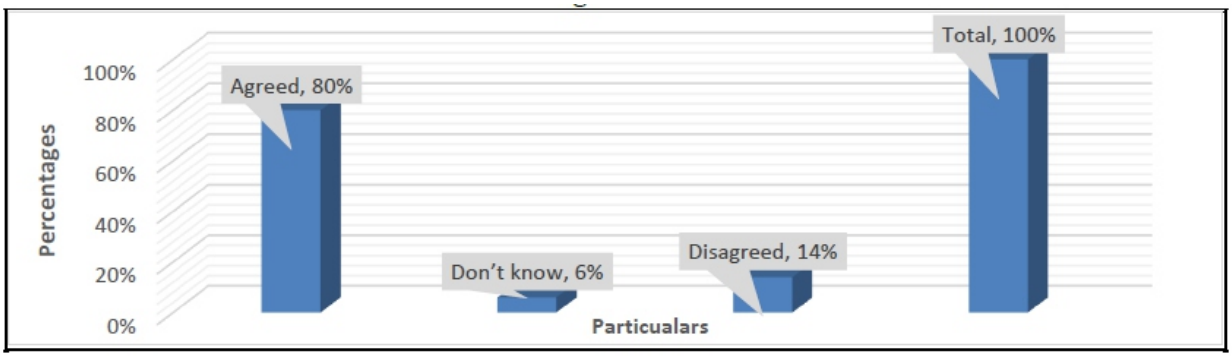

Inference

In this table, the 'Agreed' option (80%) is the highest then followed by 'Disagreed' option (14%) and 'Don't know' option (6%). It clearly indicates that the majority respondents (80%) agreed that Frontline staff has played key role in prevention of Covid-19 disease. Hence, North Coastal Andhra Pradesh region people agreed that the State government Covid-19 Frontline warriors (staff) like Medical staff, Police, Sanitation workers, local bodies staff and others have played a key role in the prevention and management of Covid-19.

Findings

1) In the Socio-economic Profile clearly evident that the respondents belong to the age group 'between 25 to 55 years' (48%), male (55%), rural region (58%) and BC Community group (50%) are the highest.
2) Hear, 84% of North Coastal Andhra Pradesh sample respondents perception towards the State government using methods and techniques for prevention of Covid-19 Pandemic are effective. Hence, the North Coastal Andhra Pradesh Region people believed that the State Government used methods and techniques like trace-test-treat method, Containment zones, Social distancing, work from home, etc., to control (mass community spread) Covid-19 Pandemic are "Effective".
3) The table, clearly shows that 81% of sample respondents perception towards AP state government's awareness campaign about the Covid-19 Pandemic is good. Hence, the North Coastal AP people accepted the State government is good in creating awareness about

Covid-19 Pandemic dangers and its preventive measures through their Communication networks like media, Government officers, etc.

4) The table, clearly shows that 81% of respondents satisfied towards the State government's supply of nutritional food and regulation of food prices. So, North Coastal Andhra Pradesh people are satisfied with the AP State Government on time supply of nutritional and essential food items (to boost the immunity system) to people through PDS (Public Distribution System) & AWC (AnganWadi Centres) at free of cost, Rythyu Bazars at cheap prices and other markets at regulating prices to control the Covid-19 Pandemic.
5) Hear, it clearly indicates that 77% of respondents satisfactory towards State government strictly implementation of Containment zones, Red zones and Buffer zones rules. So, the people of North Coastal Andhra Pradesh are satisfactory towards the strict implementation of lockdown rules in Containment zones, Red zones and Buffer zones of rural and Urban areas to restrict the spread of Covid-19.
6) Hear, it clearly indicates that majority (75%) of respondents accepted the role of Andhra Pradesh State Police Department in the implementation of Lockdown rules are good. So, the North Coastal Andhra Pradesh people opinioned that the Andhra Pradesh state police department has played a good role in the implementation of Lockdown rules like controlling people mobility in public places, social gatherings, functions, etc., to control the Covid-19.
7) It shows clearly that majority of respondents (86%) agreed the State Government of Andhra Pradesh successfully implemented the Central government Lockdown rules strictly. Hence, The People of North Coastal Andhra Pradesh believed that the State government of Andhra Pradesh successfully implemented the Central government lockdown rules i.e. restriction on public transport (aircraft, train, metro, bus, taxi, etc.), Educational institutions, Gymnasiums, Pilgrimage places, companies, Entertainment places, etc to control the spread of Covid-19 Pandemic disease.
8) It clearly indicates that majority of respondent (80%) accepted "Yes" that the testing capacity of Andhra Pradesh is high and sufficient. Hence, North Coastal AP region people accepted that the Covid-19 Testing (RT-PCR, Trunat and Rapid Kit Testing) capacity of Andhra Pradesh is high and sufficient. Andhra Pradesh State is the highest Testing Capacity in India. And this Testing is conducted according to WHO and ICMR Covid-19 testing guidelines. to control the spread of Covid-19 Pandemic.
9) The above data, clearly reveals that the majority of the respondents (81%) expressed "Good" towards the state government conduct of door-to-door survey and trace-test-treat method. Hence, the North Coastal Andhra Pradesh Region people said that the Andhra Pradesh State government conducted of the door-to-door survey, Rapid Health Check-ups and trace-test-treat method and delivery of medicine are good to prevention and control of Coviid-19 Pandemic. And this work has done with local network of ASHA workers, Auxiliary nurse midwife (ANM), village, and ward volunteer.
10) It clearly shows that majority of respondents (83%) accepted that State government has provided Surgical Masks and Home isolation Kits at free of Cost. So, The North Coastal Andhra Pradesh people accepted the State government has provided the Surgical masks and Covid-19 home isolation medical and other required medical items at free of cost in rural and urban areas and it is also useful to control and prevention of Covid-19 Pandemic disease.
11) It shows that the majority of respondents (81%) agreed the treatment, facilities and monitoring in District and State COVID Hospitals are good. So, the North Coastal Andhra

Pradesh region people accepted that the facilities, treatment and monitoring in District and State COVID Hospitals of Andhra Pradesh state government are good to control Covid-19 Pandemic.

12) It shows that majority of the respondents (78%) said the amenities and facilities in State Quarantine Centres are good. Hence, the North Coastal Andhra Pradesh region people accepted the Andhra Pradesh State government's Quarantine Centres are good in basic amenities and facilities like Healthy food, drinking water, sanitation material, Hygienic environment, etc. And this State Quarantine are very help in the control of Covid-19 spread by isolation from main stream public.
13) It clearly indicates that majority of the respondents (74%) said that Health infrastructure and medical staff are sufficient. Hence, North Coastal Andhra Pradesh region people said that the Health infrastructure (Building, Ventilators and other hospital equipment) and medical staff (Doctors, Nurses, Pharmacists and others) are sufficient to Prevention and Management of Covid-19 Pandemic.
14) It indicates that the majority respondents (80%) agreed that Frontline staff has played key role in prevention of Covid-19 disease. Hence, North Coastal Andhra Pradesh region people agreed that the State government Covid-19 Frontline warriors (staff) like Medical staff, Police, Sanitation workers, local bodies staff and others have played a key role in the prevention and management of Covid-19.

Recommendations

1) The Andhra Pradesh State government to some extent successful in creating awareness about Covid-19 - dangers and its precautions (like Community spread, Co-morbidity, fatality, Social distancing, Home Isolation, Sanitisation of Hands, wearing masks, etc.) among Urban people. But in rural areas the Covid-19 awareness among the people is inadequate. So, the State government should increase the Covid-19 awareness campaign at mass level in rural and tribal areas through it is communication networks like Print, Electronic and Social media.
2) The State Government of Andhra Pradesh should provide Sanitisers, Mask and others items to Below Poverty Level (BPL) people through Public Distribution System (PDS) or Fair price shops at free of cost or affordable prices.
3) The Frontline staff for Covid-19 prevention are Medical staff (Doctors, Nurses, Pharmacists, etc.), Sanitation workers and Police. To protect Frontline staff from the deadly Virus then the State government should provide PPE kits, Sanitisers, Masks, Medicines, Vaccines (if discovered) adequately and regular. If possible, the government should supply Nutritious food at free of cost to them to boost their immunity system.
4) The State government should provide Covid-19 special allowances (incentives) to Medical staff to increase their motivation levels to work more efficiently for preventive and management measures of Covid-19 Pandemic.
5) To increase the effective measures for Covid-19 preventive and management the Health and Medical staff should be trained with latest updated medical technology.
6) The State government should strengthen the Isolation and Quarantine centres with well-equipped facilities at every village to face second wave of Carona or any new type of flu/virus disease in future.
7) The Government has given permission to the Private Hospitals for Covid-19 disease treatment but the Private Hospitals are charging high amount of fees from the people. So, the government should regulate the fee charges of the Private Hospitals immediately.

8) The Covid-19 Testing capacity of Andhra Pradesh State is number one in India. But the state government should increase the Testing labs and reduce the time of testing reports to give quick treatment and isolation of Covid Patients.
9) The state government should provide some essential food commodities like fruits, vegetables, milk, groceries through Public Distribution System (PDS)/ Fair Price Shops to the BPL families to boost their immunity system to containment of Covid.
10) The State government should strictly implement the order of prohibiting the use and spitting of smokeless tobacco or chewable tobacco/non-tobacco product, sputum in public places.
11) The Andhra Pradesh Government has to take people cooperation by involving the people in the Control of Covid-19 disease spreading.
12) The State government should use the advanced Information and Technology like 'COVID alert tracking system', Setu appp, etc., to under control of Covid.

CONCLUSION

From this study, it is very clear that the State Government of Andhra Pradesh has taken good preventive and management measures to control Covid-19 in North Coastal Andhra Pradesh Region. Andhra Pradesh is the first highest Covid-19 testing capacity in India. From the begging of the study the Covid-19 cases are very high and end of the research period the cases are declined. If the Covid-19 Vaccine discovered in the year ending then the Union government of India should provide that vaccine first to Frontline staff, Co-morbidities and old patients immediately. If the same Covid-19 preventive and management measures are continued or even improved further will create a good name and fame to the Government of Andhra Pradesh.

REFERENCES

1) Jin, Y.H., Cai, L., Cheng, Z.S., Cheng, H., Deng, et al. A rapid advice guideline for the diagnosis and treatment of 2019 novel coronavirus (2019-nCoV) infected pneumonia (standard version). Mil. Med. Res. 7, 4

2) Imran Ali, Omar M.L. Alharbi c. et al. COVID-19: Disease, management, treatment, and social impact. Science of the Total Environment. Elsevier. Volume 728, 1 August 2020, 138861.

3) Sara Marelli., Alessandra Castelnuovo1., Antonella Somma., et al. Impact of COVID-19 lockdown on sleep quality in university students and administration staff. Journal of Neurology. https://doi.org/10.1007/s00415-020-10056-6. 4 July 2020

4) Lei Qin 1 , Qiang Sun, Yidan Wang , Ke-Fei Wu , et al. Prediction of Number of Cases of 2019 Novel Coronavirus (COVID-19) Using Social Media Search Index. International Journal of Environmental Research and Public Health; Published: 31 March 2020.

5) Tia Sherèe Gaynor & Meghan E. Social Vulnerability and Equity: The Disproportionate Impact of COVID-19. Public Administration Review, September, 2020

6) Judd E. Hollander, M.D., and Brendan G. Carr, M.D. et al. Virtually Perfect? Telemedicine for Covid-19. The New England Journal of Medicine. N engl j med 382;18 nejm.org April 30, 2020

7) CDC COVID-19 Response Team. Severe Outcomes Among Patients with Coronavirus Disease 2019 (COVID-19) — United States, February 12–March 16, 2020. Morbidity and Mortality Weekly Report Early Release / Vol. 69 March 18, 2020.

8) Hasan Muhammad Baniamin , Mizanur Rahman & Mohammad Tareq Hasan. Et al. The COVID-19 pandemic: why are some countries coping more successfully than others? Asia Pacific Journal of Public Administration. Volume 42, 2020 - Issue 3. https://doi.org/10.1080/23276665.2020.1784769.

9) Imran Ali, Omar M.L. Alharbi, et al. COVID-19: Disease, management, treatment, and social impact. Science of the Total Environment. ELSEVIER.

10) Huijuan Jin, Candong Hong, Shengcai Chen, et al. Consensus for prevention and management of coronavirus disease 2019 (COVID-19) for neurologists. Stroke Vasc Neurol: first published as 10.1136/svn-2020-000382 on 1 April 2020. Downloaded from http://svn.bmj.com. on October 5, 2020 at India:BMJ-PG

11) Amerigo Giudice, Francesco Bennardo, Alessandro Antonelli, Selene Barone and Leonzio Fortunato. COVID-19 is a New Challenge for Dental Practitioners: Advice on Patients' Management from Prevention of Cross Infections to Telemedicine. The Open Dentistry Journal, 2020, Volume 14 299.

11) Amerigo Giudice, Francesco Bennardo, Alessandro Antonelli, Selene Barone and Leonzio Fortunato. COVID-19 is a New Challenge for Dental Practitioners: Advice on Patients' Management from Prevention of Cross Infections to Telemedicine. The Open Dentistry Journal, 2020, Volume 14 299.
12) Coronavirus: Common Symptoms, Preventive Measures, & How to Diagnose It. Caringly Yours. 28 January 2020. (Retrieved 28 January 2020).
13) The Editorial Board, 29 January 2020. Is the world ready for the coronavirus? - distrust in science and institutions could be a major problem if the outbreak worsens. The New York Times Retrieved 30 January 2020
14) WHO Statement Regarding Cluster of Pneumonia Cases in Wuhan, China, 9 January 2020. www.who.int Archived from the original on 14 January 2020. Retrieved 10 January 2020.
15) CDC. Novel Coronavirus 2019, Wuhan, China. www.cdc.gov. 23 January 2020. Archived from the original on 20 January 2020. Retrieved 23 January 2020., 2019 Novel Coronavirus Infection (Wuhan, China): Outbreak Update. Canada.Ca. 21 January 2020.
16) Lu, H., 2020. Drug treatment options for the 2019-new coronavirus (2019-nCoV). Biosci. Trends. 14, 69–71.
17) https://en.wikipedia.org/wiki/Uttarandhra#:~:text=Uttarandhra%20(also%20known%20as%20North,has%20a%20population%20of%209%2C338%2C177.
18) "Coronavirus | First case of COVID-19 reported from Nellore in AP". The Hindu. Special Correspondent. 12 March 2020. ISSN 0971-751X. Retrieved 29 April 2020.
19) http://www.populationu.com/in/andhrapradeshpopulation#:~:text=Andhra%20Pradesh%20population%20in%202020,the%20projected%20population%20is%2053%2C903%2C393.
20) Roshni Duhan. Federal System in India and the Constitutional Provisions. Vol 5, Issue 1, 2016 ISSN - 2347-5544, Innovare journal of Social Sciences.
21) The States Subjects List. Vakilbabu.com. Retrieved 2013-03-25 (u can refer laxmi kant polity or others)

Arrhythmia Detection and Classification Using Convolutional Neural Network

Kishore G R[1], Dr. Shubhamangala B R[2]

[1]Research Scholar, Dept. of Computer Science & Engineering., Jain University, Bangalore, Karnataka, India e-mail: kishoregr31@gmail.com

[2]Researcher Supervisor, Dept. of Computer Science & Engineering., Jain University, Bangalore, Karnataka, India e-mail: brm1shubha@gmail.com

ABSTRACT

Healthcare and Life Sciences are among severely researched domains. With the introduction of computing paradigms and possibility of leveraging computational techniques have opened new research avenues. Heart is one among the most researched organs and the reason being trivial. With the advent of computational paradigms researchers explored ways to measure the electrical activity of the heartbeat which is known as electrocardiogram (ECG). Since then ECG has become one of the most important as well as primary tests to diagnose any irregularities in the functioning of the heart. The availability of the ECG data and possibility of employing deep learning models and their robustness has made researchers venture into leveraging them to elevate the accuracy of the ECG Analysis. To date there exists no end-to-end evaluation model based on deep learning techniques. In our present work, we identify different classes of cardiac rhythm by leveraging single-lead ECG. Our results show a significant improvement in ROC (approx. 0.97). Furthermore, our results demonstrate that we can classify a wide spectrum of arrhythmias using Deep Learning Techniques which are comparable to that of cardiologists. This approach can be used to minimize the component of human misdiagnose and help improve the quality of cardiac care.

Keywords: ECG, Deep Learning, Arrhythmia, Cardiology.

I. INTRODUCTION

Out of the large number of deaths that occur due to cardiac issues, a significant number of deaths is cause due to Cardiac arrhythmia. Annually, millions of people die of arrhythmia and hence it becomes imperative to research on this topic. A lot of researchers have already worked on arrhythmia using many techniques like wavelets, Support Vector Machines (SVM) etc. Understanding of ECG is very essential to detect and classify Arrhythmia and involves many steps including Pre-processing ECG Signal, segmentation, peak detection / feature extraction and detection / classification.

ECG is one of the most important instruments used in cardiological practices in a clinical setup. Every year millions of ECGs are ordered worldwide. ECG's output, in clinical practices is heavily relied upon for decision making as it can help in identifying several abnormalities. Advent of ECG changed the landscape of cardiac care and introduction of computational paradigms has opened new avenues in research. [1][5-7] show that some of the conventional algorithms lead to some level of incorrect diagnosis. This is also since ECG data is too complex to interpret and conventional algorithms may not scale up to handle the level of complexity. But with the advent of High-Performance Computing paradigms and possibility of implementing machine learning and deep learning algorithms, it has now become possible to use these paradigms to analyze ECG.

A lot of development that has happened over a past couple of years has paved way for deep learning models. These are the computational models with multiple layers where each layer is abstract and is designed to perform a specific task. These models have significantly increased the accuracy of techniques like speech and image recognition. These models are not just limited to speech and image but they can also be extended to research in computational life sciences and medical data analysis. Unlike conventional algorithms and machine learning deep learning and neural networks can recognize patterns from the data and interpret the features which help in feature extraction and feature engineering making them most sought after computational methods specially to interpret data like ECG.

As aforementioned, ECG Data is very complex and a lot of researchers have employed various computational methods including Machine Learning (ML) and Deep Learning (DL) Algorithms but their focus has mostly been on certain aspects of ECG analysis. Works like [5-6] have focused more on noise reduction, whereas researchers in works [7-8] have focused mostly on feature extraction ending up in detecting only a few heartbeats [9-12]. Works [13-17] detects and classify only a few types of cardiac rhythms. Most of the aforementioned works have been limited by lack of data that doesn't record / contain comprehensive cardiac rhythms.

It has been our endeavor in this work to create a novel data set that has comprehensive annotations for a wide range of rhythms. We have developed novel algorithm to detect wide range of cardiac rhythm classes. The data set contains ECG data from a single-lead ECG machine.

II. RELATED WORKS

Since the advent of newer computing paradigms like Machine Learning and Deep Learning techniques, a lot of researchers have developed lot of different techniques to detect various abnormalities, especially arrhythmia.

2.1 Detecting Arrhythmia from ECG data.

As mentioned in the previous sections, ECG signals represent the electrical activity of the heart. It is very important to study the changes in electrical signals for diagnosing arrhythmia and other cardiac abnormalities. Figure1 as shown below, shows an example of a general 2-lead ECG [18] generally, a peak can be defined as space between an apex and 2 valleys and such a peak in ECG terminology is termed as R-peak. And RR Interval (RRI) is defined as interval between 2 consecutive R-peaks. The valley on either side of an apex of the peak is studied and each such window is analyzed and features are extracted to detect arrhythmia and classify various cardiac rhythms. It becomes very trivial at this point to note how imperative it is for the feature extraction to be very accurate and effective.

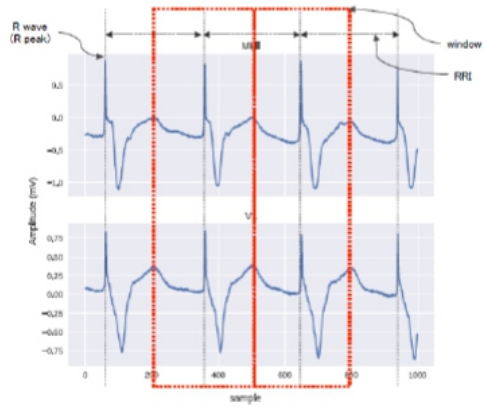

Figure 1: General Example of 2-lead ECG

Many researches have been conducted to study and detect abnormalities by leveraging computational paradigms. Most of the conventional approaches employ methods to manually extract the features from the ECG data. It is Machine Learning and Deep Learning that changed the way this type of data was being analyzed. [19] has proposed ECG classification using Conventional Neural Networks (CNN). Their model used MIT Database and focused only on VEB and SVEB. However, their approach was patient-centric which suffered from lot of variations. The work in [20] demonstrated ECG Classification by employing one-dimensional CNN. However, their approach to classification was more patient specific than being generic. Their approach to train their model was hybrid, i.e. the normal beats were recorded from the patients while the abnormal beats were emulated. Some of the other researchers who started working on a more generic approach like Zubair et al in [21] based on 1-d Convolutional Neural Network (CNN) which employed 3 layers and 1 fully connected Softmax layer. However, one of the pitfalls were that the data suffered from patient overlap in train and test data. Taking a cue from their work, researchers in the work mentioned in [22] increased the convolutional layers to 5.

Based on these works and works of many other researchers we have put forth our efforts to ensure that the data used in our work is strictly non-patient centric thus helping to clearly capture the efficiency and accuracy of our model.

III. PROPOSED ALGORITHM

The general architecture of CNN Algorithm is as shown in Figure2

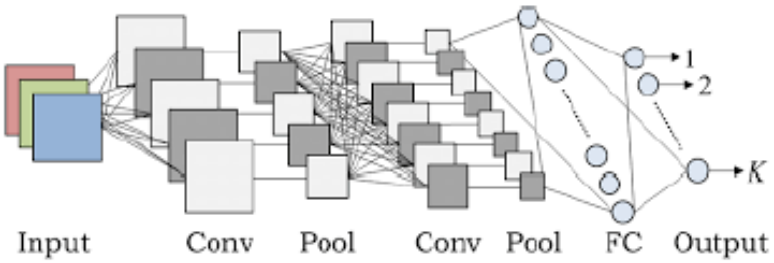

Figure 2: General Architecture of CNN

It consists of a series of input layers and pool which are connected to a fully connected layer which generates the output. The architecture is similar to the connectivity of neurons in the brain and is in-fact was inspired by the neural connection patterns in the human brain. The individual layers that perform a linear operation on the input parameters in called a convolution.

Generally, in the conventional Machine Learning Algorithms like Regression, we use normalization technique to scale the input to a range of value. This works well in a single layer but when want to extend the same technique to a CNN with multiple layers the input distribution gets changed at subsequent layers where each layer tries to normalize and the error propagates where the initial normalized values gets shifted resulting in "internal covariate shift".

To overcome this problem, we add a normalization layer between subsequent layers thereby inhibiting the hidden / convolution layers from normalizing the values. Since these layers keep normalizing the values at each layers in batches, this technique is termed as "batch normalization" [23] generally abbreviated as batch norm. A general architecture of Batch Normalization is as shown in Figure3.

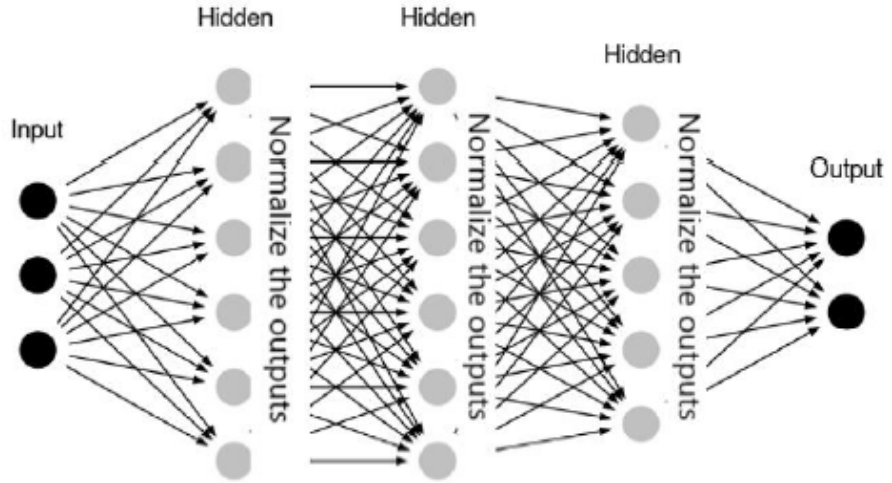

Figure 3: General Architecture of Batch Normalization

Generally, there are 4 steps involved in Batch Normalization i.e. a) batch mean b) batch-variance c) normalization d) scale and shift.

For any input batch at a normalization layerB=$\{x_1,...,m\}$,the output of that layer will be will be $\{y_i=BN_{\gamma,\beta}(x_i)\}$ [23]. Where:

$$\mu_B \leftarrow \frac{1}{m}\sum_{i=1}^{m} x_i$$

$$\sigma_B^2 \leftarrow \frac{1}{m}\sum_{i=1}^{m} (x_i - \mu_B)^2$$

$$\hat{x_i} \leftarrow \frac{x_i - \mu_B}{\sqrt{\sigma_B^2 + \epsilon}}$$

$$y_i \leftarrow \gamma \hat{x_i} + \beta \equiv \mathrm{BN}_{\gamma,\beta}(x_i)$$

We have used the data from a 200 Hz ECG Monitor and have extracted a median of a 30 sec record per record to build the dataset. Most of the records are a multiplexed representation meaning there could be different classes of rhythms in a single record. We then employed the developed algorithm, as shown in Figure4, which feeds on the ECG data that is sampled at 200Hz which are raw samples of ECG. The neural network in our work consists of 30 layers and 15 residual blocks where the batch normalization is applied along with ReLU and Dropout [24]. We have trained the network by employing the random.

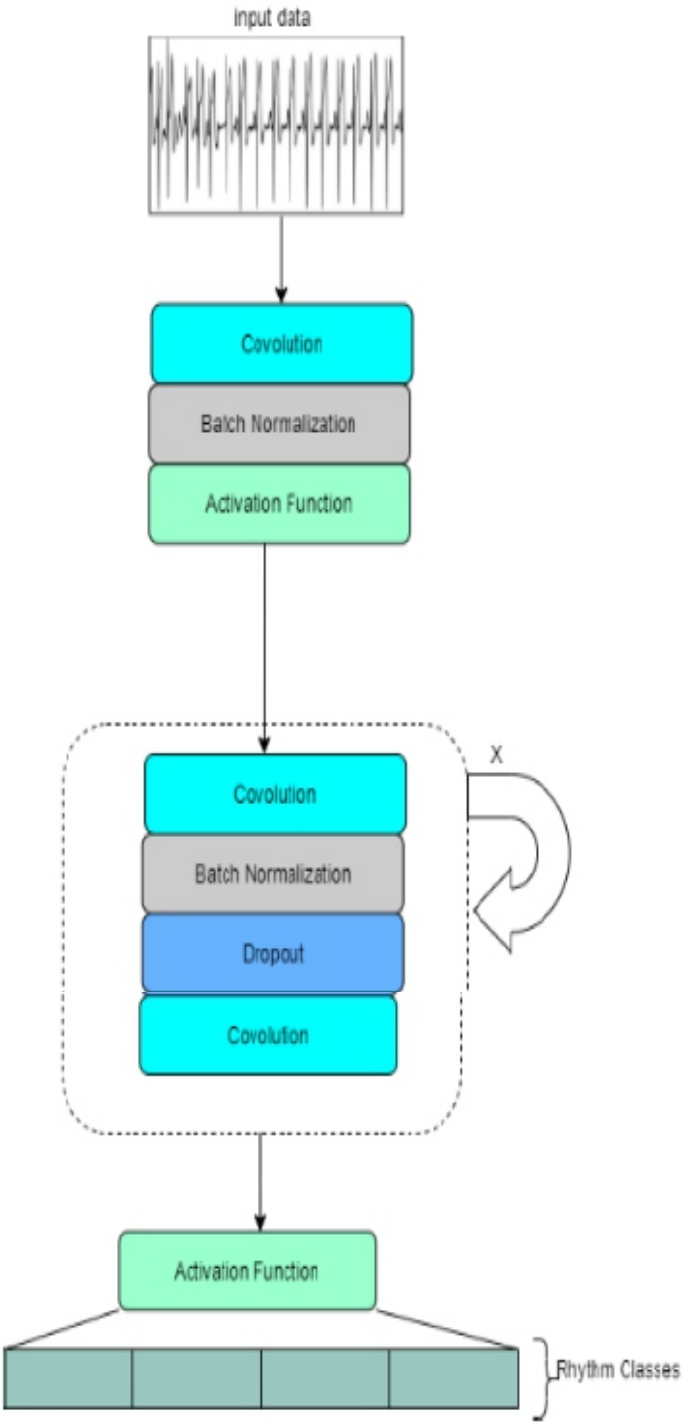

Figure 4: Proposed Algorithm

III. EXPERIMENT AND RESULT

Our work demonstrates that the accuracy of the model is around 0.97. Our study demonstrates how employing Deep Learning Methods can improve the accuracy and open new avenues for research. Figure 5 shows the AUC of the rhythm classes and we can note that the accuracy is elevated compared to the annotations.

Rhythm Class	AUC
AF	0.965
AVB	0.981
BIGEMINY	0.996
IVR	0.987
JUNCTIONAL	0.979
NOISE	0.947
TRIGEMINY	0.997
Average	0.978

Table 1: Rhythm Class AUC

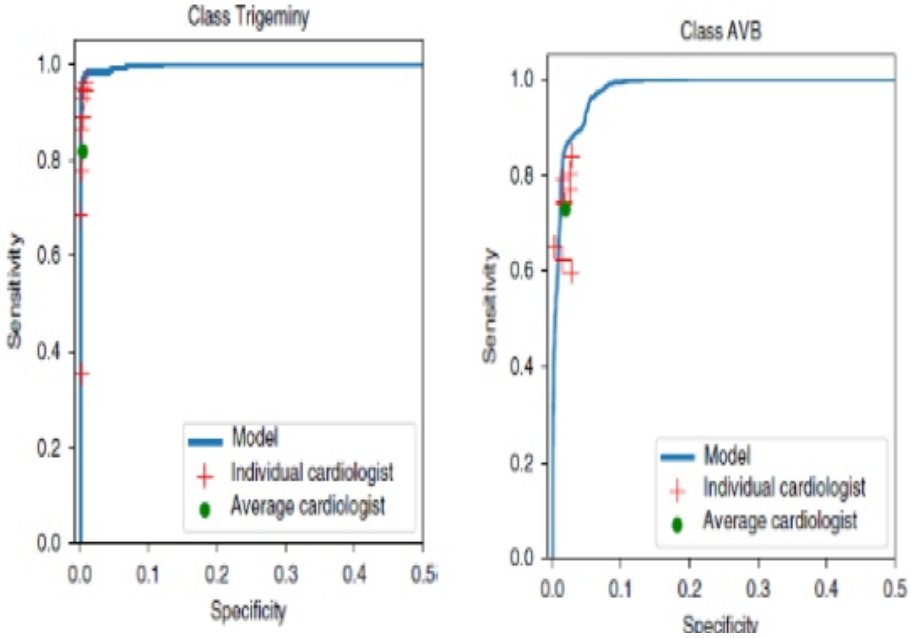

Figure 5: ROC for various rhythm classes

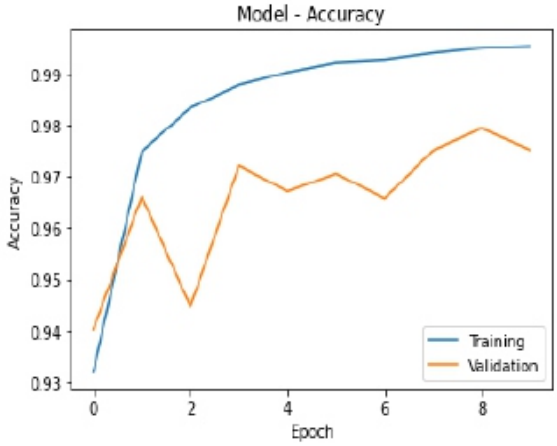

Figure 6: Model Accuracy

Figure6 shows the accuracy of the training and test sets against the number of epochs run.

IV.CONCLUSION

I believe that there is a scope for development of a more comprehensive end to end approach that employs deep learning and other neural network paradigms.

ACKNOWLEDGEMENT

Kishore G R, assistant professor, Department of Information Science & engineering, Jyothy Institute of technology, Bengaluru.

First and foremost, I wish to record my sincere gratitude to Management of Jyothy Institute of Technology and to my beloved Principal, Dr. Gopalakrishna,JIT, Bengaluru for his constant support and encouragement .

My sincere thanks to Dr. Harshvardan Tiwari, HOD, ISE, for his valuable suggestions for writing the paper

REFERENCES

[1] Schläpfer, J. & Wellens, H. J. Computer-interpreted electrocardiograms: benefits and limitations. J. Am. Coll. Cardiol. 70, 1183–1192 (2017).weights as mentioned by He et al [25] and a 128 being the size of the mini-batch.

[2] Shah, A. P. & Rubin, S. A. Errors in the computerized electrocardiogram interpretation of cardiac rhythm. J. Electrocardiol. 40, 385–390 (2007).

[3] Guglin, M. E. & Thatai, D. Common errors in computer electrocardiogram interpretation. Int. J. Cardiol. 106, 232–237 (2006).

[4] Poon, K., Okin, P. M. & Kligfield, P. Diagnostic performance of a computer based ECG rhythm algorithm. J. Electrocardiol. 38, 235–238 (2005).

[5] Poungponsri, S. & Yu, X. An adaptive filtering approach for electrocardiogram (ECG) signal noise reduction using neural networks. Neurocomputing 117, 206–213 (2013).

[6] Ochoa, A., Mena, L. J. & Felix, V. G. Noise-tolerant neural network approach for electrocardiogram signal classification. In Proc. 3rd International Conference on Compute and Data Analysis, 277–282 (Association for Computing Machinery, 2017).

[7] Mateo, J. & Rieta, J. J. Application of artificial neural networks for versatile preprocessing of electrocardiogram recordings. J. Med. Eng. Technol. 36, 90–101 (2012).

[8] Pourbabaee, B., Roshtkhari, M. J. & Khorasani, K. Deep convolutional neural networks and learning ECG features for screening paroxysmal atrial fibrillation patients. IEEE Trans. Syst. Man Cybern. Syst. 99, 1–10 (2017).

[9] Javadi, M., Arani, S. A., Sajedin, A. & Ebrahimpour, R. Classification of ECG arrhythmia by a modular neural network based on mixture of experts and negatively correlated learning. Biomed. Signal Process. Control 8, 289–296 (2013).

[10] Acharya, U. R. et al. A deep convolutional neural network model to classify heartbeats. Comput. Biol. Med. 89, 389–396 (2017).

[11] Banupriya, C. V. & Karpagavalli, S. Electrocardiogram beat classification using probabilistic neural network. In Proc. Machine Learning: Challenges and Opportunities Ahead 31–37 (2014).

[12] Al Rahhal, M. M. et al. Deep learning approach for active classification of electrocardiogram signals. Inf. Sci. (NY) 345, 340–354 (2016).

[13] Acharya, U. R. et al. Automated detection of arrhythmias using different intervals of tachycardia ECG segments with convolutional neural network. Inf. Sci. (NY) 405, 81–90 (2017).

[14] Zihlmann, M., Perekrestenko, D. & Tschannen, M. Convolutional recurrent neural networks for electrocardiogram classification. Comput. Cardiol. https://doi.org/10.22489/CinC.2017.070-060 (2017).

[15] Xiong, Z., Zhao, J. & Stiles, M. K. Robust ECG signal classification for detection of atrial fibrillation using a novel neural network. Comput. Cardiol. https://doi.org/10.22489/CinC.2017.066-138 (2017).

[16] Clifford, G. et al. AF classification from a short single lead ECG recording: the PhysioNet/Computing in Cardiology Challenge 2017. Comput. Cardiol. https://doi.org/10.22489/CinC.2017.065-469 (2017).
[17] Teijeiro, T., Garcia, C. A., Castro, D. & Felix, P. Arrhythmia classification from the abductive interpretation of short single-lead ECG records. Comput. Cardiol.
[18] George B Moody and Roger G Mark. 2001. The impact of the MIT-BIH arrhythmia database. IEEE Engineering in Medicine and Biology Magazine 20, 3 (2001), 45–50.
[19] Serkan Kiranyaz, Turker Ince, and Moncef Gabbouj. 2016. Real-time patientspecific ECG classification by 1-D convolutional neural networks. IEEE Transactions on Biomedical Engineering 63, 3 (2016), 664–675.
[20] Serkan Kiranyaz, Turker Ince, and Moncef Gabbouj. 2017. Personalized Monitoring and Advance Warning System for Cardiac Arrhythmias. Scientific Reports 7, 1 (2017), 9270.
[21] Muhammad Zubair, Jinsul Kim, and Changwoo Yoon. 2016. An Automated ECG Beat Classification System Using Convolutional Neural Networks. In 6th International Conference on IT Convergence and Security (ICITCS). IEEE, 1–5.
[22] Bahareh Pourbabaee, Mehrsan Javan Roshtkhari, and Khashayar Khorasani. 2017. Deep Convolutional Neural Networks and Learning ECG Features for Screening Paroxysmal Atrial Fibrillation Patients. IEEE Transactions on Systems, Man, and Cybernetics: Systems (2017).
[23] Ioffe et al. Batch Normalization: Accelerating Deep Network Training by Reducing Internal Covariate Shift. Proceedings of the 32 nd International Conference on Machine Learning, Lille, France, 2015. JMLR: W&CP volume 37.
[24] Srivastava, N., Hinton, G., Krizhevsky, A., Sutskever, I. & Salakhutdinov, R. Dropout: a simple way to prevent neural networks from overfitting. J. Mach. Learn. Res. 15, 1929–1958 (2014).
[25] He, K., Zhang, X., Ren, S. & Sun, J. Delving deep into rectifiers: surpassing human-level performance on ImageNet classification. In Proc. International Conference on Computer Vision, 1026–1034 (IEEE, 2015).

Analysis The Application of Lean Manufacturing with Systematic Human Error Reduction and Prediction to Reduce Defect Production

Nur Hamidah[1], Zeplin Jiwa Husada Tarigan[2*]
[1]Master of Engineering Program, Adhi Tama Institute of Technology Surabaya
[2]Magister Management, Petra Christian University

ABSTRACT

Manufacturing companies engaged in wood processing produce products in the turning process. The problem faced by the company is a waste where defects often occur in each production process. The cause of the disability arises in workers with human error. This research aims to minimize the waste in activities that do not provide added value and find the factors that cause a human error in the turning production process. For this reason, the method is used to Value Streaming Mapping illustrate the flow of products, the entry of raw materials to finished products. The research was distributing questionnaires to the production department and then processed with a waste assessment model, waste relationship matrix and waste assessment questionnaire so that the three highest wastes were obtained, namely waste defects (27,979%), waste overproduction (15,471%) and waste inventory (12,363%). Weighting waste with value stream analysis tools by selecting the two highest tools, namely process activity mapping and quality filler mapping. The causes of activities and accuracy are caused by human errors in the production process using the Systematic Human Error Reduction and Prediction method. Five activities are obtained in a critical state. The results of field implementation showed improvement with a decrease in time from 2384.2 minutes to 2247.4 minutes the value of Process cycle efficiency with the improvement of 4.9185%.

Keywords: Defect, Value Streaming Mapping, Ishikawa Diagram, SHERPA.

1. INTRODUCTION

Companies must be more competitive to survive and compete in facing competitors, so it is necessary to implement the right business strategy to stay and face the competition that occurs. Manufacturing products company in producing high-quality products is one of the advantages and guarantees consumers of products produced by the company (Kristianto and Tarigan, 2019). Lean Manufacturing application is to identify and reduce waste. Lean Manufacturing is used to identify and eliminate waste through continuous improvement. Using a pull system approach to understand better customer needs and the level of the company's inventory count is getting smaller (Abu et al. 2019). Kusbiantoro and Nursanti (2019) with the use of Value Stream Mapping (VSM) and Value Stream Analysis Tools (VSAT) state that an enormous waste is found in inventories in the form of raw materials, semi-finished goods and in finished products. Changes made to the production process system increased efficiency by 17.19% and decreased waste by 8.31%. Sinambela (2019) identifies waste in PVC pipe companies with a value stream mapping of 316.17 minutes and the total non-value-added time in 7418.73 minutes. The waste that occurs is defective products, excessive production, waiting time that causes bottlenecks, redundant processes in the form of activities setup extrude machine that requires a long time. Lean Manufacturing provides added value for companies when adequately implemented through the VSM and VALSAT methods (Lukmandono, et al. 2019; Zahra et al., 2013).

Inventory waste ranks first (19.23%), followed by defect waste (18.16%) and overproduction (16.58%), after changes in the layout of activities can reduce waste (Turseno, 2018). Lean Manufacturing with the

Single Minutes Exchange of Dies (SMED) tool applied to curing workstations can reduce internal setup time by 127.47 minutes and external setup time by 3.06 minutes. Setup activities reduced in several ways. There are converting activities classified as internal set up activities such as green tire setup, preheat mould, and tool-taking activities reduced by 63.70 minutes (Kasanah et al., 2018). Reduction of waste occurs at each workstation and impacts increasing productivity and reducing production costs caused by debris during production (Dagmar and Tarigan, 2021). The implementation of the value stream mapping that was carried out resulted in a reduction in waste at each workstation. The total waste reduction occurred of 66.97 tons/year or 18.6% in waste gel and 88.8 tons/year or 19.3% in waste powder (Ravizar & Rosihin, 2018).

Many factors cause wasteful activities or processes in the industry. One of them is an error caused by a system error or human error. System errors are usually caused by the system controlling the process, and if they are corrected, the error will not appear again. Workers can be informed about the correct procedure and have understood the procedure stan-dard (Oliveira et al. 2018). However, due to the intricate work system, there is often inconsistency in work. It is mean known as human error. Human error can be a problem in several matters relating to work safety, work effectiveness, operation, time, economic losses, and others. No one can act more than once with the same precision. Every error action taken by someone is a possibility for an error to occur. The results of research by Rochmoeljati and Firmansyah (2019) using lean Manufacturing show that the waste that occurs in the edamame production process with a total waiting time of 7.5. Suharjo (2019) using the Waste Relationship Matrix (WRM) and Waste Assessment Questionnaire (WAQ) methods in the manual production process and found that the cooling process is one of the techniques where a lot of waste is still located. Operator errors can cause losses to the company due to the many defects in the production process so that rework must be done, and the company cannot reach the specified production target. The data of recapitulation turning production in 2019, (Table 1).

Table 1 shows the amount of production with a defect that exceeds the standard tolerance set by the company, is 5%. The product defects that occur in the production process require completion, namely the lean manufacturing approach, which functions to reduce defect waste with value streaming mapping (VSM). Lean Manufacturing method can be used in identifying waste (Fercoq et al. 2016) and form factors. The production process cause can be carried out using the Systematic human error reduction and prediction method to predict human error by analyzing and identifying potential solutions to mistakes made during the production process.

Table 1. Recapitulation of Total Production Turning Year 2019

Month	Amount of production	Defects					
		size	bent	Split	Leather	knots	dead knots
January	53,000	2,770	543	1,260	1,112	412	560
February	52,500	1,223	120	1,523	670	225	1,250
March	56,000	956	1,017	1,345	1,325	1,110	125
April	53,000	1,135	430	780	1,775	2,056	430
May	53,000	780	2,215	547	320	1,125	560
June	53,000	1,050	2,754	1,110	1,112	430	1,225
July	53,600	580	1,453	1,110	1,050	320	320
August	54,000	1,017	2,112	2,050	320	438	945
September	52,500	1,549	987	1,235	716	345	1,250
October	53,000	670	1,400	2,112	715	556	1,756
November	53,000	1,678	1,070	1,015	540	540	1,011
December	53,500	1,135	430	2,780	1,775	2,056	430

Based on the results of a review of previous research conducted, the authors found several research gaps in the study. Research gap in the first research there is no use of lean Manufacturing with the SHERPA (Systematic Human error Reduction and Prediction) method in eliminating waste defects simultaneously (Mandal et al. 2015), the second application of lean Manufacturing is used to identify waste in activities that have no added value as compared to the SHERPA method to identify activities that cause human error. Third, to the knowledge of the researcher, there is no research that eliminates the waste of defect waste by improving the human error. Based on the results of previous research, this study uses a solution in minimizing defects and the factors that cause human errors that occur in the turning production process, to increase profits for the company. For this reason, an analysis of the application of Lean Manufacturing and the SHERPA method is carried out to reduce defects. The research focuses on one company in the Manufacturing of turning wood processing.

2. LITERATURE REVIEW

2.1. Lean Manufacturing

Lean manufacturing process is a production system that uses very little energy and wastes to fulfill what consumers want (Singh et al. 2018, Kasanah et al. 2018). The analytical method used to identify waste is to use the waste assessment model method. The advantage of this model is the simplicity of the matrix and questionnaires that cover many things and are able to contribute to achieving accurate results in identifying the root causes of waste. The calculation of the linkages between wastes is carried out by discussing with the company and distributing questionnaires using weighting criteria. Through this elimination of waste, lean shows its capabilities that can be applied in a business without increasing the number of workers, capital equipment, without affecting existing businesses and without hiring reliable resources. Value stream mapping (VSM) is a tool for identifying value-added and non-value-added activities, which consists of 2 activities, namely the current state map and the future state map (Dadashnejad and Valmohammadi, 2018). The current state map is a product value stream configuration using specific icons and terminology to identify waste and areas for improvement or improvement, while for the Future state map is a blueprint for the desired lean transformation in the future and provides benefits to the company. Value Stream Mapping is a definite tool as a first step in making a change process to achieve lean manufacturing conditions (Huang et al. 2019). Value stream mapping (VSM) is a tool for identifying value added and non-value-added activities in the manufacturing industry, making it easier to find root causes in the process. The purpose of VSM is to identify the production process so that materials and information can run without interruption, increase productivity, and assist in system implementtation. Therefore, VSM helps in finding waste in the production process (Steur et al. 2016).

2.2. Value Stream Analysis Tools (VALSAT)

Value Stream Analysis Tools (VALSAT) are tools used to facilitate understanding of existing value streams and make it easier to improve the waste contained in the value stream (Zahraee et al. 2020). VALSAT is an approach used by weighting waste, and then from that weighting, tools are selected using a matrix (Folinas and Ngosa, 2013). Selection of a detailed mapping tool that matches the type of waste that occurs in the production process.

2.3. Cause and Effect

Diagram A cause and effect diagram is often called a Fishbone Diagram or Ishikawa Diagram is a graphical tool used to help identify, sort, and show the causes of a problem (Simanová and Gejdoš, 2015). The cause-and-effect diagram is one of the tools used to determine and link the factors that are the

potential causes of a problem (Abu et al. 2019). This diagram is the only tool that uses verbal (non-numerical) or qualitative data (Dagmar and Tarigan, 2021).

2.4. Systematic Human Error Reduction and Prediction Approach (SHERPA)

Human error is defined as a failure to complete a specific task or job (or take actions that are not permitted) that can interfere with operating schedules or result in damage to objects and equipment (Mandal et al. 2015). Human errors can be classified into many categories, such as errors or errors made by operators. One of the causes of their occurrence is a dirty environment, complex tasks, lack of proper procedures, operator ignorance and poor operator selection and training. Maintenance errors occur in the field due to negligence by maintenance operators. Some examples of maintenance errors are faulty maintenance, incorrectly calibrated equipment, and incorrect repairs to correct equipment points. Assembly errors are the result of human error during product assembly. Some of the causes for assembly errors are low lighting, wrong blueprints and other misleading materials, poorly designed work layouts, and imperfect communication information. Installation errors occur for various reasons, including failure to install equipment or items according to manufacturer specifications and incorrect installation instructions and blueprints. Design errors are the result of inadequate design. Some of the causes for this are the failure to ensure the effectiveness of person-machine interactions to implement human needs in the design and assigning functions that are not suitable for humans. Inspection errors are the result of less than 100% accuracy of the inspection personnel. One typical example of inspec-tion error is accepting and rejecting intolerant and intolerant components and items, respectively. Mishandling occurs due to improper transportation or storage facilities. A method used to identify the mistakes related to human expertise or habits with the SHERPA method. Namely: The Hierarchical Task Analysis (HTA) step, job classification, human error identification, consequence analysis, ordinal error probability assessment, critical level analysis and making strategies for fixing errors (Naweed et al. 2018). HTA is one of the methods used in the task analysis process. HTA is the method most often used because of its very detailed, easy, and straightforward application.

3. RESEARCH METHOD

The research method is a step used to solve a defect waste problem in the turning production. The technique of collecting data by conducting observations in the field and collecting data through measurements is called field research. The second stage, the researchers conducted interviews and distributed questionnaires to workers in the company. Data collection stages are carried out by making value-streaming mapping regarding information flow, physical flow, activity time, and distance in each production process. The data obtained is then used to describe the mapping of Current State Value Stream Mapping or the initial state of the entire activity from the current state in the production process. The depiction of current state value stream mapping then created a questionnaire with the attributes used to be distributed to parties related to employees, supervisors, and managers production.

The selection of Value Stream Analysis Tools (VALSAT) is made by multiplying the average weight value of each waste from the waste identification questionnaire results with the VALSAT value for each type of waste (Zahraee et al. 2020). The tools can add value in the Process Activity Mapping (PAM) (Singh and Singh, 2020), and the Supply chain response matrix. The selected tools can categorize activities in the production process: value-added activities (VA), which are essential in the production process, non-value added (NVA). It is not added value and can be eliminated if needed, and activities that are not added value but are required in the production process or necessary non-value added (NNVA). The action that causes the most waste is then analyzed the causes of the problem to be repaired.

The most dominant factor driving the waste defect comes from operator error or human error such as negligence in checking the oven process's moisture content, which causes dry and split turning results. The next stage is human error analysis. This stage is carried out because of the waste of defects, mostly by the operator. The worklist is compiled in the Hierarchical task analysis (HTA) table, then classified according to the error type of action, checking and selection (Mandal et al. 2015; Naweed et al. 2018). Work data is collected according to the kind of error. The error identification after which an analysis of human consequences of the error occurs. Ordinal error assessment is carried out to see operator errors, including medium, low or high types, to obtain a critical level of the mistake analyzed. After that, a strategy made to reduce the errors in the form of recommendations for improvement.

4. RESULTS AND DISCUSSION

4.1 Current State Value Stream Mapping

An initial stage in understanding the physical flow and information in the turning production process. The turning process for the formation of motifs is with a turning machine. The wood before being turned is sorted whether there are defects such as holes, if there are defects, then it is put in the putty process. The refinement process using a sanding machine aims to smooth the wood and make it easier for the painting process to be satisfactory. Refining is done on good quality wood or wood that has been putty and then refined. This process takes 0.05 minutes. The painting process takes 0.035 minutes. The method of painting the dry product is then carried out by packaging the product on a unique pallet and wrapped in plastic so that when it is stored (Firmansyah and Lukmandono, 2020), and the next step is sent to the warehouse for storage before sending to the customer Figure 1.

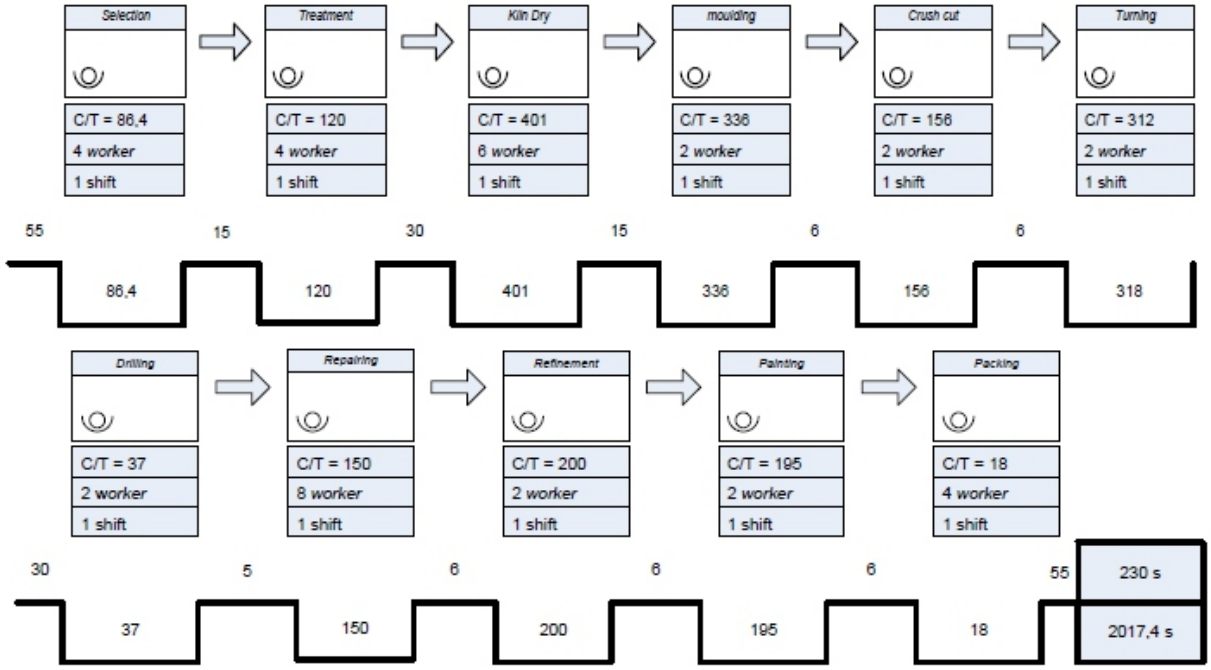

Figure 1. Current State Value Stream Mapping

4.2 Identification and Weighting of Waste

The waste identification process is carried out by distributing questionnaires to the production section regarding the relationship between the seven wastes to obtain waste weight. Here are the stages in waste identification with a seven-waste relationship, a waste relationship matrix and a waste assessment questionnaire (Table 1).

Table 1. Summary of the results of WAM, WRM and WAQ

Description	O	I	D	M	T	P	W
Score Yj	1.133	1.235	1.146	1.0548	1.070	1.045	0.980
Factor Pj	211.450	155.063	378.260	176.208	155.063	148.798	180.907
Result	239.728	191.565	433.539	185.870	165.937	155.429	177.435
Result %	15.471	12.363	27.979	11.995	10.709	10.030	11.451
Rank	2	3	1	4	6	7	5

From table 1, the recapitulation of waste results obtained the highest level of waste in the defect (D) with a percentage of 27,979%. Followed by overproduction (O) of 15,471%, inventory of 12,363 %, motion (M) 11,995%, waiting (W) 11,451%, transportation (T) of 10,709% and process (P) of 10,030. After knowing that the most dominant weighting is, then the mapping is carried out accurately using VALSAT. The selection of detailed mapping is carried out to further identify the location of waste in the value stream. Value stream Analysis Tools are a tool used to map waste by multiplying the waste weighting result from the WAQ with the scale in the VALSAT. Process activity mapping to score as many as 478 218 then Quality Filter mapping (QFM) is in second place with a score of 277,316.

4.3. Process Activity Mapping (PAM).

Process Activity Mapping is an approach that can be used for activities on the production floor. The following is the recapitulation of the turning production process activities with process mapping tools which can be seen in Table 3.

Table 3. Results of Process Mapping Tools Recapitulation

Activities	Number of activities	Time (minutes)	Percentage
Operation	12	20171.4	95.973
Transport	12	190.8	0.907
Inspection	9	193.4	0.920
Storage	2	240	1.141
Delay	3	222	1.056
Total	38	21017.6	100
VA	20	20415.8	97.136
NNVA	12	294	1.398
NVA	6	307.8	1.464
Total	38	21017.6	100

4.5. Quality Filter Mapping (QFM)

Quality Filter Mapping is a tool used to identify defects or defects in the supply chain wherein the turning production process has six types of defects. The product's highest defect was the type of split defect with a percentage of 22.55%, the kind of defect in size that was not following the percentage of 19.45% and the type of bent defect 19.43%. The following is a Pareto diagram of Product defects which can be seen in Figure 2.

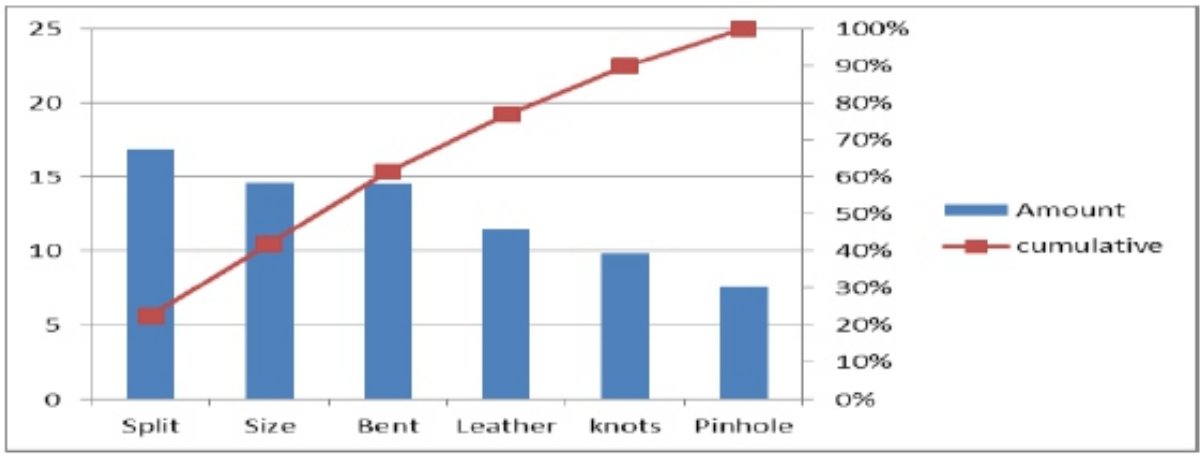

Figure 2. Pareto Diagram of Product Disability Turning

4.6. Cause and Effect Diagram

The diagram is used to analyze the factors causing the problem so that corrective action can be taken (Simanová and Gejdoš, 2015). The following is a cause-and-effect diagram of turning product defects (Figures 3, 4 and 5).

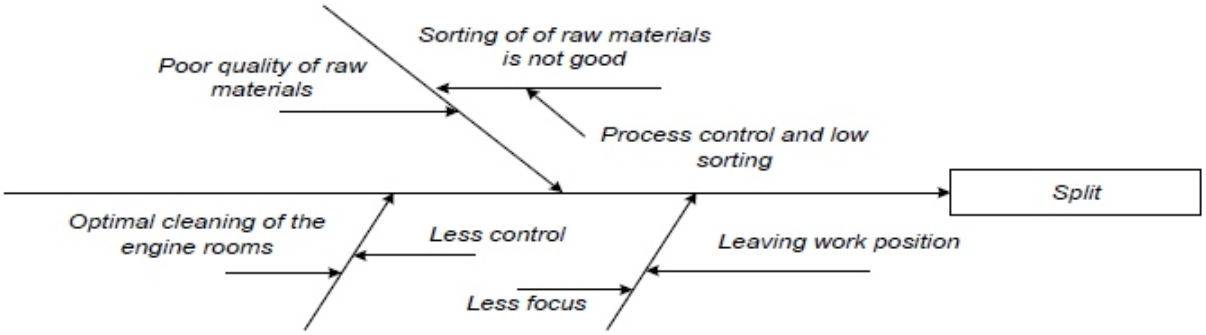

Figure 3. Cause and Effect Diagram of Split Defects

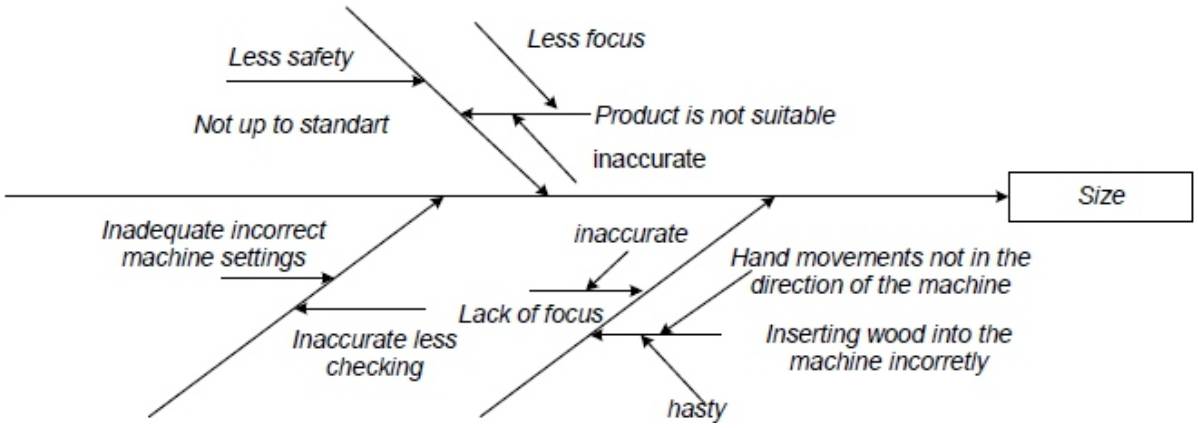

Figure 4. Cause and Effect Diagram for Size Defects

The cause-and-effect diagram of a split defect in the turning production process shows that defects occur because workers are not focused, resulting in less cleaning of the machine room. Anticipate that mistake will not happen repeatedly; it is necessary to carry out consistent supervision. Figure 4 above shows the defect size is not suitable in the turning production process due to workers' inaccuracy in inserting wood into the machine.

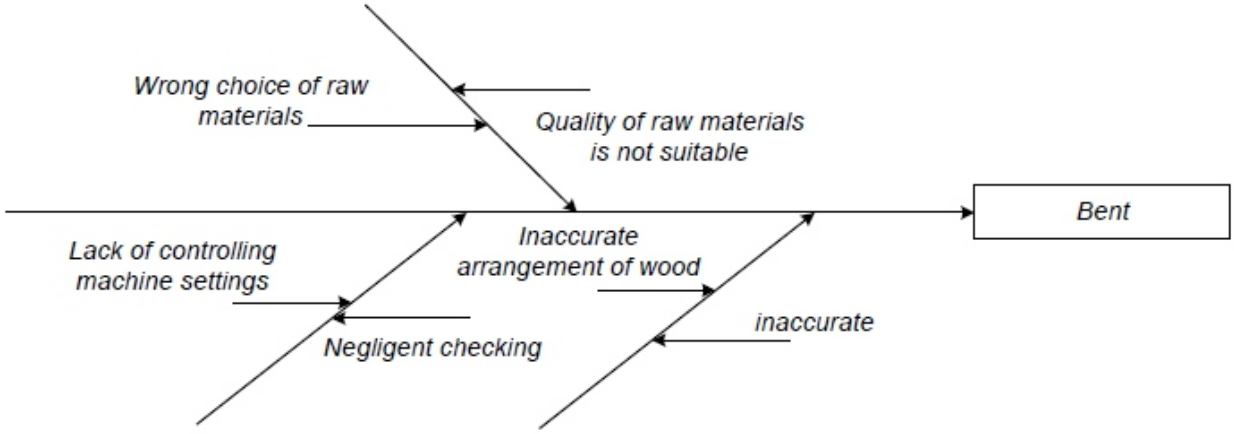

Figure 5. Cause and Effect Diagram for Bend Defects

4.7. Human Error Prediction Using by SHERPA

Method SHERPA is used to identify errors related to human expertise or habits. First, to identify a human error, create an HTA in the form of a chart of the tuning production process. The results from the HTA provide a code (!) to indicate the critical level, the turning product is likely to have many defects and require reprocessing (Table 4). The next stage of the strategic plan is drawn up as actions that must be taken to correct errors or minimize human errors. The action is adjusted according to the consequences, the critical level and the value of the probability of error.

The whole strategic plan can be concluded that there is a need for standard checklist forms for machine checking, SHS training such as personal protective equipment during production and training to improve the skills needed have an operator. After obtaining the improvements that will be carried out, it is not sure to reduce the waste defect, cycle time and lead time in each process. The next step is to use PAM analysis tools again. Recapitulation of PAM results which can be seen in table 5.

Table 4. Strategic Plan for Turning Production Process

Code	Consequences	Probability of ordinal error	Critical level	Strategic plan
1.1	Fingers punctured uneven wood surface	M	-	Implementing Safety and health system (SHS) on PPE (personal protective equipment)
1.2	Product quality decreases	L	-	Doing repetition to select wood to be more careful
2.1	Workers are hit by wood which can cause injury	M	-	Give a warning not always to apply Safety and health system (SHS)
2.2	Quality of wood that is easy to eat	L	-	Operators must carefully mix according to procedure
2.3	Eyes can be splashed with liquid and interfere with concentration	M	-	Use PPE (personal protective equipment)
3.1	Woodpiles fall from the forklift	L	-	Pick up limited according to capacity
3.2	Workers' hands are injured, or fingers scratched by wood	M	-	Apply Safety and health system (SHS) on PPE (personal protective equipment)
3.3	Eyes are exposed to dust	L	-	Use of PPE
3.4	Burns leather or workers are cold	M	-	Routine of checks
3.5	Wood becomes stringy causing the quality to decrease	H	!	Make a checklist form for routine inspection

3.6	There are parts of the wood that have not dried causing dark wood colour	M	-	Operator training and loading checklist forms
4.1	Workers are crushed by wood causing injury	M	-	Applying SHS with PPE
4.2	Products are not suitable	L	-	Repetition of the process according to size
4.3	Side surfaces are different / not match the size of	M	-	The operator must carefully
4.4	Product size does not equal	L	-	Create a form checklist routine checking
5.1	length of the product not to order	M	-	training on operator
5.2	timber quality declining	L	-	perform repetition to select wood to be more careful
5.3	cutting out of size causes defects	H	!	loggers must be careful to
5.4	fall and repeat the work	M	-	limit the extraction of wood / according to the capacity of
5.5	when the woodturning is broken or deformed	H	!	The operator must be careful
6.1	logs fall from the forklift	M	-	limit taking to capacity
6.2	fingers hit by cutting machines/accidents	M	-	increase awareness when processing is carried out
6.3	products become defective	H	!	carry out routine checks for the replacement of the chisel
6.4	wood is crushed on the leg causing injury	L	-	use of PPE
6.5	repetition time	M	-	motivation training for operators
6.5	product results are mixed between defects and good	L	-	The operator must be careful
6.6	product quality decreases	L	-	repeating to choose wood more carefully
7.1	The product falls from the forklift hitting the leg causing injury	L	-	limiting take to capacity
7.2	feet of falling wood	L	-	applies SHS with PPE
7.3	drilling depth is not suitable	M	-	The operator must be careful
7.4	process time to restart	M	-	improve operator skills
8.1	fingers pricked on uneven wood surfaces	M	-	applies SHS with PPE
8.2	some defects are not covered	M	-	The operator must be careful
8.3	many products are not suitable	M	-	The operator should be careful
9.1	pad injuries a back	L	-	increase awareness when doing poses

202

Table 5. Recapitulation of PAM Results

Activities	Number of activities	Time (minutes)	percentage
Operation	13	1951.4	86.829%
Transport	8	90	4.005%
Inspection	6	96	4.272%
Storage	2	110	4.895%
Delay	0		0
Total	29	2247.4	100

Type of activity	Number of activities	Time (minutes)	Percentage
VA	15	1926.4	85.717%
NNVA	14	321	14.283%
NVA	0	0	0
Total	29	2247.4	100

Table 5 shows the number of activities in the turning production process as many as 29 activity with a total time of 2247.4 minutes. In the type of activity, the value-added value is omitted because it has no value-added

5. FUTURE STATE STREAM MAPPING

Future state stream mapping is described after the mapping of current value stream mapping and identification of waste. This mapping depiction shows the parts that need improvement so that the turning production system conditions are improved. The following is an improvement in the mapping's turning production process, which can be seen in Figure 6. Next, compare the Current Value Stream Mapping Figure 1 and Future State Stream Mapping Figure 6. The comparison results are shown in Table 6.

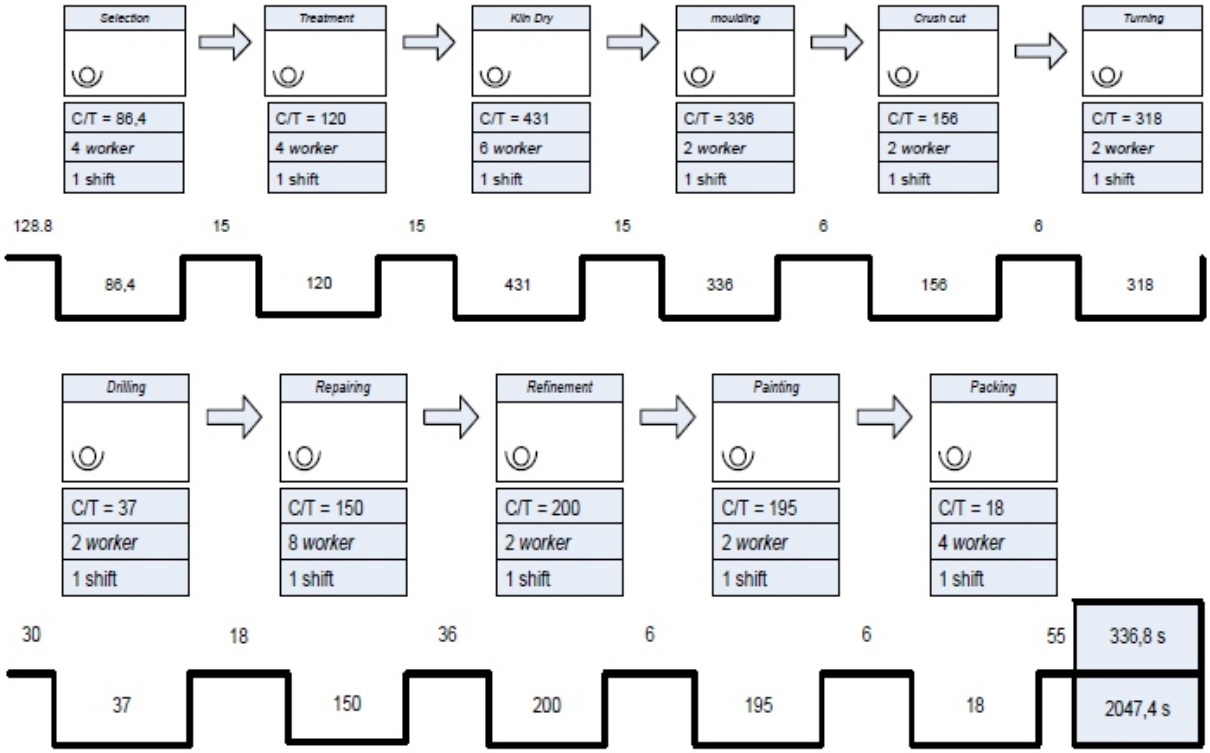

Figure 6. Future State Stream Mapping

Results Table 6 shows changes in the increase in results PCE calculation with an improvement of 4,918% (136.8 minutes). Improvement was obtained by comparing the PCE before the improvement was 80.799% (2384.2 minutes) and after the improvement was 85.717% (2247.4 minutes)

Table 6. Comparison of PAM Results

Indicator	Current (minutes)	Future (minutes)	Improvement (minutes)
VA	1926.4	1926.4	-
NNVA	333	321	12
NVA	124.8	0	124.8
Total	2384.2	2247.4	136.8
Process cycle efficiency (PCE)	80.799%	85.717%	4.918%

6. CONCLUSIONS

Data analysis identified waste from current steam mapping by distributing questionnaires to production employees regarding the relationship between the seven wastes to obtain weight. Waste that has been recognized with a seven-waste relationship between the seven wastes to obtain weight. Waste that has been recognized with a seven-waste relationship, waste relationship matrix and waste assessment questionnaire. The waste brought with the highest waste is: The highest level of waste is in defects (D) with a percentage of 27,979%. Followed by waste in overproduction (O) of 15,471%, inventory (I) of 12,363%, motion (M) of 11,995%, waiting for (W) of 11,451%, transportation (T) of 10,709% and process (P) of 10,030. The weighting of waste by selecting tools: Value stream Analysis Tools to be an obtained process activity mapping and obtained quality filter mapping. The results are 34 activities (13 operations, 12 transportation, six inspections, two storage and one delay) with the type of activity value-added 80.789%, necessary non-value-added 13,967%, and non-value added 5,234%. The comparison result of the current value stream mapping value is 80.799% (2384.2 minutes), and future state stream mapping is 85.717% (2247.4 minutes). The comparison shows the value of Process cycle efficiency with an improvement of 4.9185% (136.8 minutes). This study contributes to manufacturing companies in the turning production process in increasing value-added.

REFERENCES

1. *Abu, F., Gholami, H., Saman, M.Z.M., Zakuan, N. and Streimikiene, D. (2019). The implementation of lean manufacturing in the furniture industry: A review and analysis on the motives, barriers, challenges, and the applications. Journal of Cleaner Production, 234, 660-680, https://doi.org/10.1016/j.jclepro.2019.06.279*
2. *Dadashnejad, A.-A. and Valmohammadi, C. (2018). Investigating the effect of value stream mapping on operational losses: a case study. Journal of Engineering, Design and Technology, 16 (3), 478-500. https://doi.org/10.1108/JEDT-11-2017-0123*
3. *Dagmar, A.V. and Tarigan, Z.J.H. (2021) The application of the Six Sigma method in reducing the defects of welding on the steel material. IOP Conference Series: Materials Science and Engineering, 1010 012044, doi:10.1088/1757-899X/1010/1/012044*
4. *Fercoq, A., Lamouri, S. and Carbone, V. (2016). Lean/Green integration focused on waste reduction techniques. Journal of Cleaner Production, 137, 567-578, https://doi.org/10.1016/j.jclepro.2016.07.107*
5. *Firmansyah, A. and Lukmandono (2020). Warehouse Relayout Design with Weighted Distance Method to Minimize Time Travel. International Journal of Business Studies, 3 (1), 1-8, https://doi.org/10.9744/ijbs.3.1.1-8*
6. *Folinas, D. and Ngosa, J. (2013). Doing more with less: a pharmaceutical supplier case. International Journal of Productivity and Quality Management, 11(4), 412-433, DOI: 10.1504/IJPQM.2013.054264*
7. *Huang, Z., Kim, J., Sadri, A., Dowey, A. and Dargusch, M.S. (2019). Industry 4.0: Development of a multi-agent system for dynamic value stream mapping in SMEs. Journal of Manufacturing Systems, 52(Part A), 1-12, https://doi.org/10.1016/j.jmsy.2019.05.001*
8. *Kasanah, Y U., Suryadhini, P.P. and Astuti, M. (2018). Lean Manufacturing Application to Minimize Waste Delay at Curing Workstations at PT Bridgestone Tire Indonesia. Scientific Journal of Industrial Engineering and Management Universitas Kadiri, 2(1), 12-19. DOI: http://dx.doi.org/10.30737/jatiunik.v2i1.273*
9. *Kristianto, I. and Tarigan, Z.J.H. (2019). The impact TQM System on Supply Chain Performance through Supply Chain Integration and Employee Satisfaction. International Journal of Business Studies, 2(1),8-17, DOI: 10.9744/ijbs.2.1.8–17*

10. Kusbiantoro, C dan Nursanti, E. (2019). Implementation of Lean Manufacturing to Identify and Reduce Waste (Case Study of CV Tanara Textile), Jurnal Teknologi Dan Manajemen Industri, 5 (1), https://doi.org/10.36040/jtmi.v5i1.251
11. Lukmandono, Hariastuti, N.L.P., Suparto, and Saputra, D.I. (2019). Implementation of Waste Reduction at Operational Division with Lean Manufacturing Concept. IOP Conference Series: Materials Science and Engineering, 462, 012049, doi:10.1088/1757-899X/462/1/0120
12. Mandal, S., Singha, K., Behera, R.K., Sahu, S.K., Raj, N. and Maiti, J. (2015). Human error identification and risk prioritization in overhead crane operations using HTA, SHERPA and fuzzy VIKOR method, Expert Systems with Applications, 42 (20), 7195-7206, https://doi.org/10.1016/j.eswa.2015.05.033
13. Naweed, A., Balakrishnan, G. and Dorrian, J. (2018). Going solo: Hierarchical task analysis of the second driver in "two-up" (multi-person) freight rail operations. Applied Ergonomics, 70, 202-231, https://doi.org/10.1016/j.apergo.2018.01. 002
14. Oliveira, V.B., Ouverney, A.M.F., Cardoso, C.G.L., and Viana, C.S.C. (2018).Application of a homemade procedure for manufacturing of a rod mechanical spare part. Journal of Materials Research and Technology, 7(4), 487-491, https://doi.org/10.1016/j.jmrt.2017.03.006
15. Pratiwi, I., Masita, M., and Fitriadi, R. 2019. Human error analysis using SHERPA and HEART method in Batik Cap production process. IOP Conference Series: Materials Science and Engineering, 674,
16. Ravizar, A. and Rosihin, R. (2018). Lean Manufacturing Application to Reduce Waste in Absorbent Production. 4(1), 23-32. Jurnal INTECH Teknik Industri Universitas Serang Raya. https://doi.org/10.30656/intech.v4i1.854
17. Rochmoeljati,N.Y. and Firmansyah, R.D. (2019). Analysis of Waste in Edamame Production Using Lean Manufacturing Methods at PT. Mitratani Dua Tujuh Jember. Journal of Industrial Engineering and Management, 14(2), 51-59, DOI: https://doi.org/10.33005/ tekmapro.v14i2.55
18. Simanová, Ľ. and Gejdoš, P. (2015). The Use of Statistical Quality Control Tools to Quality Improving in the Furniture Business. Procedia Economics and Finance, 34, 276-283, https://doi.org/10.1016/S2212-5671(15)01630-5
19. Sinambela, Y. (2017). Lean Manufacturing Implementation at PT. XYZ. Industrial Engineering Journal, 6(1), 43-49.
20. Singh, J. and Singh, H. (2020). Application of lean manufacturing in automotive manufacturing unit. International Journal of Lean Six Sigma, 11 (1), 171-210. https://doi.org/10.1108/IJLSS-06-2018-0060
21. Singh, J., Singh, H. and Singh, G. (2018). Productivity improvement using lean manufacturing in manufacturing industry of Northern India: A case study. International Journal of Productivity and Performance Management, 67 (8), 1394-1415. https://doi.org/10.1108/IJPPM-02-2017-0037
22. Steur, H., Wesana, J., Dora, M.K., Pearce, D., and Gellynck, X. (2016). Applying Value Stream Mapping to reduce food losses and wastes in supply chains: A systematic review. Waste Management, 58, 359-368, https://doi.org/10.1016/j.wasman.2016.08.025
23. Turseno, A. (2018). Waste Elimination Process with Waste Assessment Model & Process Activity Mapping Method in Dispensing. Journal Industrial Manufacturing, 3(1), 45-50.
24. Zahra, A.Az., Indrawati, S. and Sulistio, J. 2020. Performance Improvement in Aerospace Production Through Lean Manufacturing Implementation. IOP Conference Series: Materials Science and Engineering 722, 012045, doi:10.1088/1757-899X/722/1/012045
25. Zahraee, S. M., Tolooie, A., Abrishami, S.J., Shiwakoti, N., and Stasinopoulos, P. (2020). Lean manufacturing analysis of a Heater industry based on value stream mapping and computer simulation, Procedia Manufacturing, 51, 1379-1386, https://doi.org/10.1016/j.promfg.2020. 10. 192

Instructions for Authors

Essentials for Publishing in this Journal

1 Submitted articles should not have been previously published or be currently under consideration for publication elsewhere.

2 Conference papers may only be submitted if the paper has been completely re-written (taken to mean more than 50%) and the author has cleared any necessary permission with the copyright owner if it has been previously copyrighted.

3 All our articles are refereed through a double-blind process.

4 All authors must declare they have read and agreed to the content of the submitted article and must sign a declaration correspond to the originality of the article.

Submission Process

All articles for this journal must be submitted using our online submissions system. http://enrichedpub.com/ . Please use the Submit Your Article link in the Author Service area.

Manuscript Guidelines

The instructions to authors about the article preparation for publication in the Manuscripts are submitted online, through the e-Ur (Electronic editing) system, developed by **Enriched Publications Pvt. Ltd**. The article should contain the abstract with keywords, introduction, body, conclusion, references and the summary in English language (without heading and subheading enumeration). The article length should not exceed 16 pages of A4 paper format.

Title

The title should be informative. It is in both Journal's and author's best interest to use terms suitable. For indexing and word search. If there are no such terms in the title, the author is strongly advised to add a subtitle. The title should be given in English as well. The titles precede the abstract and the summary in an appropriate language.

Letterhead Title

The letterhead title is given at a top of each page for easier identification of article copies in an Electronic form in particular. It contains the author's surname and first name initial .article title, journal title and collation (year, volume, and issue, first and last page). The journal and article titles can be given in a shortened form.

Author's Name

Full name(s) of author(s) should be used. It is advisable to give the middle initial. Names are given in their original form.

Contact Details

The postal address or the e-mail address of the author (usually of the first one if there are more Authors) is given in the footnote at the bottom of the first page.

Type of Articles

Classification of articles is a duty of the editorial staff and is of special importance. Referees and the members of the editorial staff, or section editors, can propose a category, but the editor-in-chief has the sole responsibility for their classification. Journal articles are classified as follows:

Scientific articles:

1. Original scientific paper (giving the previously unpublished results of the author's own research based on management methods).

2. Survey paper (giving an original, detailed and critical view of a research problem or an area to which the author has made a contribution visible through his self-citation);

3. Short or preliminary communication (original management paper of full format but of a smaller extent or of a preliminary character);

4. Scientific critique or forum (discussion on a particular scientific topic, based exclusively on management argumentation) and commentaries. Exceptionally, in particular areas, a scientific paper in the Journal can be in a form of a monograph or a critical edition of scientific data (historical, archival, lexicographic, bibliographic, data survey, etc.) which were unknown or hardly accessible for scientific research.

Professional articles:

1. Professional paper (contribution offering experience useful for improvement of professional practice but not necessarily based on scientific methods);
2. Informative contribution (editorial, commentary, etc.);
3. Review (of a book, software, case study, scientific event, etc.)

Language

The article should be in English. The grammar and style of the article should be of good quality. The systematized text should be without abbreviations (except standard ones). All measurements must be in SI units. The sequence of formulae is denoted in Arabic numerals in parentheses on the right-hand side.

Abstract and Summary

An abstract is a concise informative presentation of the article content for fast and accurate Evaluation of its relevance. It is both in the Editorial Office's and the author's best interest for an abstract to contain terms often used for indexing and article search. The abstract describes the purpose of the study and the methods, outlines the findings and state the conclusions. A 100- to 250-Word abstract should be placed between the title and the keywords with the body text to follow. Besides an abstract are advised to have a summary in English, at the end of the article, after the Reference list. The summary should be structured and long up to 1/10 of the article length (it is more extensive than the abstract).

Keywords

Keywords are terms or phrases showing adequately the article content for indexing and search purposes. They should be allocated heaving in mind widely accepted international sources (index, dictionary or thesaurus), such as the Web of Science keyword list for science in general. The higher their usage frequency is the better. Up to 10 keywords immediately follow the abstract and the summary, in respective languages.

Acknowledgements

The name and the number of the project or programmed within which the article was realized is given in a separate note at the bottom of the first page together with the name of the institution which financially supported the project or programmed.

Tables and Illustrations

All the captions should be in the original language as well as in English, together with the texts in illustrations if possible. Tables are typed in the same style as the text and are denoted by numerals at the top. Photographs and drawings, placed appropriately in the text, should be clear, precise and suitable for reproduction. Drawings should be created in Word or Corel.

Citation in the Text

Citation in the text must be uniform. When citing references in the text, use the reference number set in square brackets from the Reference list at the end of the article.

Footnotes

Footnotes are given at the bottom of the page with the text they refer to. They can contain less relevant details, additional explanations or used sources (e.g. scientific material, manuals). They cannot replace the cited literature.
The article should be accompanied with a cover letter with the information about the author(s): surname, middle initial, first name, and citizen personal number, rank, title, e-mail address, and affiliation address, home address including municipality, phone number in the office and at home (or a mobile phone number). The cover letter should state the type of the article and tell which illustrations are original and which are not.

Address of the Editorial Office:

Enriched Publications Pvt. Ltd.
S-9,IInd FLOOR, MLU POCKET,
MANISH ABHINAV PLAZA-II, ABOVE FEDERAL BANK,
PLOT NO-5, SECTOR -5, DWARKA, NEW DELHI, INDIA-110075,
PHONE: - + (91)-(11)-45525005